SOMITOGENESIS IN THE CORN SNAKE

Céline Gomez

UNIVERSITE PIERRE & MARIE CURIE
LA SCIENCE A PARIS

THESE DE DOCTORAT DE

L'UNIVERSITE PIERRE ET MARIE CURIE

Spécialité

Biologie du Développement

Présentée par

Céline GOMEZ

Pour obtenir le grade de

DOCTEUR de l'UNIVERSITE PIERRE ET MARIE CURIE

ETUDE DE LA SOMITOGENESE CHEZ LE SERPENT DES BLES

Soutenue le 19 décembre 2007

Devant le jury composé de :

Dr. Olivier POURQUIE: Directeur de thèse

Dr. Guillaume BALAVOINE: Rapporteur

Pr. Martin CATALA: Rapporteur

Pr. Muriel UMBHAUER: Examinateur

Pr. Denis DUBOULE: Examinateur

The Pierre et Marie Curie University

SOMITOGENESIS IN THE CORN SNAKE

A Thesis in

Developmental Biology

by

Céline GOMEZ

Submitted in Partial Fulfillement
of the Requirements
for the Degree of

Doctor of Philosophy

December 2007

ACKNOWLEDGMENTS

I would like to heartily thank the Dr. Olivier Pourquié for his help in many ways. Thank you for having welcomed me in your team, whereas I was struggling to escape another laboratory, after having spent one year of my PhD. You offered me an incredible scientific environment and a lot of freedom! Thank you for having given me this chance, for your trust, your tolerance, your advices, your optimism and for always having kept your words. Working with you has been a real pleasure!

In the same extent, I would like to express all my gratitude to the Pr. Muriel Umbhauer, and also the Dr. Catherine Jessus, who strongly supported and recommended me when I decided to leave my former lab. During these nasty days, Muriel has always been present and took time to listen to me, advice me with my experiments and give me back this self-confidence without which I may not be writing this thesis today.

I would also like to acknowledge the head of my doctoral school the Pr. Pierre Netter, who facilitated my moves to go to the United-States.

I am grateful to the Dr. Guillaume Balavoine, the Pr. Martin Catala, the Pr. Denis Duboule and the Pr. Muriel Umbhauer who kindly accepted to be members of my committee.

I worked with very nice and talented people. I would first like to thank the Dr. Ertuğrul Özbudak for his unconditional support (psychological and scientific). Thank you for participating to my experiments and helping me with all aspects of the analyses. Our scientific discussions were very stimulating and constructive to me. You also bucked me up when I really needed it. Lucky me!

In the same time, I was given to meet the Dr. Julian Lewis, who so kindly took time to work on our data and give us back this beautiful and elegant way to interpret them, using a mathematical model. Thank you so much again!

This work would not have happened so smoothly without the expertise of Diana Baumann and her team at the reptile facility. Thank you for the precious information you gave me throughout these years.

More generally, I thank the Stowers Institute's core facilities which are always ready to help and advice.

I, of course, received a huge support from the Pourquié Lab's members. I am thankful to Mary-Lee, Aurélie, Tada, Gonçalo, Jérôme, Joanne, Alexander, Bertrand,

Leif, Jennifer, Mitsuji, Sachin, Merry, Ertuğrul, Silvia, Michael, Cheng-Wen, Olivier Tassy, Matthias, Holly, Shaobing and Liz, as well as the former lab members Pascale, Valérie and Barbara. Thank you so much for always trying to answer my questions, your great encouragements and for your nice way to make every day life congenial. Special thanks to Joanne who edited my English in this thesis, and comforted me so many times!

I am grateful to all the people who supported me at UMR7622 before I left, especially Stéphanie Migrenne. I look forward to see you back to France!

I have met two interesting and important persons during my summer internships in Jussieu's labs. I would like to acknowledge the Pr. Dominique Higuet and the Dr. Eric Bonnivard for having given me the desire to make research while I was studying in their laboratory. This experience strongly helped me during my master and first year of PhD.

I have to thank my friends Olivia, Mélanie, Mathilde, Benoît, Xavier, Jonathan, Fabienne, Florent, Mary, David, Irène and Margot for their constant support, even from oversee.

I would like to finish by acknowledging the most important persons in my life: my family, especially my parents and my brother. There is no word to describe all the welfare you gave and still give me. Thank you for always being present, sharing my moods, joys and experiences. Nothing can replace your advices and your love.

M^{me} Tusseau, I wish so badly you could be here. I can't stop to horribly miss you. I will always keep you inside, deeply in my heart. Forever.

A mes parents,

A M^{me} Tusseau,

TABLE OF CONTENTS

LIST OF FIGURES AND TABLES……..…8
ABBREVIATIONS……..…..……..10
ABSTRACT……..…….....11
INTRODUCTION……..…..…….……12
I) Evolution of segmentation……13
II) Segmentation in the vertebrates…….....17
1) The segments are formed through a process called somitogenesis……..……..…….19
1-1) Formation of the somites…….19
1-2) Nomenclature of the somites……...…….21
1-3) Differentiation of somites……...……..21
1-4) Resegmentation……...…….....24
1-5) Regionalisation……...……..25
2) Regulation of somitogenesis and control of somite number……27
2-1) Genesis of the paraxial mesoderm and axis elongation…….27
2-2) PSM properties……...……..33
2-3) End of somitogenesis……...…….34
2-4) The Clock and Wavefront model……...……...35
3) Molecular events during somitogenesis…….…..36
3-1) The segmentation clock ……..…….…36
3-1-1) Discovery of a cellular oscillator in the PSM…36
3-1-2) Comparison between species……...…….38
3-1-3) Functional analysis of the genes involved in the segmentation clock…….…43
3-1-4) Mechanisms for the propagation of the cyclic gene wave…….……44
3-2) The determination front…….....47
3-3) Somite AP polarity specification……50
3-4) Somite boundary formation……52
III) The corn snake as a new model……. ……...54

1) Introduction to reptiles……..…….55
2) Studies (or lack of studies) on reptiles……..…….56
3) Snakes among the reptiles……..…….……...59
3-1) Generalities……..…….59
3-2) The corn snake……...……...60
4) How did snake make so many vertebrae? Evolutionary studies….63
RESULTS……...……...……..64
ARTICLE (SUBMITTED)……..……..……72
UNSUBMITTED DATA……...……...……...…...….73
I) Snake…….74
1) Are there other genes dynamically expressed in corn snake PSM?.....74
2) Cultures……..……....77
II) Lizard……...…….79
DISCUSSION……..…....……85
1) Reptile somitogenesis in evolution……...……..86
2) Control of PSM life time and somitogenesis arrest……..…….90
3) *Nrarp* and *Lfng* expression patterns……..…….……91
4) Functional studies for the future?.....92
MATERIAL AND METHODS…….……...…….94
1) Eggs and embryos…….....95
2) Cloning……..……...95
3) Whole-mount *in situ* hybridization……..……96
4) "Mesogenin1/Mespo time-course" experiment and speeds calculation…..…96
5) Corn snake skeletal prep……..…….…..….98
6) Lizard fibroblastic cell line……..……...…….98
7) Lizard fibroblastic cell line infection with RCAS virus……...……..98
8) Cultures……..…..……...98
APPENDIX ……..……..……..……102
BIBLIOGRAPHY ……..…….....108

LIST OF FIGURES AND TABLES

Figure 1. Two modes of segmentation: Synchronous and sequential…….……14
Figure 2. Phylogeny of the vertebrates…….…..……..18
Figure 3. Different forms of skeletons among the vertebrates……..…….....20
Figure 4. Organization of the body plan of vertebrate embryos……..……20
Figure 5. Nomenclature of the somites……...……..…..…..22
Figure 6. Overview of somite formation and compartmentalization in chicken embryo……...……..22
Figure 7. Schematic representation of an amniote and anamniote somite…...…..…23
Figure 8. Resegmentation…….…...……....26
Figure 9. Hox genes organization and colinearity……..……...…..26
Figure 10. Gastrulation is a continuous process in vertebrates……...…..…..29
Figure 11. A model for patterning the embryonic body in *Xenopus* and zebrafish….31
Figure 12. "Clock and Wavefront" model……...……...37
Figure 13. *c-hairy1* mRNA expression in the PSM defines a highly dynamic caudal-to-rostral expression sequence reiterated during formation of each somite……..…...39
Figure 14. *Axin2* and *Lfng* transcription oscillate out of synchrony……...…....42
Figure 15. Model of the oscillator mechanism……...……...…..46
Figure 16. The determination front is proposed to be localized at the intersection between Mesogenin1/Mespo and Mesp2/Meso2 expression……...……49
Figure 17. Model for segment formation in chicken embryo……..……51
Figure 18. Schematic representation of the regulatory mechanism underlying the clock system and of the implications of Mesp2 function in establishing the segmental boundary……...……53
Figure 19. Factors that influence reptile embryo development inside the egg…..…..57
Figure 20. Corn snake (*Pantherophis guttatus)* clutch of eggs, half a day after oviposition……...….61
Figure 21. Corn snake (*Pantherophis guttatus)* varieties……...…...…..62
Figure 22. Determination front regression speed in the PSM of four species…….....68
Figure 23. Cloning strategy for corn snake *Hes1* sequence…….....75
Figure 24. *Hes1* expression pattern in 230-somite corn snake tails…….…...76
Figure 25. Comparison on a tree of the corn snake amino acid sequence for Hes1 with chicken and mouse hairy and enhancer of split sequences……..……....78

Figure26. *Nrarp* and *Delta1* expression patterns in 230-somite corn snake tails……..…....78
Figure 27. *Lfng* expression pattern in a 3 day-old house snake embryo……..…80
Figure 28. *In vitro* culture of 3-day-old house snake tails……...…....….80
Figure 29. Picture of *Aspidoscelis uniparens* lizard……..…...……..81
Figure 30. *A. uniparens* lizard's clutch of eggs……..…….81
Figure 31. Normal developmental stages of the *A. uniparens* lizard up to mid-development post-oviposition…….....…84
Figure 32. In situ hybridization in whole-mount *Aspidoscelis uniparens* embryos....84
Figure 33. Different body forms in the lizard *Tetradactylus.*……..….89
Figure 34. Sagittal section through a corn snake tail…….…….…….93

Table 1. Name and references for cyclic genes discovered in vertebrates thus far.....40
Table 2. Sequences and melting temperatures (Tm) of the primers used for cloning corn snake's and/or lizard's genes….……..…...100
Table 3. Linearization and transcription enzymes used for the corn snake and whiptail lizard *in situ* probes……...……..…...101
Table 4. Comparison of the gene sequences cloned in corn snake and whiptail lizard with other vertebrate species……..……103

ABBREVIATIONS

AP: Antero-Posterior

bHLH: basic Helix Loop Helix

BMP: Bone Morphogenetic Protein

CS: Chicken Serum

Cyp26: Cytochrome P450 26

Dll1: Delta-like 1

EphA4: Ephrin A4

FBS: Fetal Bovine Serum

FGF: Fibroblast Growth Factor

Hes: Hairy/enhancer of split

Her: Hairy/enhancer of split related

Lef1/Tcf1: Lymphoid enhancer factor 1/ T cell factor 1

Lfng: Lunatic fringe

Mesp2: Mesoderm posterior 2

MPC: Mesodermal Progenitor Cell

PAPC: Paraxial ProtoCadherin

PCR: Polymerase Chain Reaction

PSM: PreSomitic Mesoderm

RA: Retinoic acid

Raldh2: Retinaldehyde dehydrogenase 2

RCAS: Replication-Competent Avian Sarcoma-leukosis virus

RNA: RiboNucleic Acid

RT-PCR: Reverse Transcription PCR

T: Brachyury

Tbx6: T-box 6

TGFß: Transforming Growth Factor Beta

WNT: Wingless-related MMTV integration site

ABSTRACT

The vertebrate body plan is organized in a segmented fashion, best illustrated by the repetition of the vertebrae. The first signs of segmentation arise during early embryogenesis when somites bud off in a rhythmic fashion from the anterior part of the presomitic mesoderm (PSM). The periodic formation of somites is proposed to be controlled by a molecular oscillator–the segmentation clock–acting in the PSM. The signals of the segmentation clock are converted into the repetitive serie of somites by a traveling front of maturation–the determination front–formed by a molecular gradient regressing in concert with axis elongation. In order to gain insights in the mechanisms controlling somite number, I compared the regulation of somitogenesis in a new model species exhibiting a large number of somites–the corn snake– with mouse, chicken and zebrafish. I first cloned the genes involved in corn snake's somitogenesis and analyzed their expression patterns by *in situ* hybridization. The results showed that the genes associated with the determination front had conserved expression patterns. Unexpectedly, *lunatic fringe*, a gene associated with the segmentation clock, exhibited several stripes of dynamic expression in the PSM. A comparative study based on a mathematical model suggested that this pattern reflected an accelerated pace of the clock relative to the axis growth rate. In conclusion, our studies propose that the relationship between clock and axis growth is an important factor explaining the difference in somite numbers between the corn snake and the other species.

INTRODUCTION

Segmentation is a widespread feature in the animal kingdom. It consists of the serial repetition of similar body structures. For example, the vertebrae, the digits and the rhombomeres formed during embryonic development in vertebrates, as well as the segments that form the cuticle and legs of arthropods are a form of segmentation. However, true segmentation, or metamery, refers specifically to segmentation along the antero-posterior (AP) axis of the body (Tautz, 2004). Its main role is to allow flexibility of the axial skeleton. Three major phyla share this characteristic: the annelids, the arthropods and the chordates (amphioxus and vertebrates).

I) Evolution of segmentation

Two main mechanisms of segmentation of the body axis have been described. The first one consists of the simultaneous formation of segments in a syncitium. This form of segmentation is particular to the long-germ insects, and has been extensively studied in the fruit fly *Drosophila melanogaster* (arthropod). It relies on a cascade of gene activation that in a step-by-step fashion, subdivides the embryo into smaller units, eventually resulting in the repetition of the segments patterning the AP axis (Ingham and Martinez Arias, 1992; St Johnston and Nusslein-Volhard, 1992). In short, a class of maternal genes expressed as AP gradients activates the expression of a class of zygotic genes called the gap genes. These genes are expressed as one or two broad overlapping domains along the AP axis of the syncitium, and in turn, activate the expression of the pair-rule genes. Pair-rule genes are the first to reveal a segmented pattern consisting of seven non-overlapping bands. Finally, these genes activate the expression of the segment-polarity genes as 14 bands that will simultaneously define the boundaries between the parasegments of *Drosophila* (Figure 1A). This mode of segmentation has long been considered as the reference in arthropods. However, recent studies involving other arthropods, such as the short-germ insects, the myriapods and the chelicerates (all referred to as "short-germ arthropods") show that this mechanism has more likely evolved from a more primitive mode of segmentation (reviewed in (Damen, 2007; Peel, 2004; Tautz, 2004)). This second mode of segmentation consists of the sequential addition of segments along the AP axis of the body, from a posterior growing tissue usually called the "growth zone." It is much more widespread and is shared by short-germ arthropods, annelids and chordates (Figure 1B). The main question is now whether this mode of

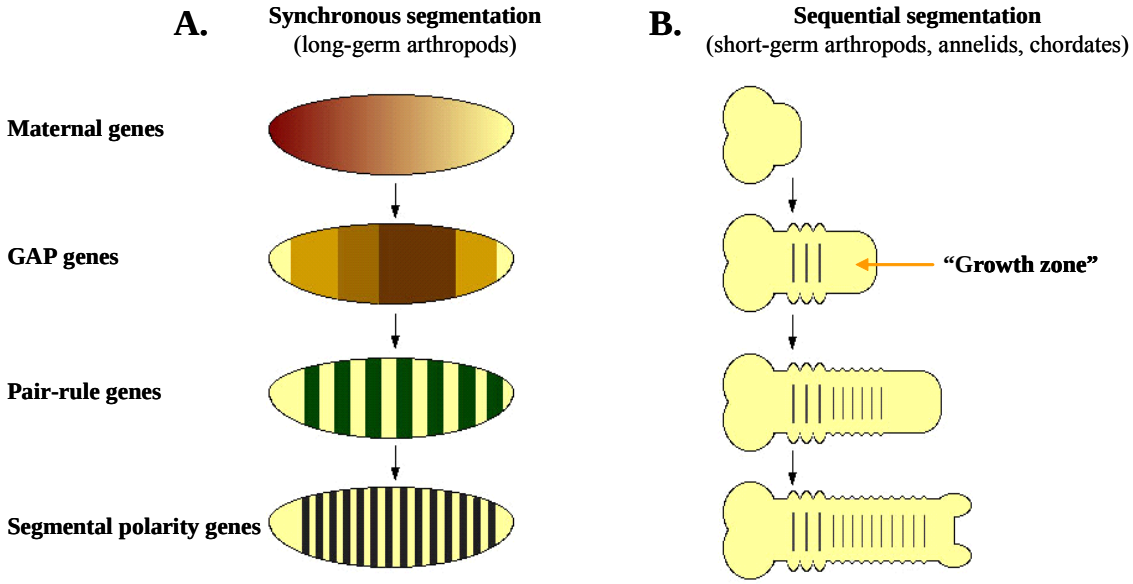

Figure 1. Two modes of segmentation: Synchronous and sequential.

A: Schematic representation of the synchronous or "parallel" mode of segmentation (based on *Drosophila melanogaster* example)

B: Schematic representation of the sequential or "serial" mode of segmentation (based on *Schistocerca gregaria* example)

Adapted from (Jaeger and Goodwin, 2002).

segmentation appeared independently in these three phyla, or if segmented common ancestors exist (Balavoine and Adoutte, 2003; Davis and Patel, 1999; De Robertis, 1997; Peel and Akam, 2003). At first glance, the existence of segmented ancestors seems unlikely. First, it would be against the principle of parsimony as it would imply the loss of the segmented character in many phyla (Jenner, 2000). Second, from a morphological point of view, these three phyla appear to segment in different ways. In arthropods and vertebrates, the growth zone generates the posterior unsegmented tissue by a seemingly diffuse cell proliferation, whereas in some annelids, the growth zone consists of stereotypical and asymmetrical divisions of large posterior teloblastic stem cells that generate separated rows of segmental founder cells. These cells divide further to generate the segments. This mode of segmentation will be referred to as "teloblastic row" (as in (de Rosa et al., 2005)). Third, the germ layers that are primarily segmented in these phyla are different. Arthropods primarily segment the ectoderm and form an exoskeleton, whereas vertebrates rather segment the mesoderm and form an endoskeleton, while annelids segment both (Tautz, 2004).

In light of these observations, it seems difficult to envision the existence of segmented common ancestors. However, some recent phylogenetic, morphological and molecular studies reveal striking similarities between the segmentation in the three phyla and have opened a burning debate on the question of the common ancestors. First, some phylogenetic studies show that loss of the segmented character is possible (Bleidorn et al., 2003; Delsuc et al., 2006; Gee, 2006; Hessling and Westheide, 2002). For example, a group of non-segmented animals, the Echiura, have changed position in the phylogenetic tree to become an ingroup of the annelids, implying that they must have lost their segmentation compared to the other annelids (Bleidorn et al., 2003; Hessling and Westheide, 2002). Second, regardless of the sequential or synchronous manner of segmentation and of the phylum, it has been observed that the first anterior segments always form faster than the rest of the segments of the body (Damen, 2007; Prud'homme et al., 2003; Tautz, 2004). This rather supports the idea of an inherited common mechanism of segmentation, which would have subsequently diverged to generate what is observed today in the three phyla. These studies emphasize the fact that organisms currently analyzed are modern and can present a derived mode of segmentation (best illustrated in *Drosophila melanogaster*) which can be misleading when looking for ancestral mechanisms of segmentation. For example, it has been shown that some crustaceans had derived the

"teloblastic row" mode of segmentation in arthropods. However, these species are not representative of ancestral taxa and therefore, likely developed this process secondarily ((Scholtz, 2002) reviewed in Tautz, 2004). Hence, the "teloblastic row" mode of segmentation is questioned in annelids. Only the leech (the most studied model in the annelid group) segments in this manner and it remains unclear whether other annelids would segment in this way (de Rosa et al., 2005). Finally, molecular studies show some striking and unexpected conserved genetic mechanisms. *Wnt/Wg* and *caudal* genes, known to be involved in vertebrate posterior axis elongation, have been observed at the posterior end of the growth zone of various short-germ arthropods, annelids and the cephalochordate amphioxus (albeit only the *caudal* gene in annelids - de Rosa et al. 2005, and *Wnt* genes in amphioxus (Schubert et al., 2000; Schubert et al., 2001)) (reviewed in Damen, 2007). Thus far, no functional studies have been performed in arthropods, annelids and amphioxus, however, this expression serves as an argument in favor of a common mechanism of the growth zone extension to the three phyla. On the other hand, the specification of the segmental boundaries was shown to be controlled by the segment polarity genes in all arthropods and in the annelid *Platyneiris durilii*, suggesting an ancestral mechanism for boundary specification among protostomes and rising the possibility that the protostome common ancestor (Urprotostomia) was segmented (Damen, 2007; Prud'homme et al., 2003). In amphioxus, the segment polarity gene *Engrailed* is also expressed at the segments borders (Holland et al., 1997), suggesting an ancestral mechanism to the three phyla. However, vertebrates do not employ segment polarity genes to specify their segment boundaries. Finally, the most striking example comes from the discovery of the Notch pathway replacing the gap genes for the regulation of the pair-rule genes in the spider, a basally branched arthropod (Schoppmeier and Damen, 2005; Stollewerk et al., 2003). This pathway is also used in vertebrate segmentation and regulates the dynamic expression in the growth zone of genes involved in segment specification, including some pair-rule genes (Henry et al., 2002; Holley et al., 2000; Jouve et al., 2000; Palmeirim et al., 1997; Shankaran et al., 2007; Sieger et al., 2004). The recruitment of the Notch pathway at the beginning of this process is a unique characteristic in both phyla, as the Notch pathway is usually required in the last steps of other processes (Irvine and Rauskolb, 2001; Rauskolb and Irvine, 1999). Moreover, the pair-rule genes in chelicerates and myriapods behave in a dynamic manner in the growth zone, which could resemble vertebrate cyclic genes. The study

of the mechanisms driving this dynamic in the short-germ insect *Tribolium* shows that it involves negative feedback loops very reminiscent of the vertebrate's (Choe et al., 2006). Further investigations in annelids and amphioxus are necessary to determine the involvement of the Notch pathway in segmentation.

In conclusion, current findings are still too sparse to definitively prove the existence of a segmented common ancestor among the three phyla. However, the last molecular studies show increasing similarities between their segmentation mechanisms. The study of more basally branched organisms in each phylum will certainly provide more information to answer this question.

The vertebrate phylum regroups fish, amphibians and amniotes (mammals, birds and reptiles) (Figure 2). Segmentation in this group has been essentially studied in fish (zebrafish and medaka), mammals (mouse), birds (chicken) and to a lesser extent in amphibians (*Xenopus laevis*), but never in reptiles. In this thesis, I will summarize what is known about vertebrate segmentation before introducing the first segmentation study in a reptile exhibiting a high number of vertebrae–the corn snake *Pantherophis guttatus*.

II) Segmentation in the vertebrates

Segmentation in vertebrates is best illustrated by the repetition of the vertebrae and ribs along the vertebral column, by their associated skeletal muscles and blood vessels, and the segmentation of the peripheral nervous system. The number of segments is highly constrained in any given species but varies tremendously among the different vertebrate species. It can range from as few as nine vertebrae in frogs, to up to several hundred in some snakes and fish (Richardson et al., 1998). Vertebrae are not identical along the vertebral column. For example, up to five different types of vertebrae, always found in the same order along the AP axis, are known in mammals. From anterior to posterior these are: the cervical, the thoracic (bearing ribs), the lumbar, the sacral (fused) and the caudal vertebrae. This vertebrae formula can change as some species (for example, humans) do not have a tail. It can also be complicated in birds by the fusion of multiple vertebrae into the 'synsacrum,' a characteristic unique to birds. In snakes, another type of vertebra with a distinct morphology is called "cloacal" and replaces the lumbar and sacral vertebrae (Polly et al., 2001). In

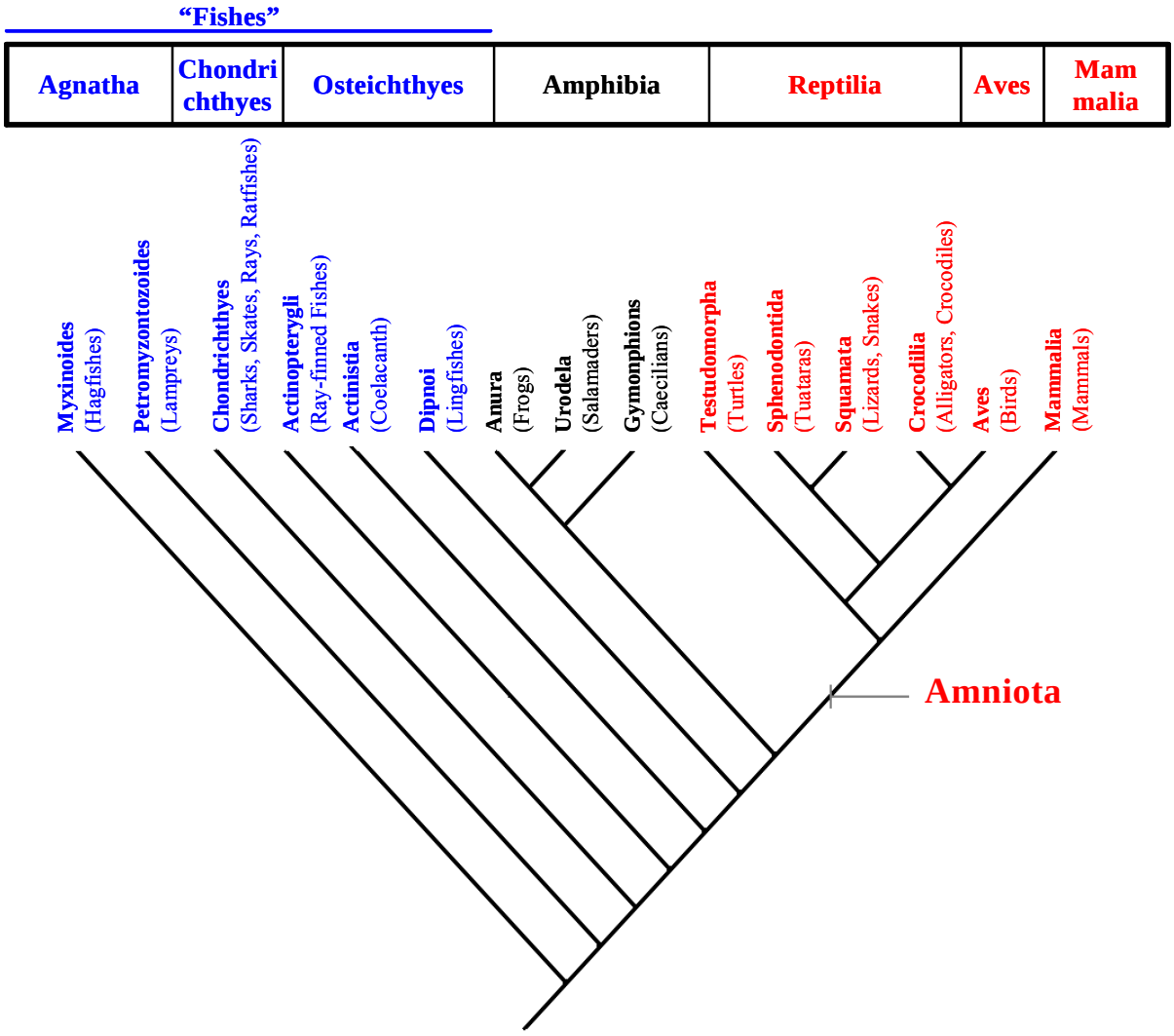

Figure 2. Phylogeny of the vertebrates.

After Steven M. Carr

(http://www.mun.ca/biology/scarr/Vertebrate_Classifications.htm)

fish, where the axial skeleton is rather uniform, a distinction is made between pre- and post-anal vertebrae, as well as the two first vertebrae which do not bear ribs (Bird and Mabee, 2003; Ward and Brainerd, 2007). Here again, the number among these different types of vertebrae varies considerably between species (Figure 3).

As we will see below, this diversity is generated during early embryogenesis. Segmentation occurs in a complex context of cellular movements involved in axis elongation. The formation of the segments and the control of their number are associated with a mechanism controlling their identity.

1) The segments are formed through a process called somitogenesis

1-1) Formation of the somites

The first signs of segmentation appear during early embryogenesis, by the process of somitogenesis, which drives the formation of transient embryonic segments called the somites. The somites are epithelial spheres of cells that are the precursors of the vertebrae, the ribs, the skeletal muscles of the body wall and limbs, and the dermis of the back (Brent and Tabin, 2002). They form soon after the beginning of gastrulation, on both sides of the neural tube from a tissue called the presomitic mesoderm (PSM) (Figure 4). The PSM is part of the paraxial mesoderm and is generated caudally during the process of gastrulation by ingression of cells through the primitive streak (in chicken and mouse)–or the blastopore (in *Xenopus laevis*) or blastoderm margin (in zebrafish),–and later, through the tail bud, a posterior condensation of cells that replaces the streak/blastopore and carry on the posterior elongation of the embryo (Catala et al., 1995; Goldman et al., 2000; Gont et al., 1993; Psychoyos and Stern, 1996; Schier and Talbot, 2005).

Somitogenesis is a highly dynamic process. The somites bud off at the anterior tip of the PSM in a rhythmic fashion, the period of which depends on the species (for example, every 30 minutes in zebrafish, 90 minutes in chicken, and 120 minutes in mouse at the standard temperatures of development). The formation of somites occurs symmetrically as a pair, and forms in a strict anterior-to-posterior fashion (reviewed in (Dubrulle and Pourquie, 2004a)). Concomitantly, the gastrulation process constantly provides cells at the posterior tip of the PSM, thus preventing its exhaustion by the segmentation process. The speed of both of these processes is regulated in a way that allows somitogenesis to continue until the species-specific

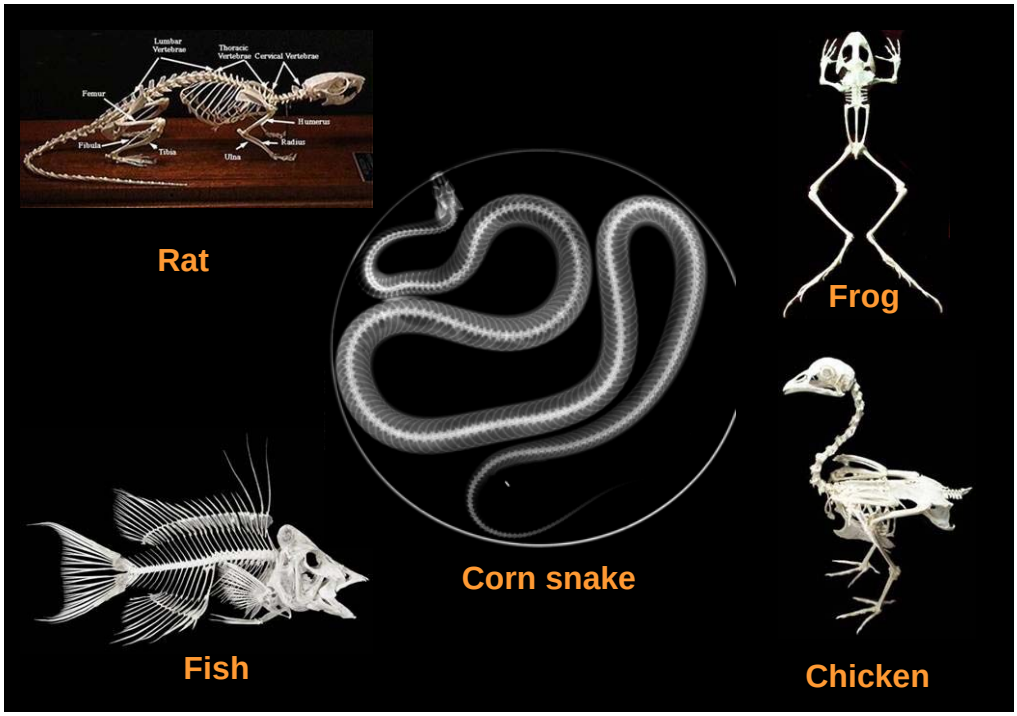

Figure 3. Different forms of skeletons amog the vertebrates.
Vertebrate axial skeletons display a segmented pattern. The number of segments (or vertebrae) can vary considerably from one species to another.

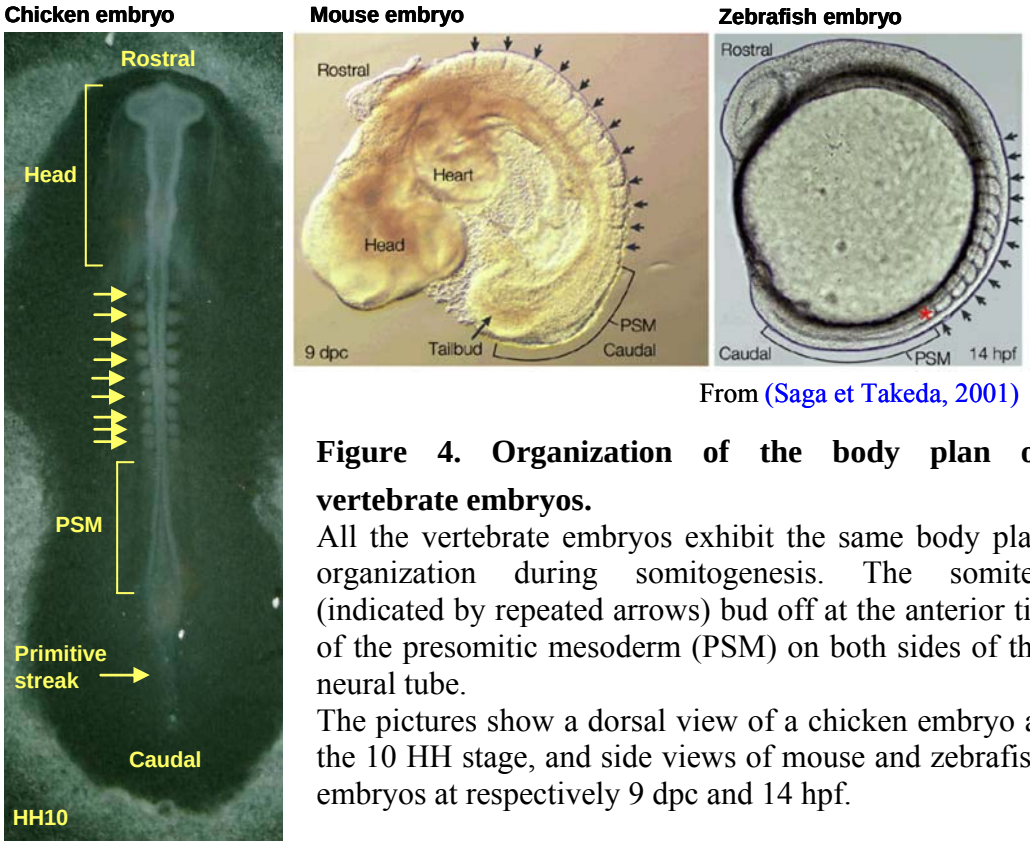

From (Saga et Takeda, 2001)

Figure 4. Organization of the body plan of vertebrate embryos.
All the vertebrate embryos exhibit the same body plan organization during somitogenesis. The somites (indicated by repeated arrows) bud off at the anterior tip of the presomitic mesoderm (PSM) on both sides of the neural tube.
The pictures show a dorsal view of a chicken embryo at the 10 HH stage, and side views of mouse and zebrafish embryos at respectively 9 dpc and 14 hpf.

total number of somites has been reached (31 in zebrafish, 65 in mouse and up to several hundred in some snakes).

1-2) Nomenclature of the somites

The sequential mode of development of the vertebrate embryo creates a gradient of differentiation along the AP axis. The newly formed posterior structures are less differentiated than the older anterior ones. In order to identify somites along different levels of the AP axis, a dynamic nomenclature has been adopted (Pourquie and Tam, 2001). The most recently formed somite is always called S1. Somites anterior to S1 are numbered increasingly until the anterior-most somite. In the PSM, the forming somite just posterior to S1 is called S0. The presumptive somites (of approximately the size of S1) are then marked with increasing negative Roman numbers (Figure 5). In this manner, a specific number always refers to a given state of differentiation along the AP axis.

1-3) Differentiation of somites

The newly formed amniote somite (at least in mouse and chicken) consists of an epithelial wall of cells surrounding a cavity containing mesenchymal cells called the somitoecele (Figure 6c and 7A). At the level of the somite S4 in chicken, the ventral cells undergo an epithelial-to-mesenchyme transition driven by signals emanating from the notochord and the neural tube floor plate (mostly Sonic hedgehog), to form a compartment called the sclerotome (Figure 6d) (Dietrich et al., 1997; Dockter and Ordahl, 1998; Fan and Tessier-Lavigne, 1994; Pourquie et al., 1993). The sclerotome will give rise to the vertebrae and ribs in conjunction with the somitocoele cells that will form the joints between the vertebrae (intervertebral discs and synovial joints) and the proximal part of the ribs (reviewed in Christ, Huang et al. 2007)(Christ et al., 2007). Somitocoele cells were designated for this reason as "arthrotome" (Mittapalli et al., 2005). The dermomyotome is the dorsal compartment of the somite that remains epithelial while the sclerotome is formed (Figure 6d). It differentiates along its mediolateral axis through signals from the lateral plate (BMP4) (Pourquie et al., 1995; Pourquie et al., 1996), the ectoderm and the dorsal neural tube (Wnts) (Fan et al., 1997; Fan and Tessier-Lavigne, 1994; Marcelle et al., 1997).

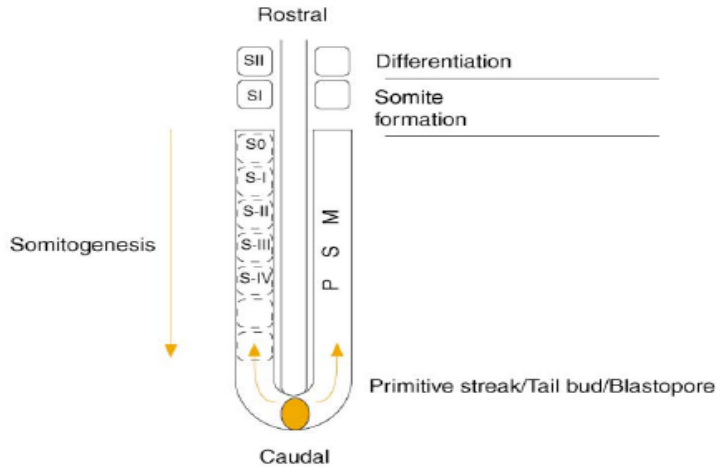

Figure 5. Nomenclature of the somites

(After Pourquié and Tam, 2001)

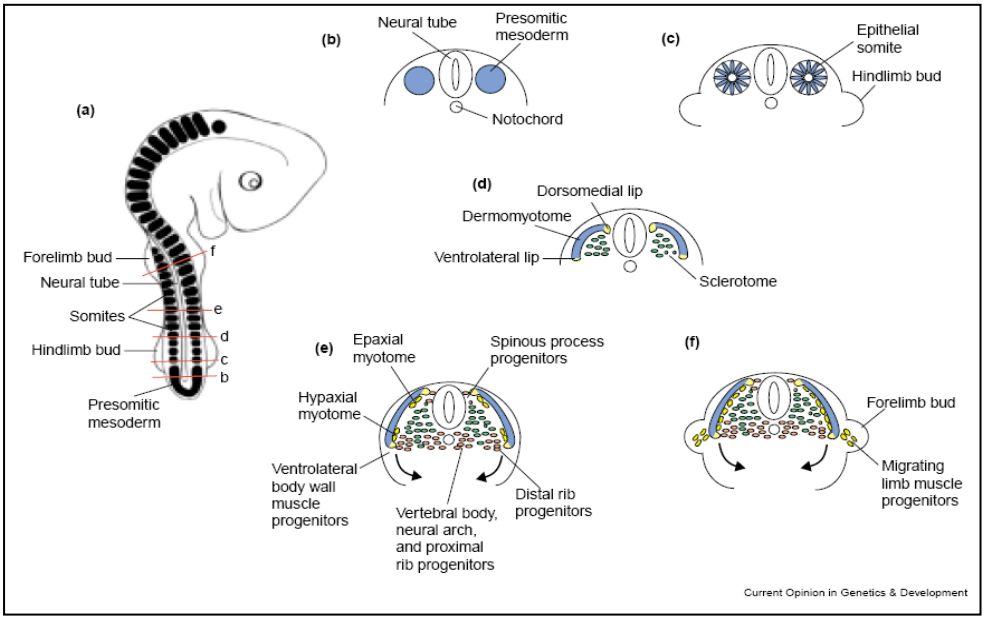

Figure 6. Overview of somite formation and compartmentalization in chicken embryo.

(a) 3-day (28 somites) chicken embryo.

(b-f) Cross-sections through the embryo at the indicated level.

The somite compartments are indicated on the scheme.

By (Brent and Tabin, 2002).

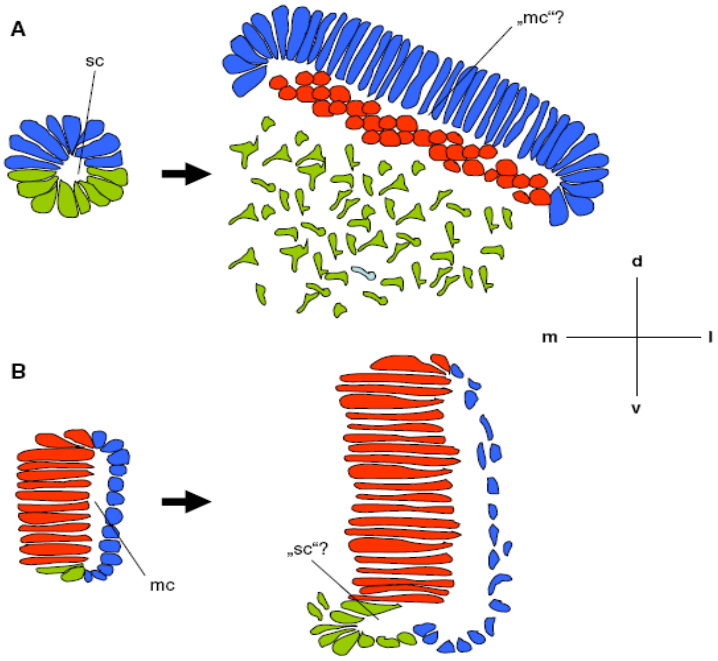

Figure 7. Schematic representation of an amniote (A) and anamniote (B) somite. On the left; an early stage of somite development, showing the epithelial somite prior to overt morphological compartmentalization. On the right; a mature somite showing distinct somite compartments. In red; myotomal cells. In blue;dermomyotomal precursor cells or dermomyotomal cells, respectively. In green; sclerotomal precursor cells or sclerotomal cells, respectively. sc the amniote somitocoel, mc the anamniote myocoel.
By (Scaal, 2006).

Dermomyotome cells ingress first in the somite to form a third compartment called the myotome (Figure 6e) (Kalcheim et al., 1999; Ordahl et al., 2000). The medial part of the myotome will generate the muscles of the back, whereas the lateral part will contribute to the abdominal musculature (Figure 6f) (Ordahl and Le Douarin, 1992). At the level of the limb buds, cells from the lateral edge of the dermomyotome delaminate and migrate into the lateral plate mesoderm to differentiate into the muscles of the limbs (Ordahl and Le Douarin, 1992). On the other hand, cells from the central dermomyotome (sometimes called dermatome) de-epithelialize to form the dermis of the back (Brent and Tabin, 2002). Finally, the myotome induces a last somite compartment from the dorsolateral edge of the sclerotome, called the syndetome (Brent et al., 2003). This compartment does not shows morphological distinction within the sclerotome and is only evidenced by the expression of the scleraxis marker. It specifically generates the tendons that attach the muscles to the vertebrae.

Differentiation of the somites in non-amniotes embryos (e.g. zebrafish and *Xenopus laevis*) has been much less studied, but shows some important differences (Figure 7) (Scaal and Wiegreffe, 2006). The myotome is the first compartment to form and represents more than 80% of the somite (Figure 7B). Thus, it has been hypothesized that the ancestral role of somites was essentially to form the body musculature (Christ et al., 2007). The dermomyotome is a thin epithelial layer of cells separated medially from the myotome by a cavity called the myocoele (and containing no cells). The sclerotome represents a very small population of ventro-medial cells with an epithelial bud that makes a protrusion toward the notochord (Figure 7B). Neither syndetome nor arthrotome have been described. Even if hedgehog secreted by the notochord has been involved in the myotome's differentiation of zebrafish and *Xenopus laevis* (Grimaldi et al., 2004; Stickney et al., 2000), the signals inducing the somite compartments remain to be further clarified.

1-4) Resegmentation

Formation of the vertebrae occurs very late during embryonic development. A fissure called von Ebner's fissure first separates the anterior and posterior halves of the sclerotomes (Von Ebner, 1888). Then, during the process called "resegmentation," the posterior half of a sclerotome fuses with the anterior half of the following

sclerotome, forming the future vertebra (Figure 8) (Bagnall et al., 1988; Christ et al., 2000; Goldstein and Kalcheim, 1992). This process does not occur in the myotomes and syndetomes, thus allowing the attachment of the muscles to two consecutive vertebrae. Thus, resegmentation is a crucial process in the flexibility of the vertebral column, and is conserved among many animal species, including arthropods (Lawrence, 1992). In zebrafish, this process is described as leaky, since cells from different sclerotome halves participate in the formation of different vertebrae (Morin-Kensicki et al., 2002).

1-5) Regionalisation

As mentioned earlier, the vertebrate body is partitioned in domains exhibiting different identities (e.g., cervical, thoracic, lombar, sacral and caudal vertebrae). The acquisition of these identities is controlled by a class of genes called *Hox* genes (Iimura and Pourquie, 2007; Krumlauf, 1994; McGinnis et al., 1984). These genes are organized into clusters in the genome. The position of the genes along a cluster reflects the order in which each gene will be expressed in time and space along the AP axis of the embryo (Figure 9) (Gaunt et al., 1988; Graham et al., 1989; Kessel and Gruss, 1991). This mechanism results in a collinear or nested expression of these genes along the AP axis, defining a code or a combination in each somite, responsible for the somite identity. Gain and loss of function experiments of *Hox* genes in mouse (and *Drosophila melanogaster*) showed nevertheless that the more posterior *Hox* gene expressed in this combination was primarily responsible for the somite identity. This gave rise to the notion of posterior prevalence (Duboule and Morata, 1994).

The anterior limit of *Hox* gene expression corresponds to limits between the future regions of the vertebral column (Burke et al., 1995). A shift in *Hox* gene expression can therefore change the number of somites harboring a given identity, and hence, change the vertebral formula (Cohn and Tickle, 1999; Economides et al., 2003; Krumlauf, 1994; Wellik and Capecchi, 2003). However, mutations in *Hox* genes have never been shown to affect the total number of somites.

Different studies have tried to relate somitogenesis and collinear activation of *Hox* genes (Cordes et al., 2004; Dubrulle et al., 2001; Iimura and Pourquie, 2006; Zakany et al., 2001). However, these mechanisms remain poorly understood.

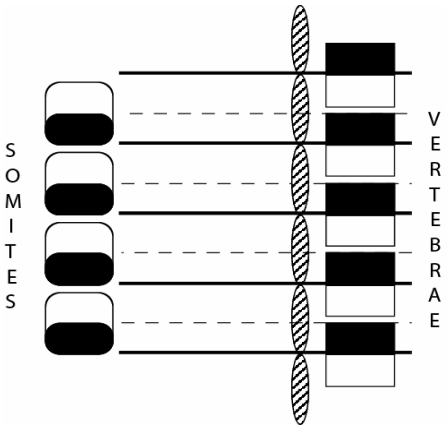

Figure 8. Resegmentation

Scheme showing the relation between embryonic (somites) and adult (vertebrae) segmentation, highlighting the resegmentation process.

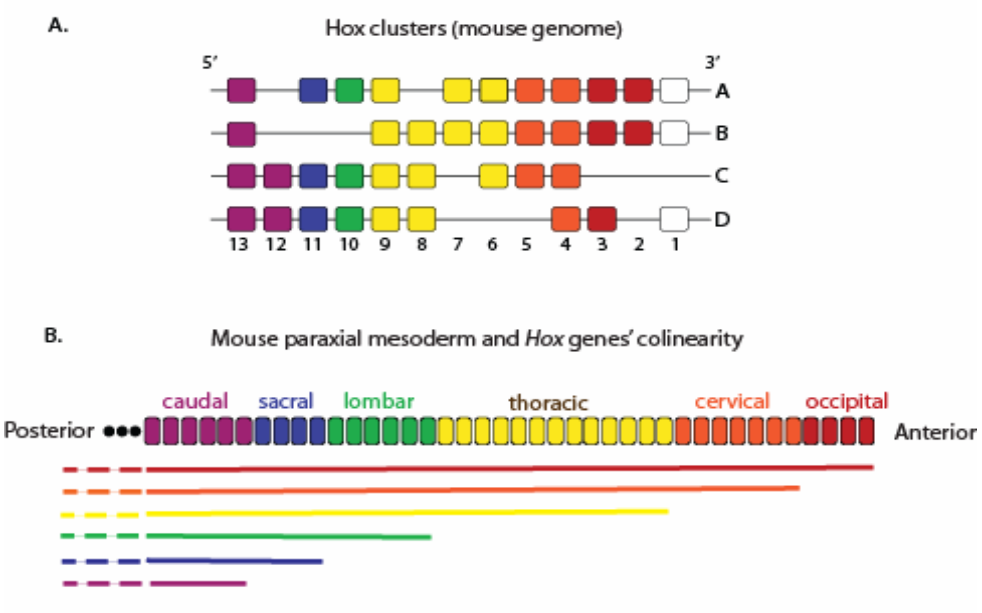

Figure 9. *Hox* genes organization and colinearity

A. Hox genes are organized into clusters in the vertebrate genomes (example of the 4 mouse clusters Hox A, B, C and D). Genes are represented by colored boxes. Horizontal lines represent chromosoms. Inter- and intragenic distances are not respected. B. Schematic representation of colinear hox gene expression (colored lines) in mouse paraxial mesoderm. Somites are represented by small colored boxes. The color in these boxes correspond to the prevalent *Hox* gene of the combination, specifying somite identity (written above using the same color). The three black dots indicate that all caudal somites are not represented. The same color code is used between A. and B. Note that the position of hox genes along the clusters reflects their position along the embryonic AP-axis.

2) Regulation of somitogenesis and control of somite number

2-1) Genesis of the paraxial mesoderm and axis elongation

Cell fate specification and cell movement are partly controlled by organizer centers located in the Hensen's node in chicken, the anterior-most primitive streak at early and mid-gastrula stages and node in mouse, the dorsal lip of the blastopore in *Xenopus laevis* and the shield in zebrafish. These organizers are maintained throughout gastrulation and have the ability to induce the formation of a secondary axis from a host tissue when grafted ectopically (Hara, 1978; Robb and Tam, 2004; Saude et al., 2000; Spemann and H., 1924). Their inductive properties change with time, so that at the early gastrula stage in newts, for example, ectopic transplantation of the dorsal blastopore lip in a host induces formation of a secondary axis mostly containing head tissue, whereas the dorsal blastopore lip of late gastrula stage embryos induces a secondary axis lacking a head but exhibiting trunk tissue (Spemann, 1931). Two contradictory views concerning the development of the posterior embryo from the tail bud–a mesenchymal structure replacing the streak/blastopore/blastoderm margin at the level of the lumbo-sacral region–have been proposed. Holmdahl considered the tail bud to be a homogenous population of pluripotent cells corresponding to a blastema and generating the posterior body by a distinct mechanism from gastrulation (Holmdahl, 1925). In contrast, Pasteels considered the tail bud as discrete populations of cells, each exhibiting a different developmental potency, as a result of the continuity of gastrulation (Pasteels, 1937b). Holmdahl's view was first supported by studies that analyzed the potency of tail bud cells using the tail bud as a "whole" (Griffith et al., 1992; Schoenwolf, 1977; Schoenwolf et al., 1985), or by a more recent experiment in *Xenopus laevis*, showing that small groups of neighboring cells in the tail bud exhibit pluripotency (Davis and Kirschner, 2000). Later, Pasteels' view gained insights from experiments in *Xenopus laevis* and chicken (Catala et al., 1996; Catala et al., 1995; Gont et al., 1993) which demonstrated the presence of these discrete populations of cells in the tail bud. "Tail organizers" that induced "tails-like" structures when grafted ectopically, were discovered in several vertebrate species. These tails organizers corresponded to the chordoneural hinge and the tip of the tail in *Xenopus laevis* (Gont et al., 1993), the chordoneural hinge and ventral tail bud in the chicken (Knezevic et al., 1998; Liu et al., 2004) and the ventral marginal zone of zebrafish embryos (Agathon et al., 2003).

Cell lineage tracing experiments showed that the chordoneural hinge derived from the dorsal blastopore lip of late gastrula in *Xenopus laevis* (Gont et al., 1993) and Hensen's node in the chicken (Catala et al., 1995; Knezevic et al., 1998), arguing in favor of the continuity of gastrulation (Figure 10). Moreover, cells in the tail bud exhibited intercalation or ingression-like movements reminiscent of the cell movements observed during gastrulation in *Xenopus laevis*, chicken and zebrafish (Gont et al., 1993; Kanki and Ho, 1997; Knezevic et al., 1998). In mouse, it is still unclear whether a tail organizer really exists. However, lineage tracing experiments identifying a population of resident cells in the anterior streak at E8.5 and in the chordoneural hinge at the tail bud stage (Cambray and Wilson, 2002; Cambray and Wilson, 2007), as well as the discovery of the ventral ectodermal ridge (VER) in the tail bud, a structure that stops axis elongation when removed (Goldman et al., 2000), are indirect proof of the existence of such an organizer. Taken together, these studies argue that gastrulation is a continuous process between early and late development. It involves an organizer, which patterns the different structures of the embryo along the AP axis by changing its inductive properties with time.

It is interesting to note that in amniotes, the anterior-most streak contain stem cells that specifically generate the medial part of the PSM, whereas the lateral part is formed through the more posterior ingression of epiblastic material (Cambray and Wilson, 2002; Eloy-Trinquet and Nicolas, 2002; Iimura et al., 2007; Selleck and Stern, 1991). This population of stem cells is found back in the tail bud at the level of the chordoneural hinge (Cambray and Wilson, 2002; Cambray and Wilson, 2007). Similarly in non-amniotes, cells closer to the organizer ingress to generate the medial part of the paraxial mesoderm, whereas cells more lateral to the organizer will generate the lateral part of the paraxial mesoderm. However, the existence of stem cells needs to be clarified in this case (Iimura et al., 2007).

Molecules controlling cell movement and specification belong to the TGFß, Wnt and FGF pathways, as well as downstream targets from the T-box family (Figure 11). The activity of these pathways (particularly TGFß and Wnt) is modulated all along gastrulation by molecules secreted by the organizer.

First, mesodermal fate is induced in the ectoderm/epiblast of the different vertebrate species by Nodal (or Nodal related molecules, which are members of the TGFß family) and FGF pathways prior to gastrulation (reviewed in (Bottcher and Niehrs, 2005; Kimelman, 2006)). Paraxial mesodermal fate is then induced by

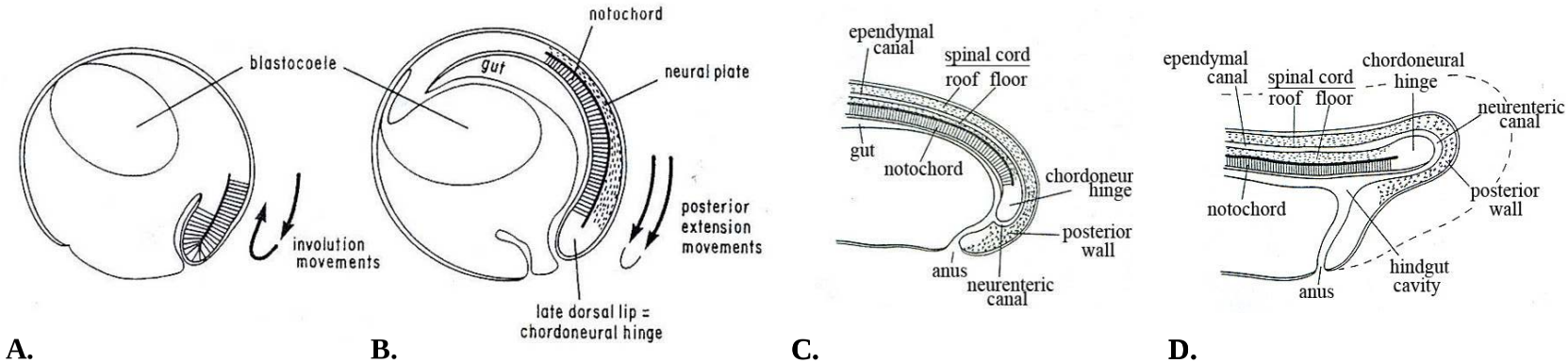

Figure 10. Gastrulation is a continous process in vertebrates.

A-B. *Xenopus laevis* embryos at mid- (A) and late- (B) gastrula stages (stages 11and 13 respectively). Side views.The late dorsal lip of the blastopore corresponds to what will be the chordoneural hinge in next stages. C-D. *Xenopus laevis* embryos at neurula and tail bud stages (stage 23 and 28 respectively). Side views. These fate mappings show the continuity of gastrulation during early embryonic development.

Adapted from (Gont et al., 1993).

patterning of the mesoderm during gastrulation. Nodal-related molecules could play a role in this process as well. They are expressed in gradients both along animal-vegetal and dorso-ventral axes in *Xenopus laevis* and zebrafish (Dougan et al., 2003; Faure et al., 2000; Gritsman et al., 2000; Schohl and Fagotto, 2002). It was shown that using Activin as a Nodal pathway activator on *Xenopus laevis* animal caps could induce different mesodermal type in a dose-dependent manner. Low activin levels induced ventral fates (e.g., pronephros) and high levels induced dorsal fates (e.g., notochord) (Green et al., 1992; McDowell and Gurdon, 1999). However, it is still unclear whether Nodal signaling gradients really play this role *in vivo*. Another member of the TGFß family, BMP, has been shown to pattern the mesoderm in interaction with molecules secreted by the organizer. BMP4 in mouse and chicken, and its antagonists Noggin and Chordin (expressed by the organizer) are expressed in a way that creates a gradient of BMP4 activity high in the lateral structures and low or null in axial structures and organizer (Miura et al., 2006; Tonegawa et al., 1997; Tonegawa and Takahashi, 1998). In this gradient, cells exposed to low BMP4 will generate axial structures (notochord), whereas cells exposed to gradually higher doses of BMP4 signal will generate gradually more lateral structures (paraxial mesoderm, intermediate mesoderm and lateral plate). In mouse, BMP4 has also been involved in mesoderm induction since the knock-out of *BMP4* results in the loss of the quasi-totality of the mesoderm (Winnier et al., 1995). Similarly in *Xenopus* laevis and zebrafish, a ventro-dorsal gradient of BMP is created by the antagonistic interaction of BMP produced by the ventral marginal zone mesoderm and the BMP antagonists produced by the organizer. In the same manner as in chicken and mouse, low doses of BMP drive anterior/dorsal fates, whereas high doses drive posterior/ventral fates (reviewed in (Dale and Jones, 1999; Kimelman and Griffin, 2000)).

As suggested above, Nodal is involved in specifying more anterior fates than BMP. For example, in zebrafish, Nodal has been found to specifically regulate the entrance of the mesodermal progenitor cells (MPC) in the PSM forming the trunk region, whereas the BMP pathway specifically controls the entrance of the MPC in the PSM at the trunk-tail transition and tail region (Szeto and Kimelman, 2006). This is in agreement with results from Agathon and colleagues showing that Nodal was necessary in specifying zebrafish trunk region, whereas, Nodal+BMP+WNT were necessary for the patterning of the tail region (Agathon et al., 2003). In mouse as well, a critical dose of Nodal signaling is required for normal anterior axis patterning,

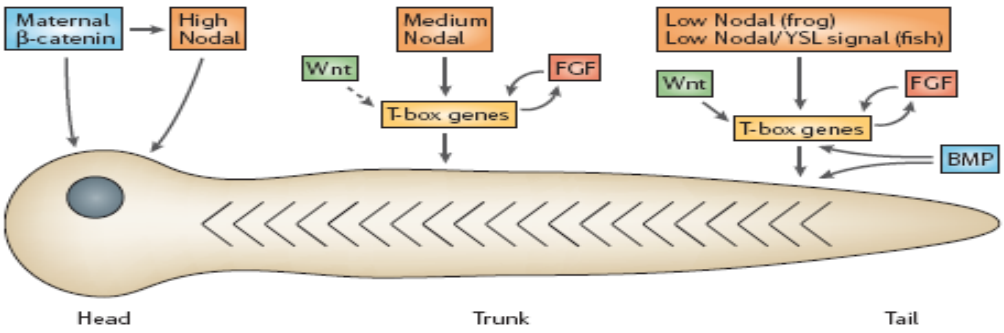

Figure 11. A model for patterning the embryonic body in *Xenopus* and zebrafish.

By (Kimelman, 2006).

whereas BMP4 is involved in the patterning of more lateral fates (Kanatsu and Nishikawa, 1996; Robb and Tam, 2004; Winnier et al., 1995).

Other pathways, such as Wnt and Fgf, also have a role in the formation and specification of paraxial mesodermal fate. A Wnt gradient is established "ventro-dorsally" in the marginal zone by antagonistic interaction between Wnt8 and its antagonists expressed in the organizer in *Xenopus laevis* and zebrafish. Wnt8 specifies ventral/posterior fates, like the BMP pathway (Hoppler and Moon, 1998; Lekven et al., 2001). Hence, the interactions between BMP, Wnt molecules and their antagonists expressed in the organizer are crucial for mesoderm patterning. The Wnt pathway has also been involved in the convergent-extension movements of the gastrulation in zebrafish and *Xenopus laevis* (Heisenberg et al., 2000; Tada and Smith, 2000). In mouse, null mutations for *Wnt3a* or its downstream effectors *Lef-1* and *Tcf-1* cause severe axis truncation immediately following the forelimb level. The paraxial mesoderm posterior to the forelimb is replaced by neural tissue (Galceran et al., 1999; Takada et al., 1994). Interestingly, mice bearing the *Wnt3a* hypomorphic mutation *vestigial tail* (*vt*) are truncated at the tail level, whereas mice bearing the *vt* allele and the *Wnt3a* knocked-out allele together exhibit an intermediate axis length, forming thoracic vertebrae and a variable number of lumbar vertebrae (Greco et al., 1996). These results show that *Wnt3a* is involved in the control of axis elongation in mouse. Similarly but to a lesser extent, null mutation of Wnt5a causes a reduction in size of all the embryo appendages (Yamaguchi et al., 1999a). The FGF pathway has been shown to control the movement of cells during gastrulation in chicken and mouse as well (Ciruna and Rossant, 2001; Sun et al., 1999; Yamaguchi et al., 1994; Yang et al., 2002). Its inhibition in *Xenopus laevis* or zebrafish causes axis truncation (Amaya et al., 1991; Griffin et al., 1995). Finally, both the Wnt and Fgf pathways have been shown to regulate the expression of the T-box genes *Brachyury/T/no tail* and *Tbx6* in vertebrates (Ciruna and Rossant, 2001; Hofmann et al., 2004; Lou et al., 2006; Yamaguchi et al., 1999b). In agreement with these observations, mutations in these mesoderm-specific T-box genes cause similar truncation phenotypes than do the mutations in the Fgf or Wnt pathways (Chapman and Papaioannou, 1998; Herrmann et al., 1990; Schulte-Merker et al., 1994; Wilson et al., 1995).

Together, these observations show that TGFß, Wnt and FGF pathways have overlapping functions in the regulation of axis elongation and mesoderm formation and specification. The patterning activity of these pathways is modulated by inhibitors

secreted by the organizer all along gastrulation. However, the precise mechanisms controlling the timing of axis elongation remain to be clarified.

2-2) PSM properties

The paraxial mesoderm gives rise to the head mesoderm before taking the name of presomitic mesoderm at the onset of somitogenesis. Several experiments have been designed to understand what signals regulate somitogenesis and what controls its sequentiality and directionality. Some of these experiments have consisted of isolating chicken or mouse PSM from one or more of their surrounding tissues *in ovo* (chicken) or *in vitro* (chicken and mouse), and observing how segmentation proceeds in the absence of these surrounding structures (Bellairs and Veini, 1980; Correia and Conlon, 2000; Packard and Jacobson, 1976; Palmeirim et al., 1998; Sosic et al., 1997). The results show that the PSM can segment normally in the absence of the neural tube, the notochord, the endoderm and the lateral plate. Only the ectoderm influences PSM segmentation both *in ovo* and *in vitro*, as epithelial somites do not form when it is absent. However, molecular segmentation is not inhibited in these explants, as stripes of *Delta1* (a marker of the posterior compartment of the epithelial somites) are formed at regular intervals of time and space at the anterior tip of the PSM in both chicken and mouse (Correia and Conlon, 2000; Palmeirim et al., 1998). This shows that the PSM is endowed with an intrinsic capacity to segment at the molecular level, and that somite epithelialization and subsequent formation of boundaries require a signal from the ectoderm.

Reversing the AP polarity of the PSM *in ovo* does not change the direction in which the PSM would have segmented if not operated (Christ et al., 1974; Menkes and Sandor, 1977). In other words, the inverted PSM segments caudo-rostrally in the embryo and accordingly forms somites with an inverted AP polarity compared to the embryonic axis. Removing the anterior half of the PSM or cutting it transversally into two pieces does not prevent segmentation of the posterior part of the PSM (Packard, 1978). In conclusion, these experiments show that no signal (within the PSM or in the surrounding structures) propagates in an anterior-to-posterior manner to drive the directional segmentation of the PSM.

The PSM is regionalized (Duband et al., 1987), with its caudal part being mesenchymal and its anterior part becoming gradually epithelial. The inversion of

small pieces of PSM (one somite in length) in the caudal part of the PSM does not have any effect on somite formation, whereas, the same inversion in the anterior third of the PSM (where it begins to epithelialize) reverses the AP polarity of the newly formed somites (Dubrulle et al., 2001). This shows that the PSM, already capable of segmenting autonomously, also acquires intrinsically a regionalization that controls the directionality and sequentiality of its segmentation.

2-3) End of somitogenesis

While the onset of somitogenesis has been examined at the molecular level (Jouve et al., 2002), the end of somitogenesis has not been as well studied. Sanders and colleagues noted that when somitogenesis was completed in the tails of chicken embryos the tails were not segmented to the tip (Sanders et al., 1986). In order to understand this, chicken tails were explanted before or after the end of somitogenesis to the chorio-allantoic membrane of 9-day host chicken embryos. The aim was to determine if extrinsic signals normally derived from the surrounding tissues of the embryonic tail bud were preventing the complete segmentation of the PSM. The results showed that explanted tails did not form more somites than they would have if the tails had not been explanted. In normal embryos, massive cell death occurs in the tail bud at the completion of somitogenesis (Sanders et al., 1986). The authors concluded that this cell death could account for the failure of the tip of the tails to segment, and proposed that apoptosis could be a contributing factor in preventing segmentation. Another approach consisted in analyzing the potency of cells from “old mouse tail buds” in which somitogenesis had recently ceased (E13.5), to participate to somite formation when grafted in the primitive streak of E8.5 embryos (Tam and Tan, 1992). The results showed that these cells still contributed to somite formation. Thus, it was concluded from these experiments that the arrest of somitogenesis is likely due to a change in the tissue surrounding the paraxial mesoderm in the tail bud rather than a loss of the cellular potency to continue somitogenesis.

Alternatively, earlier experiments aimed to understand the general control of somitogenesis and the regulation of total somite numbers (Cooke, 1975; Tam, 1981; Veini and Bellairs, 1983). This research consisted of reducing the size of embryos by removing part of their cells before gastrulation and observing how these embryos compensated for the loss of these cells. Would they form a shorter axis containing less

somites? Or, would they minimize all their structures to form a miniature embryo resembling a wild-type embryo? These experiments were performed in *Xenopus laevis*, chicken and mouse. All these embryos appeared to regulate their global size and form smaller wild-type looking embryos containing the "normal" number of somites. Cooke concluded from these experiments that formation of somites could not rely on a prepattern set up before the formation of the somites in the PSM, and proposed a theoretical model explaining how the somites could form under the control of a "clock" and a "travelling wavefront" in the PSM.

2-4) The Clock and Wavefront model

When Cooke performed the cell ablation experiment on *Xenopus* blastulae (Cooke, 1975), he was testing the validity of the hypothesis that prepatterns formed in the PSM could account for the repetition of the series of somites. These prepattern models were based on the Turing reaction-diffusion system (Turing, 1952) and were proposed to rely on physiochemical parameters (for example, involving diffusion and allosteric interaction constants for specific molecules) that determine the distance between the "peaks" in the prepattern and could therefore not be modified in the case of a reduction in size of the PSM. The hypothesis was that if prepatterns account for the formation of somites, reducing the size of the embryo by removing tissue would result in a reduction of the number of somites in proportion to the amount of tissue removed, provided that the amount of tissue removed is larger than one segment. The results showed that these embryos never exhibited a reduced number of somites, hence ruling out the prepattern hypothesis. This prompted Cooke, in collaboration with Zeeman, to propose a different concept explaining somite formation (Cooke and Zeeman, 1976). In this concept, a gradient formed in the PSM would give positional information to the cells. At a given value of this gradient, called the "wavefront," the cells would receive the information allowing them to form a somite. This wavefront (and gradient) would constantly be displaced posteriorly, in concert with axis elongation, and thus gradually instructing the cells to form somites. For this model to work, a periodic signal matching the time of the somites formation, or "clock" would interact with the wavefront to instruct the cells when to form a boundary. This clock was proposed to be an intracellular oscillator that synchronized PSM cells. The interaction between the clock and wavefront was described as follow: "*We conceive*

the oscillator as interacting with the wavefront by alternately promoting and then inhibiting its otherwise smooth passage down the body pattern. It could do this by affecting periodically either the onset of catastrophe in cells, or else those particular expressions of the rapid change which cause the new locomotory-adhesive behaviour." (Cook and Zeeman, 1976, p467). By "catastrophe," the authors meant a rapid change of state in the cell, like for example, suddenly changing adhesive properties to allow the periodic formation of the boundaries defining the somites. Therefore, while the clock maintains the cells of the PSM in an inhibitory state, a certain number of cells pass through the wavefront and become competent to execute the program to form a somite. They do not do so because of inhibition by the clock. When the clock switches to its permissive state, a catastrophe is induced in the cells passing the wavefront, hence allowing the cells to form a somite (Figure 12). This model gained a lot of insights thanks to molecular discoveries in the last decades.

Other theoretical models of somitogenesis exist and will not be discuss here. These include the "Cell cycle model" (Primmett et al., 1989; Primmett et al., 1988), the "Model of Meinhardt" (Meinhardt, 1986), and the "Clock and trail" (Kerszberg and Wolpert, 2000).

3) Molecular events during somitogenesis

3-1) The segmentation clock

3-1-1) Discovery of a cellular oscillator in the PSM

Twenty-one years after the publication of the "Clock and Wavefront" model, the first molecular evidence for a cellular oscillator or "clock" was provided in the chicken by the discovery of the periodic expression of *cHairy1*, a chicken homolog of the *Drosophila melanogaster* pair-rule *Hairy* gene, in the PSM (Palmeirim et al., 1997). Palmeirim and colleagues noticed that this gene had a dynamic expression pattern between different chicken embryos when analyzed by *in situ* hybridization at the same stage. An ingenious culture system, using the principle that somitogenesis is a synchronous process between left and right sides, allowed them to reorder these different patterns. It consisted of culturing the left and right sides of a bissected embryo during different times, and checking how the dynamics of the pattern had changed between the left and right PSM within this timeframe. This allowed the reconstitution of the *cHairy1* pattern as a wave of mRNA, sweeping across the PSM,

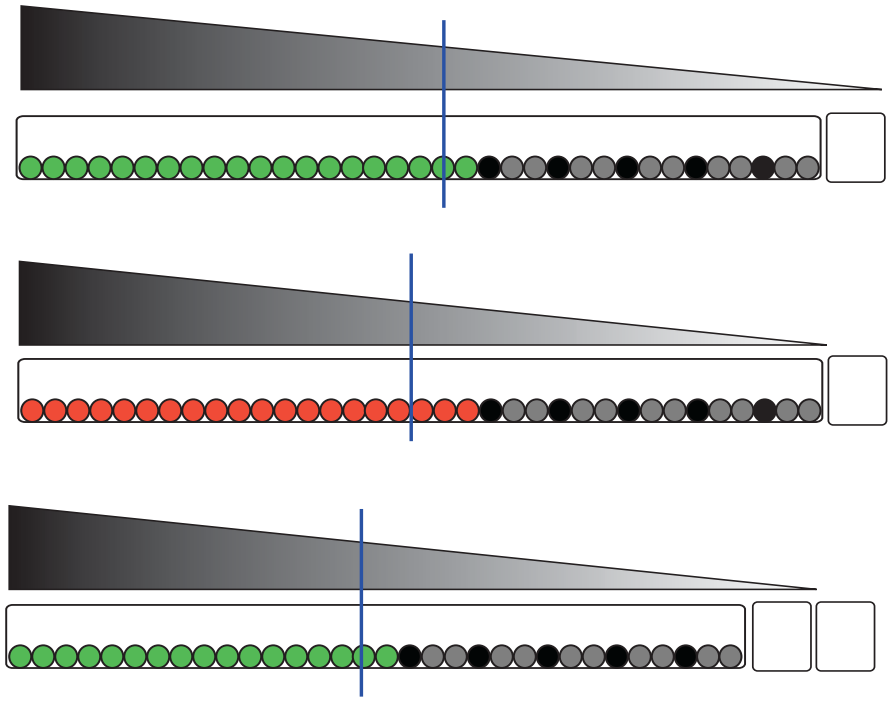

Figure12. “Clock and Wavefront” model

In this model, the PSM cells oscillate under the influence of a clock (iluustrated by the switch green-red-green). Simultaneously, a “wavefront” (blue line) moves slowly down the AP axis of the embryo. The cells that are in a permissive state (in red) when they meet the wavefront become competent to form a boundary (in black).

starting at its posterior end and stopping at its anterior end, within the time of one somite formation (Figure 13). This wave is re-initiated at the posterior tip of the PSM each time a somite forms, thus matching the time of somite formation as predicted in the Clock and Wavefront model. Labeling experiments show that this mRNA wave does not result from cell displacement, but from a very synchronous way the cells upregulate and downregulate the expression of the gene to allow propagation of the wave (Jiang et al., 2000), as predicted again by the Clock and Wavefront model. This characteristic is intrinsic to the PSM, as removing surrounding tissues does not prevent the propagation of the wave (Palmeirim et al., 1997). To describe the embryos more easily, the "cyclic" pattern of *cHairy1* has been divided into three phases. During phase I, *cHairy1* is expressed in a broad domain in the caudal PSM. During phase II, the domain of expression shifts toward the middle of the PSM, and during phase III, it becomes a narrow band close to S0. The duration of these phases was shown to be different. Phase I lasts 20-25 % of the cycle, whereas phase II and III last 75-80 % (Maroto et al., 2005). The slowing down of the wave propagation in the anterior PSM explains the timing of these phases (Giudicelli et al., 2007; Morimoto et al., 2005). This periodic expression pattern has definitively been proven later in mouse by real-time imaging (Masamizu et al., 2006).

The discovery of the periodic expression of *cHairy1* in the PSM matching the time of somite formation provided the first molecular evidence for the existence of a cellular oscillator linked to somitogenesis. For this reason, *cHairy1* was called a "cyclic gene," and the mechanism underlying its expression was called the "segmentation clock."

3-1-2) Comparison between species

Additional cyclic genes have been discovered in chicken and other species since then (see Table 1). The majority belong to the Notch pathway: *Hairy2, Hey2, Lfng* in chicken (Aulehla and Johnson, 1999; Jouve et al., 2000; Leimeister et al., 2000; McGrew et al., 1998), *Hes1, Hes7, Hey2, Lfng, Delta1* in mouse (Bessho et al., 2001; Forsberg et al., 1998; Jouve et al., 2000; Leimeister et al., 2000; Maruhashi et al., 2005), *her1, her7, her11, her12, her15, deltaC* in zebrafish (Henry et al., 2002; Holley et al., 2000; Jiang et al., 2000; Shankaran et al., 2007; Sieger et al., 2004), *her1/11, her5, her7* in medaka (Gajewski et al., 2006) and *esr9* and *esr10* in *Xenopus*

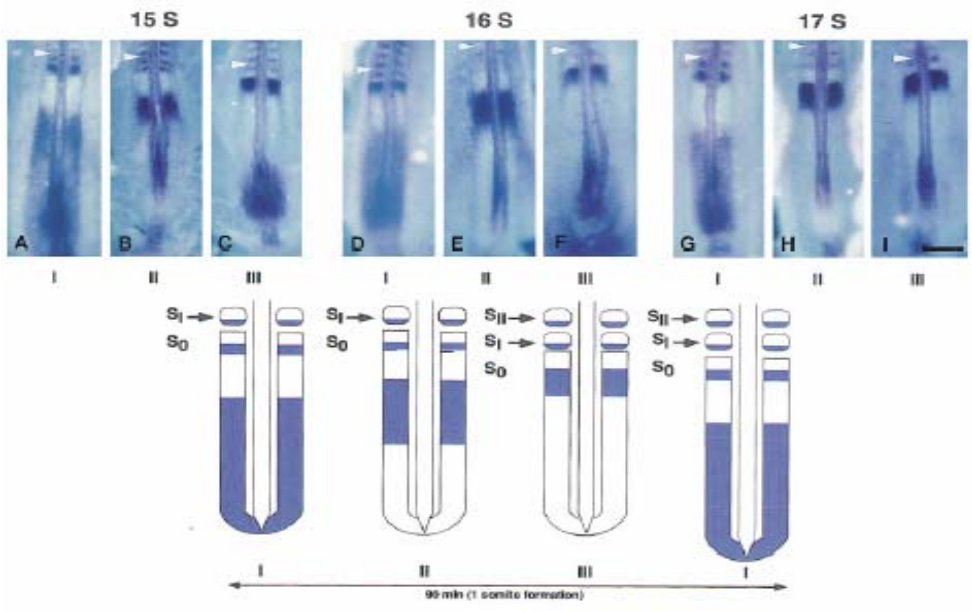

Figure 13. *c-hairy1* mRNA expression in the PSM defines a highly dynamic caudal-to-rostral expression sequence reiterated during formation of each somite.

(Top) *In situ* hybridization with *c-hairy1* probe showing categories of *c-hairy1* expression patterns in embryos aged of 15 (A, B and C), 16 (D, E and F) and 17 (G, H and I) somites. Rostral to the top. Arrowheads point to the most recently completely formed somite (somite I: SI). Bar = 200 µm.

(Bottom) Schematic representation of the correlation between *c-hairy1* expression in the PSM with the progression of somite formation.

By (Palmeirim et al., 1997).

	Notch pathway	Wnt pathway	FGF pathway
Mouse	***Hes1*** (Jouve et al, 2000); ***Hes7*** (Bessho et al, 2001b); ***Hey2*** (Leimeister et al, 2000); ***Lfng*** (Forsberg et al, 1998); ***Delta1*** (Maruhashi et al, 2005); ***Hes5*** (Dequeant et al, 2006) ***Hey1*** " ***Nkd1*** " ***Nrarp*** " ***Id1*** "	***Axin2*** (Aulehla et al, 2003); ***Nkd1*** (Ishikawa et al, 2004); ***Snail1*** (Dale et al, 2006); ***Dact1*** (Suriben et al, 2006); ***Dkk1*** (Dequeant et al, 2006) ***c-myc*** " ***Tnfrsf19*** " ***Sp5*** " ***Phlda1*** " ***Has2*** "	***Snail1*** (Dale et al, 2006); ***Dusp6 (*** Dequeant et al, 2006) ***Sprouty2*** " ***Bcl2l11*** " ***shp2*** " ***Hspg2*** " ***efna1*** "
Chicken	***hairy1*** (Palmeirim et al, 1997); ***hairy2*** (Jouve et al, 2000); ***Hey2*** (Leimeister et al, 2000); ***Lfng*** (McGrew et al, 1998; Aulehla and Johnson, 1999)	***snail2*** (Dale et al, 2006)	***snail2*** (Dale et al, 2006)
Zebrafish	***her1*** (Holley et al, 2000); ***her7*** (Henry et al, 2002); ***her11*** (Sieger et al, 2004); ***her12*** (Shankaran et al, 2007); ***her15*** " ***deltaC*** (Jiang et al, 2000)		
Medaka	***her1/11*** (Gajewski et al, 2006) ***her5*** " ***her7*** "		
Xenopus laevis	***esr9*** (Li et al, 2003) ***esr10*** "		

Table 1. Name and references for cyclic genes discovered in vertebrates thus far.
Genes either belong to or are regulated by the pathway indicated on top of the columns. Genes in green are regulated by two pathways.

laevis (Li et al., 2003). All of these genes cycle in synchrony, even if some qualitative differences can be observed in their expression patterns either due to a difference in the mRNA stability (*Hes7-Lfng* in mouse (Bessho et al., 2001)) or to specific domains of expression (*her11, her12* and *her15* in zebrafish (Shankaran et al., 2007)). The Notch pathway is involved in cell-cell communication. *Notch* encodes a transmembrane receptor that recognizes two sets of transmembrane ligands, Delta and Serrate (Artavanis-Tsakonas et al., 1999). The affinity of Notch for its ligand can be modified by differential glycosylation mediated by the Fringe protein (Bruckner et al., 2000; Moloney et al., 2000). Upon ligand binding, Notch undergoes a number of proteolytic cleavages leading to the translocation of its intracytoplasmic domain into the nucleus where, together with the transcription factor Su(H)/RBPjk, it activates the transcription of downstream targets genes such as those of the enhancer of split family *(Hairy/Hes/her/esr* genes). The genes from this family encode negative regulators of the Notch pathway.

Cyclic genes from the Wnt pathway, *Axin2, Dact1* and *Nkd1*, have been recently discovered in mouse (Aulehla et al., 2003; Ishikawa et al., 2004; Suriben et al., 2006). *Nkd1* cycles in synchrony with the cyclic genes from the Notch pathway. In contrast, *Axin2* and *Dact1* exhibit the same periodicity but cycle out of synchrony with these genes, meaning that when *Axin2* and *Dact1* are in a given phase, the Notch pathway cyclic genes and *Nkd1* are in another phase (Figure 14). Interestingly, *Axin2*, *Dact1* and *Nkd1* are negative regulators of the Wnt pathway (Cheyette et al., 2002; Kikuchi, 1999; Wharton et al., 2001).

More recently, a large-scale approach using mouse microarrays led to the discovery of new cyclic genes in both Notch and Wnt pathways, but also in the FGF pathway (Dequeant et al., 2006), which was shown just before to drive, in coordination with Wnt pathway, the cyclic expression of S*nail1* and S*nail2* in mouse and chicken, respectively (Dale et al., 2006). FGF and Notch cyclic genes cycle out of synchrony with Wnt cyclic genes. The common point between all these cyclic genes is that most of them encode negative regulators of the pathways. As we will see later, this characteristic is required in the mechanism controlling the propagation of the cyclic gene wave in the PSM.

Whereas the cycling behavior of the genes is conserved in the PSM between different species (implying that the mechanisms of the segmentation clock are conserved as well), it is interesting to note that it involves different players. For

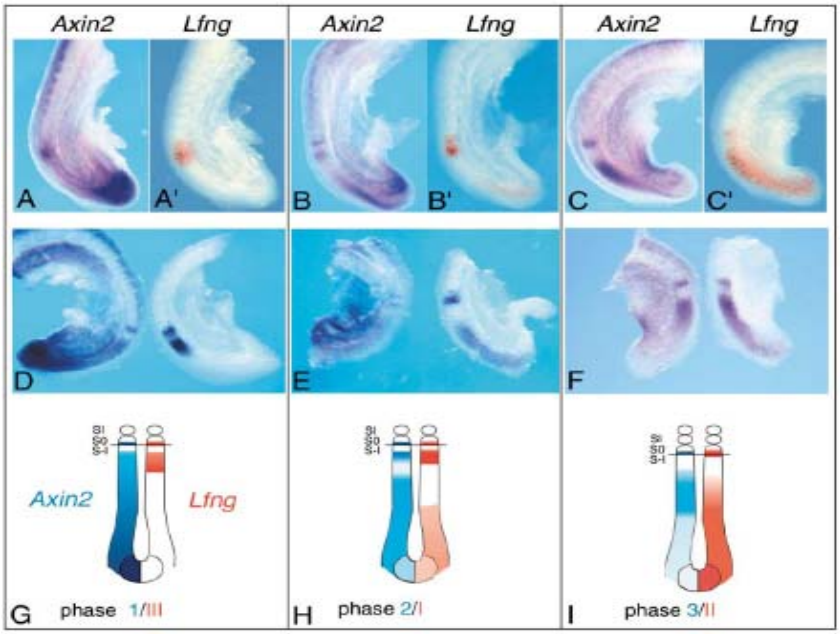

Figure 14. *Axin2* and *Lfng* transcription oscillate out of synchrony.
Whole-mount in situ hybridization of 9.5 dpc mouse embryos (A–C') or embryo halves (D–F), stained for *Axin2* and *Lfng*.
(A–C') The same embryos were stained first for *Lfng* (A'–C') and then for *Axin2* (A–C).
(D–F) Embryo halves were stained for either *Axin2* (left) or *Lfng* (right).
(G–I) Schematic representation of expression patterns shown for phase 1 (A, A', and G), phase 2 (B, B', and H), and phase 3 (C, C', I) of the *Axin2* expression cycle in relation to cyclic *Lfng.* Note the alternating waves of *Axin2* and *Lfng* expression in the tail bud and posterior PSM, while expression of both genes overlaps and is stable in the anterior PSM.
By (Aulehla et al., 2003).

example, *Lfng* is cycling in amniotes, but expressed as a single band in the anterior-most PSM of lower vertebrates such as zebrafish (Leve et al., 2001; Prince et al., 2001; Wu et al., 1996), or not clearly expressed in the mesoderm in *Xenopus laevis* (Wu et al., 1996). The Hairy and enhancer of split family also involves non-orthologous genes between the different species. For example, *her9*, homologue of the mouse cyclic gene *Hes1* and the chicken cyclic gene *hairy2,* in zebrafish and medaka is not expressed in the PSM (Gajewski et al., 2006; Leve et al., 2001). Finally, Delta-ligand was not shown to cycle in the chicken PSM.

In conclusion, the segmentation clock involves a complex mechanism driving the fine regulation of different cyclic genes in the different vertebrate species. It involves cross-talk between at least three pathways in the mouse, the mechanisms of which are poorly understood. The involvement of the Wnt and FGF pathways in zebrafish and chicken embryos remains to be explored.

3-1-3) Functional analysis of the genes involved in the segmentation clock

Null mutant mice for genes involved in the Notch pathway all exhibit somitogenesis defects. The severity of these defects depends on the mutated gene. For example, null mutant mice for *Notch1, Dll1* or *Rbpjk* die before birth (Conlon et al., 1995; Hrabe de Angelis et al., 1997; Oka et al., 1995). Their somites are irregular in size, and present defects in their epithelialization and AP polarity. Null mutant mice for *Hes7, Lfng, Dll3, Presenilin1* (an enzyme involved in the Notch clivage) and *Mesp2* (a gene involved in somite boundary specification interacting with the Notch pathway) also exhibit defects in somite boundaries and AP polarity, and their skeleton accordingly exhibits defects such as fused vertebrae and ribs, split vertebrae, vertebrae of irregular shapes, missing vertebrae and/or caudal truncation (Bessho et al., 2001; Evrard et al., 1998; Kusumi et al., 1998; Saga et al., 1997; Shen et al., 1997; Wong et al., 1997; Zhang and Gridley, 1998). In these mutants, the dynamics of the cyclic genes are affected (Bessho et al., 2001; del Barco Barrantes et al., 1999; Jouve et al., 2000).

A study of the Wnt3a hypomorph mutant "vestigial tail" (Greco et al., 1996) shows that the Wnt pathway is upstream of the Notch pathway to control the dynamic

expression of the cyclic genes (Aulehla et al., 2003). A null mutation of the Wnt target *Mesogenin*, generates severe defects in somitogenesis and skeleton formation (Wang et al., 2007; Yoon and Wold, 2000). Surprisingly, null mutant mice for the cyclic genes *Axin2* or *Nkd1* do not show any somitogenesis defects (Li et al., 2005; Lustig et al., 2002; Yu et al., 2005; Zhang et al., 2007), showing that these genes are not essential for somitogenesis process.

In zebrafish, genes involved in somitogenesis have been identified by a screen for mutants that exhibit defects in somitogenesis, or by a morpholino approach and *in situ* hybridizations (Gajewski et al., 2003; Geling et al., 2002; Henry et al., 2002; Holley et al., 2002; Jiang et al., 1996; Oates and Ho, 2002; Shankaran et al., 2007; Sieger et al., 2003; Sieger et al., 2004; van Eeden et al., 1996). This screen identified *after eight/DeltaD*, *deadly seven/notch1a*, *beamter/deltaC* and *mindbomb* (a Notch component encoding a RING E3 ligase), *her1, her7, her11, her12, her15* and *Su(h)*. Interestingly, all the defects identified in mouse and zebrafish mutants start after the first five to seven somites are formed, implying a possible different regulation of the segmentation in the anterior region of the body.

At last, in humans, mutations in *Mesp2, Lfng* and *Delta 3* result in severe defects in the vertebral column causing congenital scoliosis (Bulman et al., 2000; Sparrow et al., 2006; Whittock et al., 2004).

All these studies show the importance of genes from the Notch and Wnt pathways in somitogenesis. The mild phenotypes of the mice mutants for a cyclic gene is, however surprising if we consider that cyclic genes are the effectors of the segmentation clock. This can be interpreted by a possible redundancy between the cyclic genes, or perhaps the main component of the segmentation clock remains to be unravelled.

3-1-4) Mechanisms for the propagation of the cyclic gene wave

The fact that most of the cyclic genes encode negative regulators or ligands for a given pathway suggested a potential mechanism for generating the periodic expression of the cyclic genes and the synchronization of their expression between cells (Lewis, 2003). Lewis proposed that the periodic expression of the cyclic genes depends on the ability of the genes from the Hairy and enhancer of split family to directly inhibit their own transcription (as well as the transcription of other cyclic

genes). In zebrafish, this model was based on the *her1/her7* genes and showed that their periodic expression depends mainly on the time delays that allow their transcription (Tm), their translation (Tp) and the life times of their mRNA and proteins (Figure 15A). Tm and Tp delays correspond to the "on" state when the mRNA is detectable in the cell. Then, when the protein is made and functional, it switches through a negative auto-feedback loop mechanism to the "off" state where the mRNA ceases to be transcribed and disappears by decay. This "off" state depends on the life time of both the mRNA and protein of these genes. The shorter they are, the shorter the "off" state. At least, for this mechanism to work and return to the "on" state again, the life time of the mRNA and proteins of the *her* genes must be shorter than the delays Tm + Tp. Computational simulations show that if these conditions are respected, robust oscillations of *her1* and *her7* can be obtained. Then, this model proposes that *her* genes can repress the expression of *deltaC*, thus generating the periodic expression of *deltaC*. Upon binding periodically to the Notch receptor, deltaC induces periodic activation of the Notch pathway in the neighboring cell (Figure 15B). This provides a mechanism explaining how the periodic expression of cyclic genes can be synchronized between cells via the Notch pathway. This mechanism can work, provided again that the life time of deltaC is short, as for the products of *her* genes. This model was recently experimentally proven, by measuring the transcriptional and translational delays of *her1, her7* and *deltaC in vivo*, and by confirming the inhibitory relationships between these genes (Giudicelli et al., 2007).

The synchronization of cells by the Notch pathway had already been proposed based on cyclic gene expression in various zebrafish Notch mutants (Jiang et al., 2000). It was at the origin of the proposition of the model above, and also proposed at that time an explanation of why the first somites always appear to form normally in the Notch mutants. The model above can be transposed to mouse and chicken, where *hairy* or *Hes* genes would play the role of zebrafish *her* genes, and *Lfng* gene, the role of *deltaC* (except that *Lfng* would inhibit periodically the Notch activity). Some studies tend to prove that this model would work in mouse and chicken (Bessho et al., 2003; Bessho and Kageyama, 2003; Dale et al., 2003; Hirata et al., 2004; Hirata et al., 2002; Monk, 2003; Morimoto et al., 2005).

In conclusion, the discovery of the cyclic genes provided the first evidence of a cellular oscillator linked to somitogenesis. The PSM cells behave as coupled oscillators that allow the propagation of the clock signal throughout the PSM at

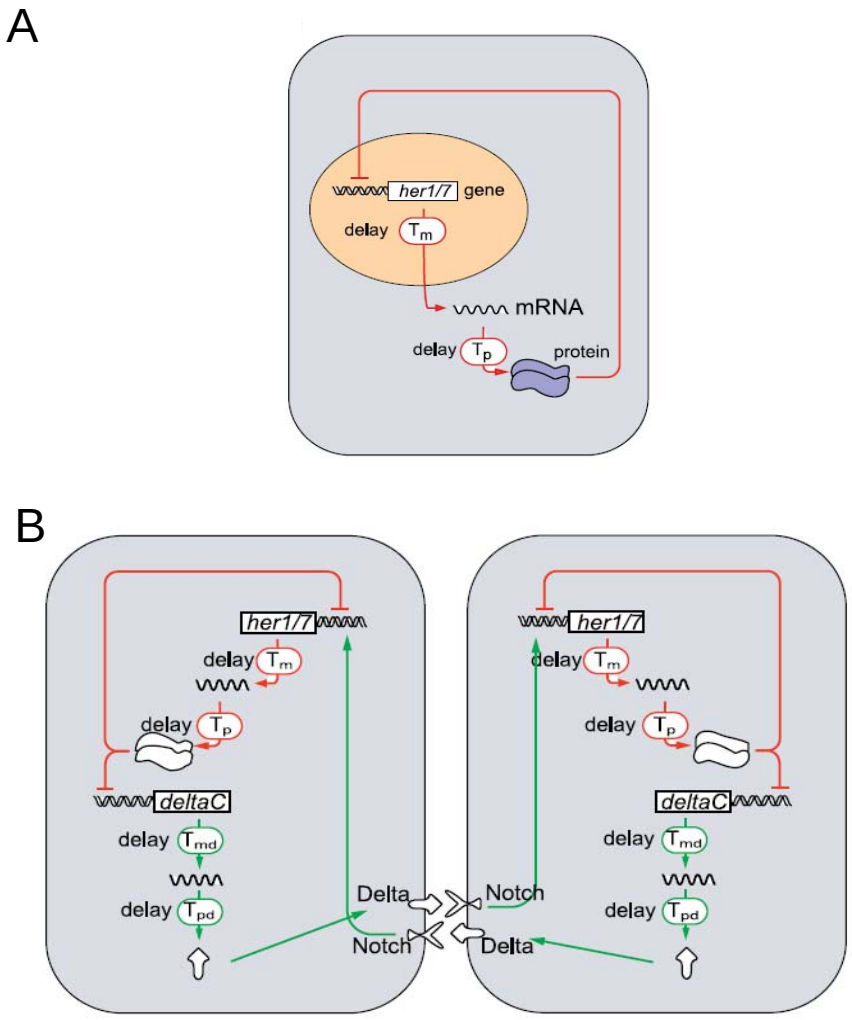

Figure 15. Model of the oscillator mechanism.

A. In each cell of the presomitic mesoderm, it is proposed that a *her1* or *her7* autoinhibition negative feedback loop generates oscillations.

B. Communication via the Delta-Notch pathway is proposed to keep oscillations in adjacent cells synchronized. The oscillations depend critically on the delays (Tm, Tp, Tmd, and Tpd) in the feedback loops.

By (Giudicelli et al., 2007).

regular intervals of time, corresponding to the somite formation. The clock system relies at least on three pathways: the Notch, Wnt and Fgf pathways.

3-2) The determination front

In 2001, the first evidence of the existence of a "wavefront" arose from works in chicken and zebrafish (Dubrulle et al., 2001; Sawada et al., 2001). By inverting small pieces of PSM of one somite in length in chicken, Dubrulle and colleague were able to localize a region in the PSM above which the cells become determined to form a somite. This region was localized at the level of the presumptive somite S-IV and was called the "determination front." The position of the determination front was shown to correspond to a threshold of fgf8 signaling activity (Delfini et al., 2005; Dubrulle et al., 2001; Sawada et al., 2001). *Fgf8* is expressed as a gradient in the PSM, the peak of which is at the level of the tail bud. Cells exposed to a high level of fgf8 activity in the posterior PSM are maintained in an immature state. They express *Brachyury/T, Tbx6* and *Mesogenin*, a marker of the posterior PSM. Below a given threshold of fgf8 activity, cells become competent to form a somite. This transition from an immature to a competent state can be visualized by the downregulation of the Mesogenin marker at the level of the determination front and the upregulation of the Mesp2 factor right in the same area (Figure 16) (Buchberger et al., 2000; Yoon et al., 2000). As we will see later, *Mesp2* is involved in the starting of the somitogenesis program in the cells.

The determination front is constantly displaced caudally in the PSM at the same time that the axis is elongating, hence, gradually allowing the cells to commit to form a somite. *In situ* hybridization using intronic probes against *fgf8* showed that its mRNA was only produced in the tail bud (Dubrulle and Pourquie, 2004b). Therefore, the regressing gradient is created by the gradual *fgf8* mRNA decay occurring in cells exiting the tail bud. Changing the position of the determination front by treating embryos with the drug SU5402, an inhibitor of fgf signaling, leads to the formation of larger somites. Conversely, implanting Fgf8-soaked beads in the posterior PSM leads to the formation of smaller somites (Dubrulle et al., 2001). Analysis of the dynamics of the cyclic genes and of the periodicity of somite formation in these conditions shows that both are unaffected. These effects can be interpreted as acceleration or slowing down of the determination front regression. For example, the SU5402

treatment imitates a sudden acceleration of the *fgf8* front regression, hence allowing more cells to commit and to form a larger somite at the clock signal. Inversely, fgf8-soaked beads displace rostrally *fgf8* expression, as if the determination front was regressing very slowly, allowing less cells to form a somite between two signals of the clock. In conclusion, the determination front, in concert with the segmentation clock, controls the size of the somites. This description of the determination front corresponds well to the prediction of the "Clock and Wavefront" model. The determination front relies on a gradient regressing caudally, giving positional information along the AP axis and controlling the competence of the cells to form a somite in interaction with the clock.

More recently, a gradient of Wnt signaling "parallel" to the fgf gradient was shown to be involved in the positioning of the determination front. As with fgf8, grafting a pellet of wnt3a-expressing cells in the posterior PSM leads to the formation of smaller somites (Aulehla et al., 2003). Moreover, the fgf8 expression is down regulated in the Wnt3a vestigial tail mutants, suggesting that FGF8 acts downstream of WNT3a.

Finally, a last gradient that antagonizes both fgf8 and wnt3a gradients is involved in the positioning of the determination front (Diez del Corral et al., 2003; Moreno and Kintner, 2004). It is comprised of retinoic acid (RA) and functions by triggering differentiation of PSM cells. The RA gradient is strong anteriorly and weak caudally due to the expression pattern of the RA synthesis enzyme Raldh2 that is strongly expressed in the anterior PSM and the formed somites, and the expression pattern of the RA degradation enzyme Cyp26 expressed at the tail bud of the embryos (Blentic et al., 2003; Niederreither et al., 2003; Sakai et al., 2001). Embryos deficient in RA exhibit smaller somites (Diez del Corral et al., 2003; Maden et al., 2000). Accordingly, the fgf8 domain is shifted anteriorly in these embryos. In contrast, RA-treated embryos were shown to antagonize fgf8 activity and to induce the formation of larger somites (Moreno and Kintner, 2004). These gradients have been described in *Xenopus laevis*, zebrafish, chicken and mouse, showing the conservation of these mechanisms between vertebrate species.

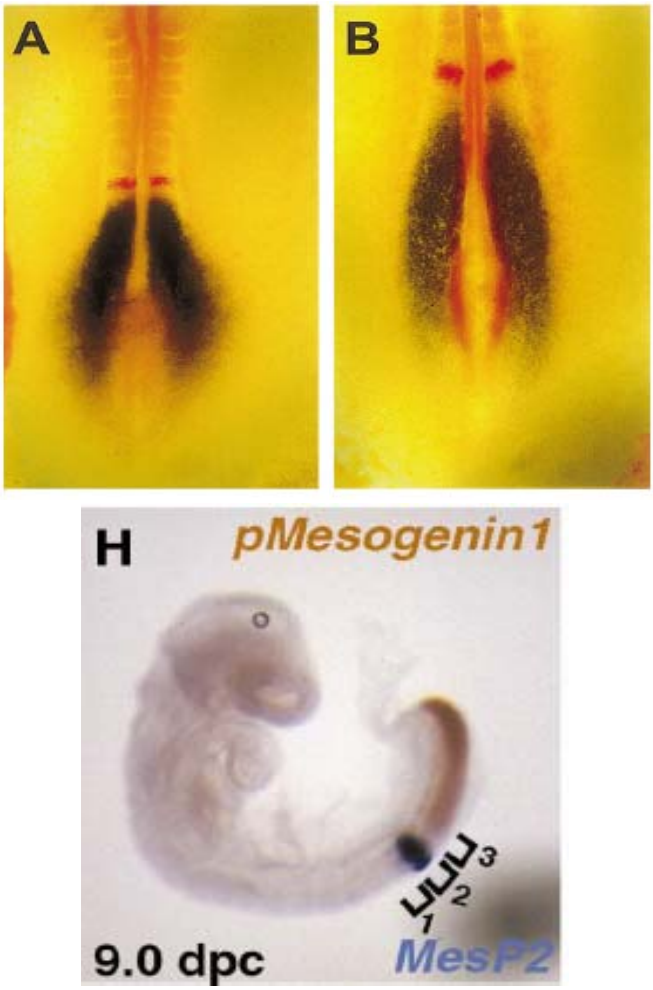

Figure 16. The determination front is proposed to be localized at the intersection between Mesogenin1/Mespo and Mesp2/Meso2 expression.

(Top) Double in situ hybridizations of *cMespo* (dark blue) and *cMeso2* (red) on HH stage 9±10 chicken embryos.

By (Buchberger et al, 2000).

(Bottom) Double in situ hybridizations of *pMesogenin1* (brown color) and *MesP2* (dark blue) in 9.0-dpc mouse embryos.

By (Yoon et al. 2000).

In conclusion, the regression of the determination front is regulated by mutually inhibitory and dynamic gradients of FGF/WNT and RA signaling–a caudorostral gradient of FGF/WNT that prevents the cells from initiating their segmentation program; and a rostrocaudal RA gradient that relieves this inhibition by antagonizing FGF activity and/or directly activating genes involved in the segmentation process. In concert with the segmentation clock, the determination front regulates the size of the somites formed (Figure 17).

3-3) Somite AP polarity specification

As mentioned earlier, cells activate their somitogenesis program at the determination front level. The bHLH factor, Mesp2, has been shown to play an important role in the control of this program. Mice carrying a null mutation for *Mesp2* do not specify the anterior compartment of their somites, which results in severe segmentation defects (Saga et al., 1997). Moreover, Mesp2 has been shown to directly activate the expression of a member of the Ephrin family, EphA4, thought to be later involved in the somite boundary formation (Durbin et al., 1998; Nakajima et al., 2006). Therefore, *Mesp2* would play a role in both controlling the set up of the AP polarity of the somites and activating the molecules that will be involved in the somite boundary formation.

Mesp2 is activated as one stripe of about one somite in length at the level of the determination front by the contiguous action of *Tbx6* and Notch signaling (Koizumi et al., 2001; Yasuhiko et al., 2006). This expression pattern is also regulated by the inhibitive activity of FGF signaling (Delfini et al., 2005). Mesp2 activates and stabilizes *Lfng* expression in its own domain of expression, and represses *Dll1* expression. Upon its upregulation by Mesp2, Lfng downregulates Notch1 activity. This results in the segregation of the expression of *Dll1* in a posterior compartment, and *Lfng* and *Mesp2* in an anterior compartment (Figure 18) (Morimoto et al., 2005; Takahashi et al., 2000). The size of these compartments is gradually refined along the anterior PSM until reaching S0, where these compartments correspond to the two halves of the somite.

The fact that Mesp2 stabilizes and refines *Lfng* expression as one stripe in the anterior compartment of the future somite and excludes the expression of other genes in the posterior compartment, is thought to account for the sudden slowing down of

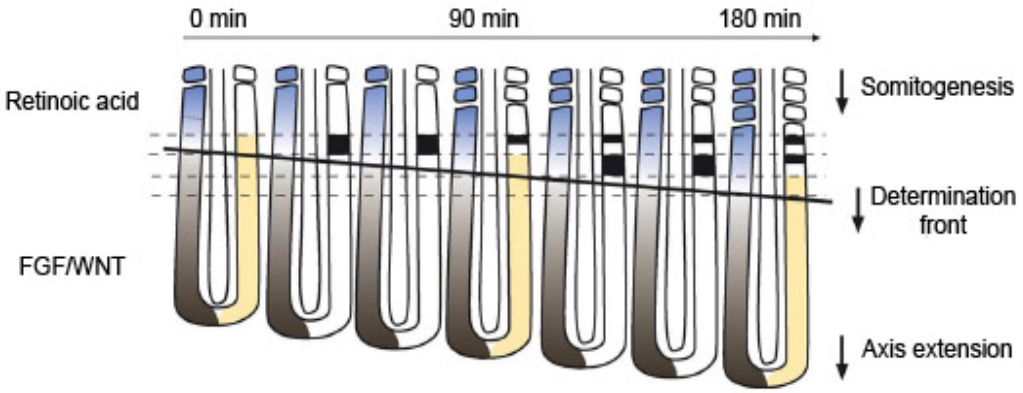

Figure 17. Model for segment formation in chicken embryo.

On the left side of the embryos are shown the antagonistic gradients of FGF/WNT signaling (in grey) and of retinoic acid (in blue), which define the position of the determination front (thick black line).

On the right side of the embryos, the periodic signal of the segmentation clock is shown in yellow as the phase I expression of Notch-related cyclic genes. Cells reaching the determination front which are exposed to this periodic signal activate the expression of segmental genes such as *Mesp* (in black) in a segment-wide domain thus establishing the segmental pattern. Subsequently, rostro-caudal identity of the prospective somite is established and ultimately somite boundaries are formed.

After (Pourquie, 2004).

the cyclic genes in the anterior PSM. It is also in agreement with the finding that the expression of cyclic genes such as *her1* in zebrafish or *Lfng* in mouse is controlled by two different regulatory elements in their promoter: one which drives cyclic expression in the posterior PSM, and the other that controls expression in the anterior PSM (Cole et al., 2002; Gajewski et al., 2003; Morales et al., 2002).

New factors have recently been involved in the control of the somitogenesis program in conjunction with Mesp2 and belong to the Ripply family. Three *Ripply* genes exist in mouse, human and zebrafish, two of which have been involved in somitogenesis. They exhibit a stripy expression pattern in the anterior PSM (*Ripply2*), or in the anterior PSM and anterior compartment of the formed somites (*Ripply1*). *Ripply2* is a direct target of Mesp2. Both *Ripply1* and *Ripply2* function to repress the expression of *Mesp2*. They were shown to play a crucial role in the specification of the AP polarity of the somites and in boundary formation (Kawamura et al., 2005; Morimoto et al., 2007).

In conclusion, the activation of factors such as Mesp2, Ripply1 and Ripply2 in the anterior PSM results in the set up of AP polarity of somites. This AP polarity was shown to be required for the formation of somite boundaries (Durbin et al., 2000), as well as for the ulterior resegmentation process (see above). In amniotes, it is also required for the segmentation of the peripheral nervous system, as it restricts migration of the motor neurons and neural crest cells through the anterior part of sclerotomes (Bronner-Fraser, 2000; Bronner-Fraser and Stern, 1991; Stern et al., 1991).

3-4) Somite boundary formation

Somite formation requires tissue epithelialization and boundary formation. Epithelialization begins dorsally and ventrally in the anterior PSM at the level of the determination front. PSM cells secrete various extracellular matrix proteins, such as fibronectin or laminin which will form the future basal lamina, and upregulate the expression of adhesion molecules such as NCAM, N-cadherin and cadherin11 (Duband et al., 1987; Horikawa et al., 1999). *Paraxis* may be involved in regulating this process as null mutant mice for *Paraxis* fail to form epithelial somites all along the axis (Burgess et al., 1996). Somite boundary formation *per se* has been studied by time-lapse movie. It showed that somite border formation does not occur via a simple

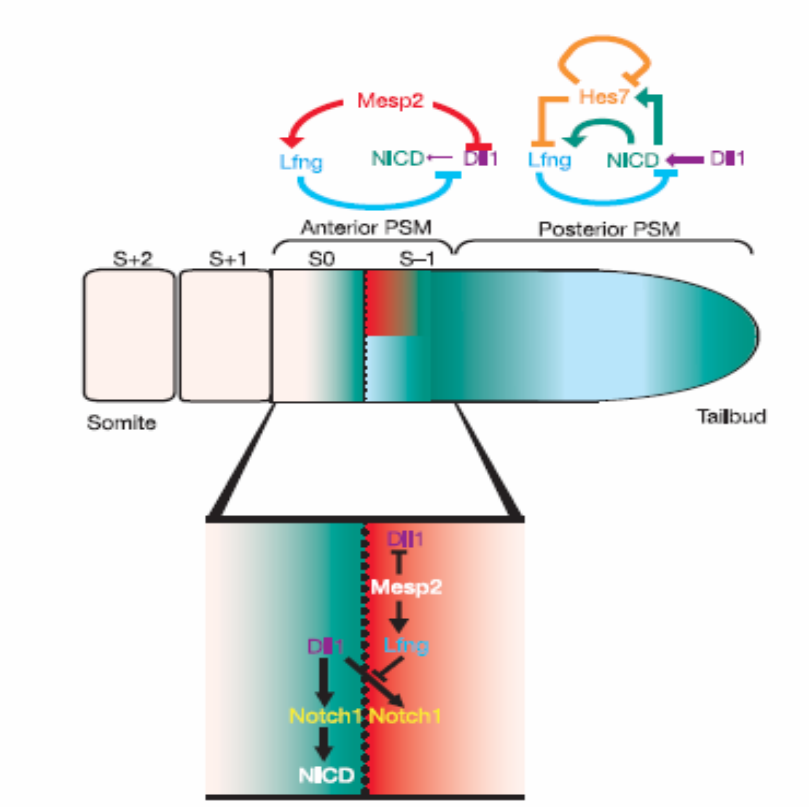

Figure 18. Schematic representation of the regulatory mechanism underlying the clock system and of the implications of Mesp2 function in establishing the segmental boundary.

In the posterior PSM, the Dll1–Notch signal initially activates both *Lfng* and *Hes7*. *Hes7* is a strong transcriptional repressor of *Lfng* and of the *Hes7* gene itself, whereas *Lfng* is a negative modulator of the Notch receptor in this cellular context. The positive and negative feedback loops thus generates oscillation of Notch1 activity. In the anterior PSM, the Notch1 activity and *Lfng* waves are no longer subject to negative regulation by *Hes7*, as *Mesp2* now becomes a major regulator of *Lfng* activation and *Dll1* suppression. As a result, both Notch1 activity and *Lfng* waves are arrested and generate a clear boundary between the Notch1 activity domain and the *Mesp2* expression domain, which produce the next segmental boundary.

By (Morimoto et al., 2005).

segregation mechanism. Cells on both sides of the presumptive boundary exchange place several times before definitively stabilizing their position as the boundary forms (Kulesa and Fraser, 2002). Boundary formation requires expression of specific molecules, such as ephrins and cadherins. The knock-down of *EphA4* by the injection of dominant-negative constructs in zebrafish results in the abnormal formation of somite boundary (Durbin et al., 1998). In *Xenopus laevis*, the protocadherin PAPC has been shown to also play an important role in this process (Kim et al., 2000). In mouse, members of the EPH family were shown to be downstream targets of Notch signaling (del Barco Barrantes et al., 1999). However, null mutant mice for *EphA4* or *PAPC* have no somitic phenotype, suggesting a possible redundancy between the members of these large families (Dottori et al., 1998; Yamamoto et al., 2000).

In conclusion, vertebrate body metamery is set up during early embryogenesis by the somitogenesis process. This process is tightly linked to gastrulation and involves a molecular oscillator, the segmentation clock, which drives the periodic expression of the cyclic genes in the PSM. The periodic signals of this clock are translated in the serie of somites by a travelling determination front, regressing caudally in the PSM and controlling cell maturation. Interactions of both clock and determination front was shown to regulate somite size.

III) The corn snake as a new model

Although the molecular mechanisms involved in somite specification begin to be well documented, the mechanisms controlling the total number of somites are poorly understood. Precedent studies primarily focused on mechanisms regulating the whole body size or on signals that could regulate the arrest of somitogenesis. Another way to address this issue is to use a model that exhibits many more vertebrae than the current model species used in developmental biology and to compare how somitogenesis is regulated. Snakes are good candidates for this approach.

1) Introduction to reptiles

Reptiles include chelonians (turtles), crocodilians, tuatara and squamates (lizards and snakes) (Figure 2). Although they represent at least 8,000 species, the majority of which are squamates, they have been very under studied compared to other vertebrate species. For comparison, about 4,800 species of mammals, 9,000 species of birds and 5,300 species of amphibians have been categorized (Pough, 2004a). Reptiles form a chorion, an allantois and an amnion during their embryonic development. For this reason, they have been classified in the group of the amniotes (close to the birds). The closest relatives to the birds are the crocodilians, and a complete list of the extant reptiles would actually have to include birds. However, birds are so different from the other group of reptiles that they are normally excluded from herpetology and the term "reptile" is used to mean non-avian reptiles (Pough, 2004a). Reptiles live in a variety of habitats from the sea, to the land, forests, deserts and mountains. Compared to birds, which are endothermic (maintaining a constant body temperature), reproduce sexually and lay hard-shelled eggs; all reptiles are ectothermic animals (regulating their body temperature by absorbing external heat), and reproduce either sexually (chelonian, crocodilian, tuatara and most of the squamates) or asexually. The asexual reproduction is called "parthenogenesis." and is associated with mostly lizards, although at least one snake species (the typhlopid *Rhamphotyphlops braminus*) has been found to also reproduce by parthenogenesis - (Pough, 2004b). Over 80% of reptiles lay eggs (Kohler, 2005a). All crocodilians, chelonians and tuaturas are oviparous, while ovoviviparity has been developed by the squamates. Ovoviviparity means that embryos develop in an egg inside the mother's body. The nutrients are supplied to the embryo entirely by the egg, or by the egg and the mother according to the species. The eggs are laid before hatching. However, different degrees of ovoviviparity exist and the eggs can be laid by the mother at various times before hatching. For simplicity, people often call the species that lays eggs "oviparous," and the species that gives birth to live offspring "viviparous." One case of complete viviparity has been, however, discovered in the lizard *Mabuya heathi*, in which the egg is one millimeter in diameter and nutrients are transferred from the mother to the embryo by a placental connection, accounting for 99% of the dry mass of the embryo at the time of birth (Pough, 2004b). The shell of the reptile eggs can be of two types: rigid (hard-shelled) or flexible (soft-shelled), depending on

the arrangement and the quantity of minerals in the shell (Kohler, 2005b; Pough, 2004b). Hard-shelled eggs are laid by all the crocodilians, some turtles and the gekkonidae lizard species, whereas soft-shelled eggs are laid by all snakes, non-gekkonidae lizards and other turtles. The size of the eggs and of the clutches depends on the species, and can vary from less than 1 gram to 300 grams for one egg, and from one egg to several hundred eggs for one clutch. One other important difference between reptile and bird eggs is the lack of chalazae. After deposition, the embryo attaches to the inner top portion of the shell via the chorion. Changing the position of the eggs after deposition can be lethal to many reptile species, as no rotation of the yolk brings the embryo back to its original position (Kohler, 2005b). In the face of such diversity, it is quite surprising that so few studies have been conducted on reptiles.

2) Studies (or lack of studies) on reptiles

A good model species for developmental studies is one that is readily available, easily maintained, lays large numbers of eggs at frequent intervals and produces embryos that can be easily harvested at early time points in development (Billett et al., 1985). For genetic studies, short generation times are also appreciated.

Reptiles are far from meeting these criteria. For example, few species are commercially available and animals must therefore often be caught in the wild. Very little is known about the behavior and physiology of the species brought to the laboratories, which makes the maintenance and the successful breeding of the captive species particularly difficult and uncertain (Holder and Bellairs, 1962). Then, the nature of the eggs themselves (particularly the soft-shelled), makes successful incubation difficult (Kohler, 2005c). The development of the embryos is influenced, and can be impaired, by various environmental factors (Figure 19). Most of the reptiles are seasonal, breed and lay eggs once, or a few times per year. For the most part, the clutches do not contain enough eggs for reproducible experiments, and the stage of development may or may not be suitable for some particular experiments (New, 1966). The development of the embryo is slow compared to birds and small rodents used in the laboratories and therefore, is not suitable for short-term studies (New, 1966). In addition, the time before reaching sexual maturity can range from months to several decades, which does not favor genetic studies.

A

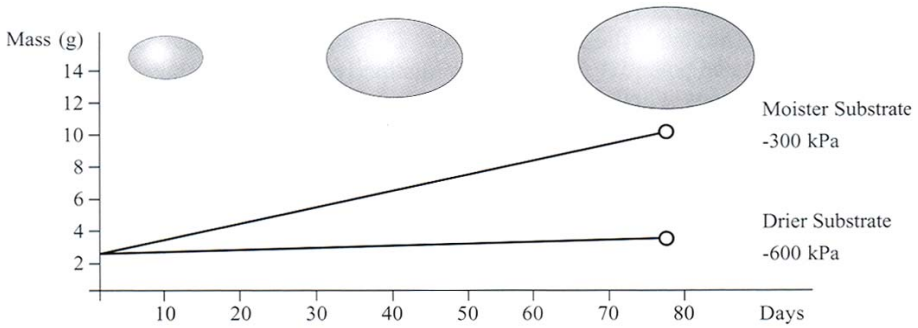

B

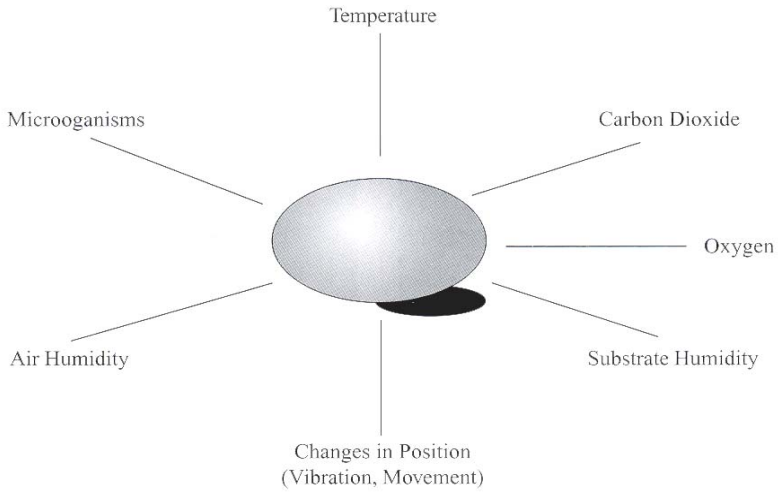

Figure 19. Factors that influence reptile embryo development inside the egg.
A. Diagram showing that soft-shelled reptile eggs increase their mass by uptaking water during incubation period. Successful incubation requires moister substrate.
B. Different factors that influence embryo development inside the egg.
Figures by (Kohler, 2005).

However, a number of experiments has been performed on reptiles, notably in medicine, to discover new curative molecules from snake venom, to study the regeneration of damaged brain tissue in some lizards, or to test the procedures of open-heart surgery on crocodilians (Grenard, 1994). In developmental biology, several staging sequences of normal development have been described (Lizards: (Dufaure and Hubert, 1961; Mathukkaruppan et al., 1970) (Lemus et al., 1981); Turtles: (Beggs et al., 2000; Crastz, 1982; Greenbaum, 2002; Greenbaum and Carr, 2002; Guyot et al., 1994; Mahmoud et al., 1973; Miller, 1985; Renous et al., 1989; Tokita and Kuratani, 2001; Yntema, 1968); Crocodilians: (Magnusson and Taylor, 1980; Reese, 1915); Tuatara: (Dendy, 1899; Moffat, 1985); Snakes: (Hubert and Dufaure, 1968; Hubert et al., 1966; Treadwell, 1962; Zehr, 1962)). Some tools and protocols to culture whole embryos have been developed (Bellairs, 1951; Holtzman and Halpern, 1989; Lutz and Dufaure, 1960; Pasteels, 1937a; Raynaud, 1959a; Raynaud, 1959b; Shinde and Goel, 1980; Yntema, 1964), but culturing reptiles remains difficult due to fungal infections (Holtzman and Halpern, 1989). Pasteels was the first to use vital dyes to trace *in ovo* the movement of the cells during gastrulation of the turtle Clemmys leprosa (Pasteels, 1937a). Gastrulation was also described in the lizard *Lacerta vivipera* and the snake *Vipera aspis*, and some other reptiles (Gilland and Burke, 2004). Most of the gastrulation aspects were shown to be quite uniform throughout the reptiles and are reminiscent of gastrulation in chicken in some ways (e.g., flat organization of the embryo at the surface of the yolk or formation of the hypoblast layer by epiblast cells delamination). However, no reptile has been found to possess an elongated primitive streak and node as in mammals and birds. Instead, a posterior slit similar to the amphibian blastopore (called "blastoporal plate") has been described. More recently, exciting developmental studies have been performed, and aimed at unraveling the mechanisms of the turtle carapace formation. These studies consisted of grafting turtle somites in place of the somites of a chicken host and observing how the turtle somites differentiate (Nagashima et al., 2005), or looking for factors inducing carapacial fate (Cebra-Thomas et al., 2005; Gilbert et al., 2001; Loredo et al., 2001), or again, studying the turtle "Hox code" and *Msx* genes (Ohya et al., 2005; Vincent et al., 2003). Neural crest cells have been shown to contribute to the plastron formation (Cebra-Thomas et al., 2007; Clark et al., 2001). Turtle PSM has also been cultured *in vitro* (Packard, 1980; Packard and Meier, 1984).

No genome sequence is available for any reptile as yet. The Green Anole

lizard, *Anolis carolinensis* genome should, however, be sequenced soon. Finally, some BAC libraries on different reptile species have been constructed (see http://www.nsf.gov/bio/pubs/awards/bachome.htm).

3) Snakes among the reptiles

3-1) Generalities

Snakes represent 2,900 species divided into 18 families that live in various ecosystems (e.g., sea, underground, forests, deserts, mountains). The phylogenetic relationships between these families are not always well understood (Zug et al., 2001). Nevertheless, for simplicity, three large groups can be derived from these families. The first group contains snakes called "the blind-snakes" (three families). They do not have eyes, are worm-like, very short (150 to 400mm in length) and have a fossorial life style. The second group contains snakes referred to as "primitive snakes" (11 families), among which are the phythonidae (pythons) and boidae (boas) that can exhibit giant sizes (up to 10 meters for the reticulated python). They are non-venomous snakes that kill their prey by constriction. They are unique in exhibiting vestigial hindlimbs as "spurs" on both sides of their cloaca. The third and last group contains the snakes considered as the most evolved (four families) and groups notably the viperidae (vipers, copperheads), the elapidae (cobras, coral snakes) and the colubridae (e.g., garter snakes, corn snakes, king snakes). These snakes do not exhibit any vestigial limbs. They have developed fangs (for the elapidae, the viperidae and a few colubridae) that allow them to kill their prey through biting and injecting the venom. The most sophisticated venom delivery system has been developed by the viperidae.

The snake's evolutionary history is reconstituted from diverse fossils and molecular phylogenies studies (Apesteguia and Zaher, 2006; Caprette et al., 2004; Greene and Cundall, 2000; Vidal and Hedges, 2004). One hypothesis is that snakes evolved from lizards. The forelimbs would have been lost first, followed by the progressive loss of the hindlimbs (thus placing pythons and boas at an intermediate stage), accompanied by body elongation. Snakes would also have lost their eyelids and otic pits compared to lizards, and developed special jaw bones that allowed them to open their mouths extremely wide, thus allowing snakes to eat large prey.

Several studies have also focused on understanding body shapes and behaviors

of snakes in relationship to their ecosystems and metabolism (Shine, 2000; Shine, 2003). One important example, which can have consequences when working on snakes in a laboratory, concerns the reproductive strategies. It was shown that female snakes can control the timing of fertilization by storing the sperm in their reproductive tract and using it only when they have enough energy to form a clutch (Shine, 2003). Females can also influence the number and quality of their offspring by controlling the number of matings, the choice of the male(s), storing sperm from different males and generating sperm competition in their reproductive tract, as well as selecting the nest site. In corn snakes, fertilization can be delayed up to one year after mating (personal observation). Thus, it is very difficult to know the time of fertilization when working with corn snakes.

3-2) The Corn snake

Corn snakes (*Pantherophis guttatus*) belong to the colubridae family. They are between 100cm and 150cm in length, non-venomous, and kill their prey (rodents) primarily by constriction. They live in the pine forests and grasslands of the southeast United States, in an area encompassing Florida, stretching north to the New Jersey, and west to Arkansas and Louisiana. The name "corn" snake is said to derive from cultivators that often found them in the corn storage bins where mice and rats were abundant, or from the marked resemblance of their belly to an ear of Indian corn (Soderberg, 2006).

Corn snakes are ovoviviparous and lay once a year during early summer (early May to end of July) in one to two clutches of 10 to 25 soft leathery-shelled eggs that stick to each other (Figure 20). The eggs hatch within a two-month period (early fall) and the baby snakes are already autonomous. They acquire their sexual maturity within 18 to 24 months. They are commercialized in America and are good-tempered animals and easily kept as pets (where they can live up to 20 years!). They are also very much appreciated by breeders for their varieties of colors (Figure 21).

Figure 20. Corn snake (*Pantherophis guttatus)* clutch of eggs, half a day after oviposition.
The red arrow indicates an unfertile egg.

Figure 21: Corn snake (*Pantherophis guttatus)* varieties.
(a) “Okeetee” (wild type); (b) “Snow” (combine amelanistic and anerythristic traits, causing the lack of both black and red pigment) ; (c) “Reverse Okeetee” (amelanistic Okeetee); (d) “Striped amelanistic”; (e) “Ghost Bloodred” (very pale, like a ghost, erythristic corn snake); (f) “Lavender” (anerythristic corn snake, lavender in shade).
Pictures by (Don Soderberg, 2006).

4) How did snake make so many vertebrae? Evolutionary studies

A number of evolutionary studies have aimed to document the transition between a lizard-like tetrapod body to a snake-like limbless elongated body (Berger-Dell'Mour, 1985; Sanger and Gibson-Brown, 2004; Wiens, 2004; Wiens and Slingluff, 2001). In the lizard group, several examples of body elongation coupled with limb reduction or loss have been reported. This implies that there may be a mechanism coupling the size of the axis with the formation of the appendages. This mechanism may include *Hox* genes, as published by Cohn and Tickle in python (Cohn and Tickle, 1999).

Other studies have compared the size and numbers of the pre- and post-cloacal/anal vertebrae in snakes and elongated fish. These studies, showing that the number of these vertebrae can change independently in some species, proposed the existence of "modules". In this case, the pre- and post-cloacal vertebrae represent two modules, regulated by two different developmental processes (Polly et al., 2001; Ward and Brainerd, 2007).

Finally, the majority of the studies comparing body size with the number of vertebrae show a positive correlation between these two criteria (the longer the body, the more vertebrae). This positive correlation is called "pleomerism" (Lindell, 1994). A recent study showed that the pleomerism was not respected in the case of giant snakes. The number of vertebrae was found reduced to what it should have been compared to the body size of the snake (Head and David Polly, 2007). This implies that in this case, the body size is regulated by somatic growth following the segmentation process.

In conclusion, evolutionary studies can aid in to discerning some features, such as developmental modules, that would not be evident without a large-scale comparison. These analyses can be very helpful in orientating studies in the evo-devo field.

RESULTS

When I arrived in the laboratory, it was proposed that I work with a reptile model (snake or lizard). A reptile facility had been opened at the institute, housing corn snakes (*Pantherophis guttatus*), a parthenogenetic lizard species (*Aspidoscelis uniparens*) and bearded dragons (*Pogona vitticeps*). Diana Baumann, a herpetology specialist, directed this facility and had the knowledge to enable the reproduction of these captive species and the successful incubation of the eggs. The corn snake colony was composed of enough females to obtain about 150 eggs at the laying season (early summer).

I chose to work with the corn snake to address the following question: How is the total number of somites regulated in a given vertebrate species? The idea was to compare the differences in the regulation of somitogenesis between the corn snake that forms a large number of somites (315), and those species currently studied in the somitogenesis field (mouse, chicken, zebrafish) that form less somites.

Using a reptile as an animal model was a new approach in the laboratory. Developmental stages of corn snake embryos had never been described and gene sequences or expression never characterized. Specific techniques, such as *in situ* hybridization or embryo culture, needed prerequisite adaptations.

Corn snake embryos develop fairly slowly compared to other model vertebrates. Eggs required an incubation period of two months at 28ºC before hatching, and the time between fertilization and oviposition was estimated at about one month. Therefore, corn snake embryos developed for a total of about three months between fertilization and hatching. In comparison, chicken required three weeks, zebrafish two days and mouse three weeks (between fertilization and birth).

At oviposition, corn snake embryos had accomplished half of their somitogenesis (Article Figure 1). Depending on the egg clutch, embryos could exhibit between 170 and 200 somites and required about one week to complete somitogenesis. Therefore, we estimated somitogenesis time at about two weeks in corn snake, compared to 16 hours in zebrafish, four days in chicken and six days in mouse. Occasionally, corn snake embryos exhibited less than 170 somites at oviposition, but never less than 100 somites, so that I always missed the first part of somitogenesis. Within a clutch, embryo stages were quite homogenous. I could count a 20-somite difference at most between embryos from large clutches.

I have done the following work with the help of Dr. Ertuğrul Özbudak, a post-doctoral researcher who arrived in the laboratory during the last year of my PhD; Dr.

Julian Lewis, who leads a laboratory in the developmental biology field in the United Kingdom and Dr. Olivier Pourquié, my advisor. Ertuğrul generated the data on zebrafish embryos and helped me, with Julian and Olivier, to analyze the results of the comparative study (which I will present below) using mathematical tools.

Summary of the article results

Corn snake embryos exhibit a large number of somite (315) compared to mouse (65), chicken (55) and zebrafish (31). I first checked how much of the segmentation mechanism was conserved in corn snake by cloning and visualizing the expression of the different genes associated with somitogenesis by *in situ* hybridization. Genes associated with the determination front *(Fgf8, Wnt3a, Mespo, EphA4, Raldh2* and *Paraxis*) and the somitic compartments *(Uncx4.1* and *MyoD*) exhibited a conserved expression pattern, suggesting that the gradient system involved in forming the determination front, as well as somite specification and differentiation, were conserved between corn snake and other vertebrates (Article Figure 2b,e,g,k,l,m, and article supplemental Figure 1). Surprisingly, among cyclic genes, *Lfng* expression consisted of multiple stripes (up to nine), dynamically expressed in the PSM. No expression was ever detected in the tail bud (Article Figure 2h-j). The diversity in the *Lfng* expression patterns observed on 39 embryos strongly suggested that *Lfng* stripes corresponded to several traveling waves in the PSM, hence arguing that *Lfng* could be cyclic in the corn snake PSM. I did not observe any cyclic genes from the Fgf (*Sprouty2* and *Dusp6*) and Wnt (*Axin2*) pathways (Article Figure 2 c,d,f).

I compared the amino acid sequences of corn snake cloned translated fragments of DNA with the corresponding orthologous sequences in chicken, mouse, *Xenopus laevis* or *tropicalis* and zebrafish (Table 4 in appendix). These sequences were cloned by nested PCR using primers designed from conserved regions between species and do not represent full-length sequences, except for *Paraxis*. Interestingly, all the corn snake sequences were closer to chicken, with 67% to 98 % identity according to the protein. This is consistent with birds being the closest relatives to reptiles. I did not find any good chicken sequences for *Uncx4.1* gene. In this case, corn snake *Uncx4.1* fragment was closer to mouse sequence, with 85.4 % identity (see Table 4 in appendix for further comparisons between species).

In conclusion, the conservation of gene expression patterns suggested that

corn snake somitogenesis relied on mechanisms based on the "Clock and Wavefront" model, like other vertebrates. However, *Lfng* expression pattern suggested a difference in the segmentation clock regulation.

We postulated that the increased somite number observed in corn snake could depend on factors regulating its axis growth and its somite size (for example, the smaller the somites dividing the axis length, the more somites). Somite size was proposed to be determined by the distance travelled by the determination front in the PSM within one clock period (Dubrulle et al., 2001). Hence, reducing somite size in a given species could be achieved by accelerating the clock pace or slowing down the speed of the determination front regression in the PSM. This would result in fewer cells allocated per somite. Therefore, clock pace and determination front regression speed were compared between corn snake and other species. The corn snake's clock pace was estimated by calculating the difference in somite number between embryos from the same clutch, incubated during different amounts of time. By this approach, the corn snake's clock period was estimated at 90 minutes per somite formation. The same was observed in chicken, whereas a clock period of 120 minutes was described in mouse and 30 minutes in zebrafish.

Mesogenin1/Mespo represents a good marker to locate the determination front position in the PSM (see Figure 16 in introduction). *In situ* hybridizations using this marker were performed on chicken, mouse, zebrafish and corn snake embryos throughout somitogenesis (Article Figure 3). The speed of the determination front was calculated for each species (see "Material and Methods"), and the corn snake's speed was found to be twice as slow as other species (Figure 22). As corn snake clock ticks at the same speed or faster than chicken and mouse clocks, respectively, a slower regression of the determination front in corn snake should lead to smaller somites compared to mouse and chicken. Zebrafish clock is three and four times faster than chicken and mouse, respectively, and the speed of regression of its determination front is similar. Therefore, zebrafish somites should be smaller than mouse and chicken somites as well. When the newly formed somite (called "S1") sizes were finally compared on each embryo of the time course, smaller somites were indeed observed in corn snake and zebrafish, compared with chicken and mouse (Article Figure 4c). Hence, these results explain perfectly somite size in the different vertebrate species.

What information about the regulation of somite number can be extracted

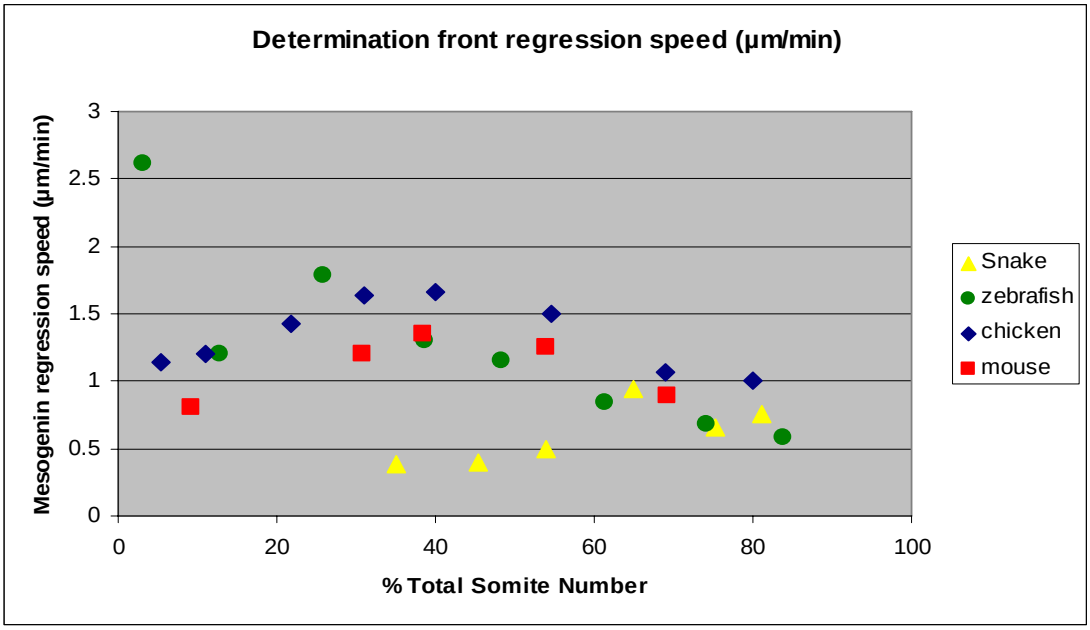

Figure 22. Determination front regression speed in the PSM of four species. Speeds have been calculated in µm/minute (y-axis) and are presented as a function of the percentage of total somite number (x-axis) for corn snake (yellow), zebrafish (green), chicken (blue) and mouse (red).

from these measurements? How can we compare clock paces and determination front regression speeds between species that do not develop at the same rate? In other words, is there a manner to compare the somitogenesis of these species in a normalized way, which could make the measurements comparable and help identify the parameters responsible for somite number variation? Further investigations are presented below.

PSM size was measured on each embryo from the *Mesogenin1/Mespo* time-course experiment. Results showed that in amniotes, PSM first increased in size before decreasing until somitogenesis terminated (Article Figure 4a). Maximal PSM lengths were not drastically different, even if corn snake had the longest PSM. In zebrafish, PSM size decreased almost since the start of somitogenesis (Article Figure 4a).

The ratio between *Mesogenin1/Mespo* domain size and PSM size was calculated. This ratio gives the relative position of the *Mesogenin1/Mespo* anterior limit of expression (or determination front) in the PSM of the different species. This position appeared to be regulated in the same manner in all the species. The determination front was always at the same relative position in the PSM of each species both during the increase and the decrease of PSM size (Article Figure 4e). These results suggested that over the course of somitogenesis, mechanisms controlling the determination front position in the PSM were conserved between vertebrate species. This also suggested that the determination front position and regression was linked to axis growth. Hence, the similar regulation of determination front position in the PSM between species suggested that the speed of the determination front regression in the PSM could not be a parameter explaining variation in somite number. Therefore, the slow speed of determination front regression observed in corn snake does not correspond to a difference in somitogenesis regulation *per se*, but rather illustrates the slow rate of development of this species compared to the others.

A mathematical model using an equation describing the exponential growth of a population of cells, and taking into account the clock pace, the total somite number of each species as well as the measurements of PSM and somite S1 lengths, enabled us to estimate the time and number of "PSM generations" needed to generate the specific number of somites in each species (Article Box 1 and supplementary Box). "PSM generation" in our model is defined by the time needed by the PSM for

doubling its size. Corn snake PSM generation time was found to be significantly longer, in agreement with its overall slow rate of development. Interestingly, it appeared that the number of PSM generations (that is the number of times the PSM doubles in size, up to the end of somitogenesis) were quite close between amniotes, suggesting that they use similar mechanisms to grow their axis. In conclusion, these results suggested that among amniotes, axis growth and determination front regression speed were similarly regulated and for this reason, could not play a preponderant role in explaining the variation of total somite number.

Therefore, the only parameter that appeared differently regulated between amniotes was the clock pace relative to the PSM generation time, or axis growth rate. A clock pace of 90 minutes in corn snake appears much faster relative to its slow developmental rate than a clock pace of 90 minutes in chicken. Hence, according to our data, the difference in the regulation of clock pace relative to axis growth rate in corn snake would mainly account for the difference in total somite number with other amniotes.

In zebrafish, things are slightly different. First, the number of PSM generations needed to complete somitogenesis is much smaller than in amniotes, suggesting that a "premature" arrest of axis growth in zebrafish explains the reduced total somite number (See supplementary box in the article, Table 1). Second, zebrafish somite size is close to corn snake, suggesting that zebrafish clock pace relative to its axis growth rate is close to the corn snake's. Therefore, these results suggested that the main parameters explaining the reduced somite number in zebrafish compared with corn snake was the small capacity of zebrafish axis growth.

A recent study in zebrafish showed that the cyclic gene expression patterns obtained by *in situ* hybridization could be used to describe the dynamics of the propagation of the cyclic gene waves in the PSM (Giudicelli et al., 2007). The propagation of these waves is characterized by a gradual slowing down along the postero-anterior axis of the PSM, which is amplified when the wave passes the determination front. The number of waves traveling at the same time in the PSM reflects the number of cycles (or number of times a wave has been initiated at the posterior end of the PSM) by which the anterior PSM cells are delayed relative to posterior PSM cells. Measurements of the distance between each cyclic gene wave on *in situ* hybridization pictures, and the positioning of these waves relative to PSM length can be used in a mathematical model to extract parameters (like the local

wavelength, or local period of the cells) describing the wave propagation in the PSM. This method was applied to the corn snake *Lfng* expression pattern (Article Figure 4f and Box 2). Figure 4f in the article represents the local period of the corn snake and zebrafish PSM cells (y-axis) as a function of PSM length (x-axis). The posterior PSM is at the "zero" level on the x-axis, and the anterior PSM is at the "1" level, indicating its full length in a normalized way. The curves show that the cell period lengthens as the wave moves anteriorly, reflecting the slowing down of the cyclic gene wave. This slowing down is suddenly amplified (at 60% of the PSM length) which is thought to reflect the passage through the determination front. Corn snake *Lfng* waves behaved similarly to zebrafish cyclic gene waves in the PSM as shown by the overlapping curves, suggesting similar mechanisms of cyclic gene waves slowing down in the PSM of both species. If the mechanisms of slowing down of cyclic genes are conserved between species, our mathematical modeling indicates that the number of cyclic gene waves in the PSM become proportional to the clock period relative to the time of cell divisions (PSM growth rate). Hence, our model indicates that in snake, the increased number of *Lfng* waves in the PSM is due to a faster clock period relative to the slow rate of axis growth. More generally, the faster the clock period compared with axis growth rate, the more stripes of cyclic genes in the PSM (Article Box 2).

In conclusion, our studies suggest that two main parameters regulate somite number in vertebrates: the number of PSM generations (which is the parameter that contributes the most to zebrafish somitogenesis compared with amniotes) and the speed of somite formation (clock pace) within the time to complete the number of PSM generations (which is the parameter that contributes the most to amniote somitogenesis). The number of cyclic gene waves traveling at the same time in the PSM can be considered as a readout of the clock pace relative to axis growth rate.

ARTICLE (SUBMITTED)

Control of segment number in vertebrate embryos

Céline Gomez[1], Ertuğrul M. Özbudak[1], Diana Baumann[1], Julian Lewis[2], Olivier Pourquié[1,3]

[1]Stowers Institute for Medical Research, Kansas City, Missouri 64110 USA.
[2]Vertebrate Development Laboratory, Cancer Research UK, London Research Institute, London WC2A3PX, UK.
[3]Howard Hughes Medical Institute, Kansas City, Missouri 64110, USA.

The vertebrate body axis is subdivided into repeated segments, best exemplified by the vertebrae that derive from embryonic somites. The number of somites is precisely defined for any given species but varies widely from one species to another. To determine the mechanism controlling somite number, we have compared somitogenesis in the embryos of zebrafish, chick, mouse and corn snake. Here we present evidence that in all these species, a similar Clock-and-Wavefront mechanism operates to control somitogenesis, and in all of them, somitogenesis is brought to an end through a process in which the presomitic mesoderm, having first increased in size, then gradually shrinks until it is exhausted, terminating somite formation. In snake embryos, however, the rate of ticking of the segmentation clock is much faster relative to growth rate than in other amniotes, leading to a greatly increased number of smaller-sized somites.

Vertebrate segment formation is thought to depend on a periodic signal generated by an oscillator or clock acting in the presomitic mesoderm (PSM)[1,2]. This signal is translated into the periodic series of somites by a traveling wavefront of maturation slowly moving posteriorly along the embryonic axis[1]. The Clock-and-Wavefront model is supported by the existence of a molecular oscillator known as the segmentation clock, which operates in the PSM to drive the periodic activation of a signaling network involving the Notch, Wnt and FGF pathways[2,3]. The wavefront, or determination front, is defined by a gradient system involving FGF and Wnt signaling that regresses in concert with axis elongation[4-6]. At a particular threshold of FGF/Wnt signaling (the determination front), cells of the PSM become committed to form segment boundaries according to the rhythmic signal generated by the clock. This process at the level of the determination front results in the periodic generation of stripes of expression of the gene *Mesoderm posterior 2* (*Mesp2*) that codes for a key transcription factor that defines the boundaries and establishes the rostro-caudal identity of future segments[7].

The number of somites, and hence of vertebrae, is highly variable among vertebrate species[8]. For instance, frogs have around 10 vertebrae, while humans have 35 and snakes can have more than 300. To gain insight into the mechanisms controlling somite numbers in vertebrates, we compared somitogenesis in a reptile, the corn snake *Pantherophis guttatus*, which makes a large number of somites (315), with three other vertebrate species that make far fewer: a teleost, the zebrafish *Danio rerio* (31); a bird, the chicken *Gallus gallus* (55) and a mammal, the mouse *Mus musculus* (65).

The corn snake belongs to the highly derived family of colubrids. Its vertebral column comprises around 295 vertebrae, including two cervical, 219 thoracic, four cloacal, and 70 post-cloacal caudal (Fig. 1a). The female lays eggs once a year in one to two clutches of 10 to 25 eggs. Eggs are laid around 30 to 50 days after mating, but the exact time of fertilization is difficult to determine precisely because the females can store the sperm for long periods of time. Eggs hatch after a two-month incubation period at 28°C. Depending on the clutch, corn snake embryos exhibit between 110 to 200 somites at oviposition and add somites progressively until the total number of 315 somites is reached within days 7 to 9 post-oviposition (Fig. 1b). Thus, the snake develops much slower compared to zebrafish, chick or mouse and takes far longer to generate its full set of somites.

We next examined, by in situ hybridization, the expression of the corn snake homologues of genes involved in the generation of the Wnt and FGF gradients and the positioning of the determination front (Fig. 2a). These include *Fibroblast growth factor 8 (Fgf8*) (Fig. 2b) and its targets, *Sprouty 2* (*Spry2*) (Fig. 2c), and *Dual specificity phosphatase 6* (*Dusp6*) (Fig. 2d)[3,9], as well as *Wnt3a* (Fig. 2e), and its PSM targets *Axin2* (Fig. 2f)[6]and *Mesogenin1/Mespo* [10](Fig. 2g) . Except for *Spry2*, which was not detected in the PSM, all of these genes were expressed in analogous domains when compared to their fish or amniote counterparts[5,11,12]. *Eph receptor A4* (*Epha4*), one of the direct targets of the Mesp2 transcription factor[13] that marks the determination front level, shows two to four stripes of expression in the anterior PSM (Fig. 2k). The position of these stripes is consistent with their lying anterior to the determination front, whose position would thus be located immediately anterior to the *Mesogenin1/Mespo* domain as in fish, chick and mouse[14-16].

We then examined the expression of genes activated anterior to the determination front. In snake embryos, both *Raldh2*, the retinoic acid biosynthetic enzyme (Fig. 2l) that was shown to establish a gradient antagonizing the posterior FGF gradient[17,18], and *Paraxis* (Fig. 2m), that is required in the anterior PSM for somite epithelialization[19], were expressed in the segmented region and in an anterior domain of the PSM complementary to the *Mesogenin1/Mespo* domain. Expression of mature somite markers, such as *Uncx4.1* that labels the posterior compartment of the forming somites[20] and *MyoD* whose expression is associated with the developing muscle lineage[21,22], suggests that somites are patterned and develop in a similar fashion to other amniotes (Supplementary Fig. 1) and that a Wnt/FGF posterior gradient system opposes an anterior retinoic acid gradient in snakes as in other vertebrates[11,12,23].

Studies in chick have shown that the *Fgf8* gene is transcribed in cells of the tail bud, which thus creates the high point of a signaling gradient in the PSM[24]. While cells are removed from the PSM anteriorly by somitogenesis, the cells within the PSM proliferate, and new cells strongly expressing FGF and Wnt ligands are continually added caudally, elongating the body axis. The FGF signal, in concert with Wnt signals, is thought to keep the PSM cells in an uncommitted, oscillating, proliferative state and thus, governs the balance between somitogenesis and tail extension[11,12]. As long as appropriate production of these factors is maintained or increased, the size of the PSM will be maintained or increased, and segments will continue to be formed. Conversely, if production or efficacy of these factors declines, the PSM will progressively shrink until it becomes entirely segmented into somites, bringing somitogenesis to an end.

Figs. 3 and 4a show our measurements of the changing size of the PSM. In zebrafish, the PSM length decreases from the beginning of somitogenesis. In contrast, in amniote embryos, it first increases and finally decreases in size until the arrest of somitogenesis. Strikingly, even though snakes make the longest PSM, this maximal length is not very different among the four species (Fig. 4a). Moreover, in all four species, the PSM becomes shorter and shorter as somitogenesis nears its end. Therefore, our data support a model in which termination of somitogenesis is caused by exhaustion of the PSM. It is also evident that there is an important difference between fish and amniotes in the timing of the onset of the PSM shortening process.

How do these findings help to explain the remarkable species differences in somite numbers? If we assume a conserved somite patterning mechanism, then the final

somite number will be solely determined by the number of cycles of the segmentation clock prior to depletion of the PSM. This logic predicts that either the snake segmentation clock is faster than in other vertebrates, or that the relative developmental lifetime of the snake PSM is extended to allow additional rounds of somite formation, or both. To test this prediction, while accounting for the different developmental time scales between species, we used the generation time of the PSM cell population (in other words, roughly speaking, the average cell-cycle time in the PSM; see Box 1 for a precise definition) as a standard biological time unit. In the steady state when PSM growth and segmentation are in balance so that somites are being generated steadily and at a steady size, the length of each new somite will equal the length of new tissue generated in the PSM in the course of one tick of the segmentation clock. The shorter the clock period relative to the PSM generation time, the smaller this length will be. Thus, the length of a newly formed somite, s_1, as a fraction of the length of the PSM, L, (Fig. 4b) gives a measure of the duration of a segmentation clock cycle as a fraction of the PSM generation time (Box 1). This argument can be generalized to the non-steady-state case where the PSM is changing in length (see Supplementary Information). We observed that snake somites are clearly smaller when compared to other amniotes (Fig. 4c). When compared to PSM size, we see that in the snake, the somite size, s_1 is on average only about 5% of the PSM length as compared with 18% in the mouse, 19% in the chick and 11% in the zebrafish (Fig. 4b). This leads to the unexpected conclusion that the difference in somite number among these amniotes is almost entirely because the snake segmentation clock period is short compared with the PSM generation time: the calculated number of PSM generations in the snake (~21), from the beginning of somitogenesis to the time of PSM exhaustion, is only a little greater than in the mouse (~16) or the chick (~13) (see Supplementary Information). The zebrafish, however, with a PSM that lasts for only 2.8 generations, is very different from the three amniotes. The rapid exhaustion of the PSM in the fish and its lack of an initial phase of PSM enlargement suggest that its mechanisms of PSM maintenance may be markedly different.

Given the large quantitative differences of somite number and developmental tempo, one must ask whether the Clock-and-Wavefront mechanism operates according to similar principles in the various species. We have already seen that the wavefront seems to be determined similarly (Fig. 2), but how is this coupled to the behavior of the clock? To answer this question, we first examined the expression of the *Mesogenin1/Mespo* gene. The anterior boundary of this gene's expression domain lies within the PSM, and its regression provides a marker of the regression of the wavefront. We first measured the speed of the *Mesogenin1/Mespo* anterior boundary posterior regression during somitogenesis in all four species, and show that it moves by one somite length during one period independent of the stage of somitogenesis and the species type (Fig. 3 and Fig. 4d and Supplementary Fig. 2). Therefore, this validates an important prediction of the Clock-and-Wavefront model–that somite size corresponds to the distance traveled by the wavefront during one oscillation period. We then plotted the ratio of *Mesogenin1/Mespo* expression domain to PSM size as a function of stage for each species (Fig. 4e). Strikingly, a similar ratio was observed throughout somitogenesis in all four species, suggesting that although the size of the PSM varies dramatically according to stage and species, similar processes are occurring but scaled proportionately.

To further explore how the regulation of the snake segmentation clock compares with that of other vertebrates, we measured the average rate of somite formation by sampling embryos from the same clutch at various times of incubation. The segmentation cycle time (the time taken to make one pair of somites) of the snake averages 90 minutes; the corresponding time of the chick embryo is also 90 minutes, for the mouse 120 minutes and for the zebrafish 30 minutes. However, this period has to be related to the comparatively slow development of reptiles [25]. This supports the idea that the increase in total somite number observed in snakes could be accounted for by a relative acceleration of the segmentation clock compared to the growth rate.

We examined the expression of cyclic genes associated with the amniote segmentation clock in snake embryos. No oscillations of the FGF or Wnt target genes *Spry2*, *Dusp6*[3] or *Axin2*[6]could be evidenced (Fig. 2c, d, f). The Notch target *Lunatic fringe (Lfng)* exhibited within the PSM a very unexpected expression pattern that consisted of up to nine stripes of variable size and spacing, and lacked the posterior-most expression domain seen in mouse and chick (Fig. 2h-j)[26,27]. Thirty-nine snake embryos were hybridized with *Lfng* and virtually all of them showed a different expression pattern, consistent with this gene oscillating in the snake embryo (Fig. 2h-j and data not shown). Altogether, these observations support the existence of an oscillator driving cyclic gene expression in the PSM of snake embryos. However, its regulation at first sight appears quite different from that of other vertebrate species studied thus far.

We next investigated the basis for this striking increase in the number of *Lfng* stripes observed in snake embryos. The stripes of cyclic gene mRNAs are a reflection of the gradual slowing of the gene expression oscillations in the cells as they move from the posterior PSM (where the oscillation runs fastest) to the anterior border of the PSM (where the oscillation is arrested). Hence, the number of stripes in the PSM reflects the total phase difference between cells at opposite ends of the PSM ($\Delta\Phi$, see Box 2); that is, the number of clock cycles by which the cells at the anterior end of the PSM lag behind those in the posterior PSM. The slowing down of the segmentation clock waves has recently been analyzed in zebrafish embryos. From measurements of the local interstripe distance (the spatial wavelength), one can obtain a graph of the oscillation period in the PSM as a function of distance along its length[28]. We have used the same method to study the slowing down of the oscillations in the snake as indicated by the *Lfng* waves. Fig. 4f shows the graph for the snake based on measurements from 230-somite-stage embryos, overlaid with the previously published zebrafish data and with the distances in each species scaled in proportion to the length of the PSM in that species. The profile of the slowing down of the oscillations in the snake is remarkably similar to that seen in the zebrafish, suggesting that the mechanism controlling this process is similar. As explained in Box 2, the same manner of slowing down in the snake and the zebrafish entails very different numbers of the PSM stripes simply because of the different ratios of oscillator rate to growth rate. Slow growth of the PSM in the snake means that its cells take a long time to move from the posterior of the PSM to its anterior end, and during this period they fall behind the posterior PSM cells by a large number of oscillator cycles, reflected by the large number of stripes in the spatial pattern. Specifically, if we focus on the state of affairs midway through somitogenesis, we see from Fig. 4b that the PSM is about 35 times longer than the length s_1 of a newly formed somite in the snake, but only eight times longer than s_1 in the zebrafish and only five times longer than s_1 in the mouse or

chick, implying that the ratio of the PSM generation time to clock cycle time is about four to seven times greater in the snake than in the other species (see Box 1). From the analysis in Box 2, we hence predict that there should be four to seven times as many stripes in the PSM at this stage; this agrees with the observations and suggests that the model accurately describes the behavior of the traveling waves generated by the segmentation clock in these different species and that the FGF/Wnt gradient controls the slowing and arrest of the clock in a similar way in all four species.

Taken together, our data show that the basic Clock-and-Wavefront mechanism operates according to similar principles in snake, chick, mouse and zebrafish. The period of the segmentation clock, however, bears no fixed relation to the rate of development as defined in terms of PSM cell generation time or to the time for which somitogenesis continues. This argues strongly that the segmentation clock and the cell cycle represent two independent, uncoupled oscillation mechanisms. Our modeling suggests that one parameter that changes rather little among amniotes is the number of PSM generations for which somitogenesis continues.

This then raises the question of what determines the number of PSM generations that elapse in the course of somitogenesis; in other words, what determines when the process ends? In all four species, somitogenesis ends with a progressive shrinking of the PSM. This shrinking presumably reflects a gradual extinction of the signals that maintain the PSM character of cells at the tail end of the embryo. Our data indicate that these signals are extinguished after a roughly similar number of PSM generations in snakes, mouse and chick. The proximity of the anterior retinoic acid domain to the tail bud caused by the PSM shrinking could trigger the differentiation or the death of these precursors, thus causing the arrest of axis elongation and termination of somitogenesis.

We show that in the four species studied here, there is a "timing mechanism" that dictates when the switch between the PSM elongation mode to the shortening mode occurs. In the zebrafish, the early PSM enlargement phase seen in amniotes is absent, and this correlates with a small somite number. In amniotes, a switch from PSM enlargement to PSM shrinkage occurs at the transition between the trunk and tail region, suggesting that it might be under the control of regional regulators such as *Hox* genes. Our work indicates that evolution plays freely on the segmentation clock pace and on the cell cycle, and that the ratio of these two parameters ultimately controls segment number.

Methods

Corn snake eggs (176) were placed in humidified vermiculite and incubated at 28°C in a humidified incubator. Fertilized chick eggs were obtained from Ozark Hatcheries (Neosho, MO) and incubated at 38ºC in a humidified incubator. Embryos were staged according to Hamburger and Hamilton (HH)[29]. Wild-type CD1 mice embryos were harvested from timed-mated pregnant females between 8.0 and 13.5 days postcoitum (dpc). Zebrafish (*Danio rerio*) embryos were obtained from natural crosses (Zebrafish International Resource Center at the University of Oregon [ZIRC]) AB strain, maintained at 28.5°C and staged according to hours post-fertilization at 28.5°C. Embryos of the different species were harvested at different days of incubation and fixed overnight at 4°C in 4% formaldehyde and dehydrated in methanol. Total RNA from a one-day incubated, frozen snake embryo was isolated by Trizol extraction (Invitrogen) and used for PCR amplification of the snake genes using standard protocols. Sequences of the

snake genes used in this study were deposited in GeneBank. Antisense Digoxygenin-labeled probes were produced from the cloned snake constructs. Whole-mount in situ hybridization was performed as described[30] with a hybridization temperature of 58°C. For measurements, embryos or tails of embryos of the four species were hybridized with a *Mesogenin1/Mespo* probe in whole mount, and flat-mounted and photographed. Then, the size of the PSM, the somite s_1 size and the size of the *Mesogenin1/Mespo* domain in μm were measured using a Zeiss LSM image browser software. Embryos were pooled in groups of five based on their somite number. Measurements corresponding to each pool were averaged and the standard deviation calculated (see Supplementary Fig. 2). For the calculation of the slowing down of the period along the PSM in corn snake, interstripe distance was measured using the Zeiss LSM software in two-day-old embryos stained with *Lfng* and calculations were performed as described[28]. Alizarin staining was performed according to standard procedures.

Figures legends

Figure 1 Vertebral formula and somitogenesis in the corn snake.
a, Alizarin staining of a corn snake showing the 295 vertebrae, including two cervical, 219 thoracic, four cloacal (distinguishable by their forked lymphapophyses), and 70 caudal.
b, Time-course of corn snake development from day 1 after egg laying (118-somite embryo on the far left), until the end of somitogenesis at day 9 (315 somites).

Figure 2 The corn snake determination front and segmentation clock.
a, Schematic drawing of a corn snake tail showing the position of the determination front in the PSM. **b-m,** Whole-mount in situ hybridizations of 230-somite (**b-k**) and 260-somite (**l,m**) corn snake embryo tails: *Fgf8* (**b**), *Spry2* (**c**), *Dusp6* (**d**), *Wnt3a* (**e**), *Axin2* (**f**), *Mesogenin1/Mespo* (**g**), *Lfng* (**h-j**), *Epha4* (**k**), *Raldh2* (**l**) and *Paraxis* (**m**). Anterior to the top.

Figure 3 Dynamics of the PSM size in zebrafish, corn snake, chick and mouse.
a-t, Developmental series of four vertebrate species hybridized with *Mesogenin1/Mespo* in whole mount. Zebrafish embryos are shown at one somite (**a**), 8 somites (**e**), 12 somites (**i**), 19 somites (**m**), and 30 somites (**q**). Corn snake embryos are shown at 165 somites (**b**), 202 somites (**f**), 251 somites (**j**), 291 somites (**n**), and 310 somites (**r**). Chick embryos are shown at six somites (**c**), 17 somites (**g**), 22 somites (**k**), 30 somites (**o**), and 44 somites (**s**). Mouse embryos are shown at six somites (**d**), 20 somites (**h**), 35 somites (**l**), 45 somites (**p**), and 55 somites (**t**). Anterior to the top. Scale bars correspond to 100 μm for zebrafish and 200 μm for corn snake, chick and mouse. Graphs to the right show the size evolution (in micrometers) in time of the PSM, of s_1 (green) and the *Mesogenin1/Mespo* domain (purple) in chick, corn snake, mouse and zebrafish embryos.

Figure 4 Comparison of somitogenesis parameters.
a-f, Graphs show measurements in zebrafish (turquoise), corn snake (lavender), chick (dark blue), and mouse (red) embryos. (**a**) Dynamics of the PSM size during somitogenesis. (**b**) Dynamics of s_1 size during somitogenesis. (**c**) Variation of the PSM

size to s_1 size ratio during somitogenesis. (**d**) Speed of the *Mesogenin1/Mespo* boundary in period units normalized by s_1 size. (**e**) Variation of the ratio of the *Mesogenin1/Mespo* domain size over the PSM size during somitogenesis. (**f**) Slowing down of the oscillation period along the PSM.

References

1. Cooke, J. & Zeeman, E.C. A clock and wavefront model for control of the number of repeated structures during animal morphogenesis. *J.Theor.Biol.* 58, 455-476 (1976).
2. Palmeirim, I., Henrique, D., Ish-Horowicz, D. & Pourquié, O. Avian hairy gene expression identifies a molecular clock linked to vertebrate segmentation and somitogenesiss. *Cell* 91, 639-648 (1997).
3. Dequeant, M.L. *et al.* A complex oscillating network of signaling genes underlies the mouse segmentation clock. *Science* 314, 1595-1598 (2006).
4. Dubrulle, J., McGrew, M.J. & Pourquie, O. FGF signaling controls somite boundary position and regulates segmentation clock control of spatiotemporal Hox gene activation. *Cell* 106, 219-232 (2001).
5. Sawada, A. *et al.* Fgf/MAPK signalling is a crucial positional cue in somite boundary formation. *Development* 128, 4873-4880 (2001).
6. Aulehla, A. *et al.* Wnt3a plays a major role in the segmentation clock controlling somitogenesis. *Dev Cell* 4, 395-406 (2003).
7. Morimoto, M., Takahashi, Y., Endo, M. & Saga, Y. The Mesp2 transcription factor establishes segmental borders by suppressing Notch activity. *Nature* 435, 354-359 (2005).
8. Richardson, M.K., Allen, S.P., Wright, G.M., Raynaud, A. & Hanken, J. Somite number and vertebrate evolution. *Development.* 125, 151-160 (1998).
9. Delfini, M.C., Dubrulle, J., Malapert, P., Chal, J. & Pourquie, O. Control of the segmentation process by graded MAPK/ERK activation in the chick embryo. *Proc Natl Acad Sci U S A* 102, 11343-11348 (2005).
10. Wittler, L. *et al.* Expression of Msgn1 in the presomitic mesoderm is controlled by synergism of WNT signalling and Tbx6. *EMBO Rep* 8, 784-789 (2007).
11. Dubrulle, J. & Pourquie, O. Coupling segmentation to axis formation. *Development* 131, 5783-5793 (2004).
12. Aulehla, A. & Herrmann, B.G. Segmentation in vertebrates: clock and gradient finally joined. *Genes Dev* 18, 2060-2067 (2004).
13. Nakajima, Y., Morimoto, M., Takahashi, Y., Koseki, H. & Saga, Y. Identification of Epha4 enhancer required for segmental expression and the regulation by Mesp2. *Development* 133, 2517-2525 (2006).
14. Yoo, K.W. *et al.* Characterization and expression of a presomitic mesoderm-specific mespo gene in zebrafish. *Dev Genes Evol* 213, 203-206 (2003).
15. Yoon, J.K., Moon, R.T. & Wold, B. The bHLH class protein pMesogenin1 can specify paraxial mesoderm phenotypes [In Process Citation]. *Dev Biol* 222, 376-391 (2000).

16. Buchberger, A., Bonneick, S. & Arnold, H. Expression of the novel basic-helix-loop-helix transcription factor cMespo in presomitic mesoderm of chicken embryos. *Mech Dev* 97, 223-226 (2000).
17. Niederreither, K., Subbarayan, V., Dolle, P. & Chambon, P. Embryonic retinoic acid synthesis is essential for early mouse post-implantation development. *Nat Genet* 21, 444-448 (1999).
18. Diez del Corral, R. *et al.* Opposing FGF and retinoid pathways control ventral neural pattern, neuronal differentiation, and segmentation during body axis extension. *Neuron* 40, 65-79 (2003).
19. Burgess, R., Cserjesi, P., Ligon, K.L. & Olson, E.N. Paraxis: a basic helix-loop-helix protein expressed in paraxial mesoderm and developing somites. *Dev Biol.* 168, 296-306 (1995).
20. Mansouri, A. *et al.* Paired-related murine homeobox gene expressed in the developing sclerotome, kidney, and nervous system. *Dev Dyn.* 210, 53-65 (1997).
21. Sassoon, D. *et al.* Expression of two myogenic regulatory factors myogenin and MyoD1 during mouse embryogenesis. *Nature* 341, 303-307 (1989).
22. Pownall, M.E. & Emerson, C.P.J. Sequential activation of three myogenic regulatory genes during somite morphogenesis in quail embryos. *Dev Biol.* 151, 67-79 (1992).
23. Diez del Corral, R. & Storey, K.G. Opposing FGF and retinoid pathways: a signalling switch that controls differentiation and patterning onset in the extending vertebrate body axis. *Bioessays* 26, 857-869 (2004).
24. Dubrulle, J. & Pourquie, O. fgf8 mRNA decay establishes a gradient that couples axial elongation to patterning in the vertebrate embryo. *Nature* 427, 419-422 (2004).
25. Zug, G.R., Vitt, L.J. & Caldwell, J.P., *Herpetology : an introductory biology of amphibians and reptiles*, 2nd ed. (Academic Press, San Diego, Calif., 2001).
26. McGrew, M.J., Dale, J.K., Fraboulet, S. & Pourquie, O. The lunatic fringe gene is a target of the molecular clock linked to somite segmentation in avian embryos. *Curr Biol* 8, 979-982 (1998).
27. Forsberg, H., Crozet, F. & Brown, N.A. Waves of mouse Lunatic fringe expression, in four-hour cycles at two-hour intervals, precede somite boundary formation. *Curr.Biol.* 8, 1027-1030 (1998).
28. Giudicelli, F., Ozbudak, E.M., Wright, G.J. & Lewis, J. Setting the Tempo in Development: An Investigation of the Zebrafish Somite Clock Mechanism. *PLoS Biol* 5, e150 (2007).
29. Hamburger, V. & Hamilton, H.L. A series of normal stages in the development of the chick embryo (1951). *Dev.Dyn.* 195, 231-272 (1992).
30. Henrique, D. *et al.* Expression of a Delta homologue in prospective neurons in the chick. *Nature* 375, 787-790 (1995).

Supplementary Information is linked to the online version of the paper at www.nature.com/nature.

Acknowledgments We thank M. Gibson, B. Rubinstein, P. Francois and members of the Pourquié Laboratory for critical reading and discussions, members of the Reptile & Aquatics Department, and S. Esteban for artwork. Research was supported by Stowers Institute for Medical Research and in part by DARPA grant HR 0011-05-1-0057. Zebrafish were obtained from the Zebrafish International Resource Center at the University of Oregon and is supported by grant #RR12546 from the NIH-NCRR. O.P. is a Howard Hughes Medical Institute Investigator.

Author contributions C.G. and O.P. designed the experiments, C.G. cloned the snake genes and performed the in situ hybridizations, C.G. and E.O. performed the measurements and analyzed the data with O.P. D.B. established the corn snake and zebrafish colony and produced the embryos. J.L. performed the mathematical modeling. C.G., E.O., J.L. and O.P. wrote the manuscript. All authors discussed the results and commented on the manuscript.

Author information Sequences of genes described in this paper are accessible through GeneBank under accession number XXXXXXXXXXXXX. Reprints and permission information are available at www.nature.com/reprints. Correspondence and request for materials should be addressed to O.P. (olp@stowers-institute.org).

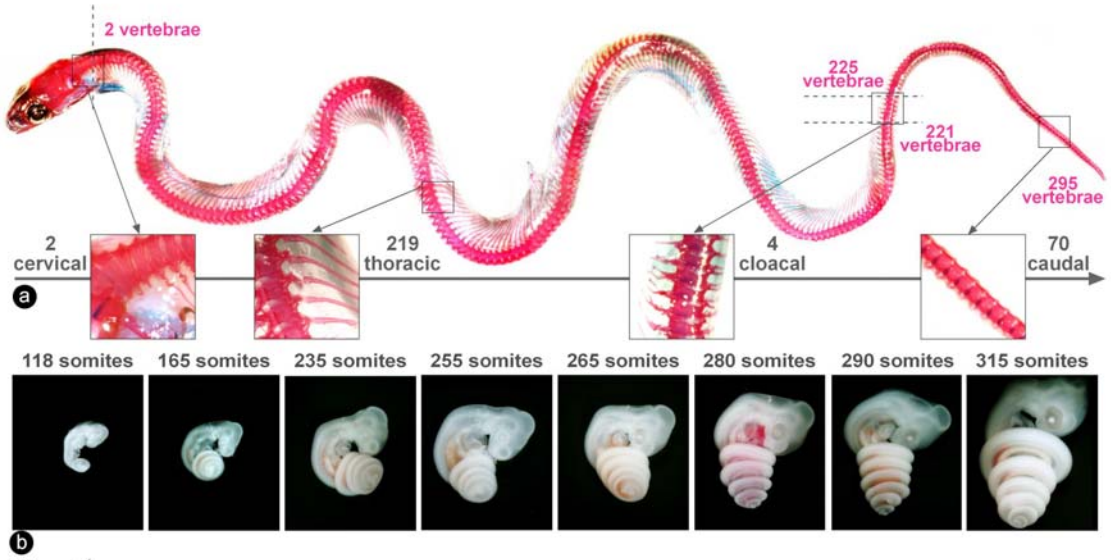

Figure 1

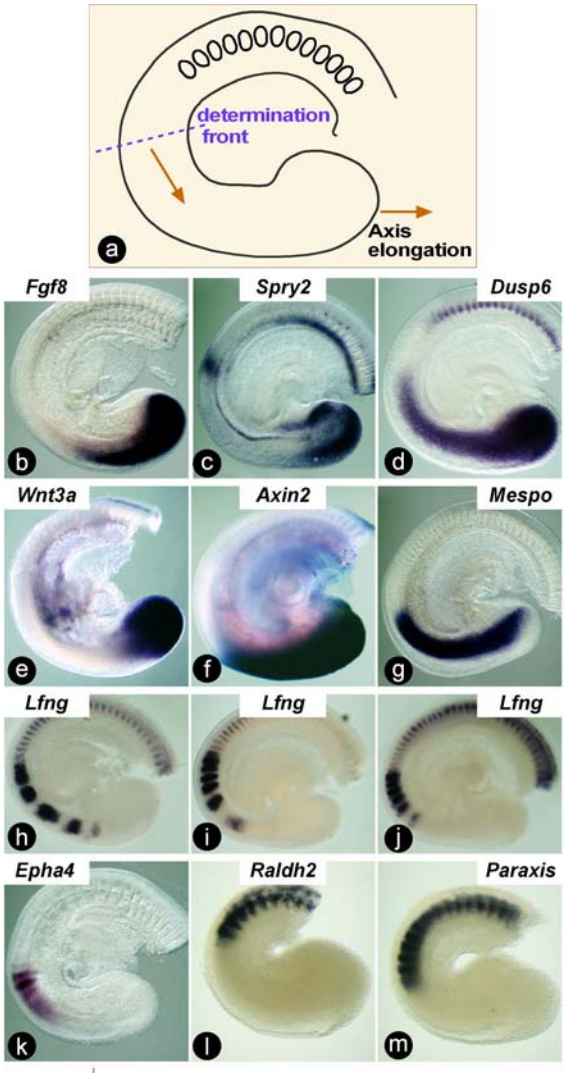

Figure 2

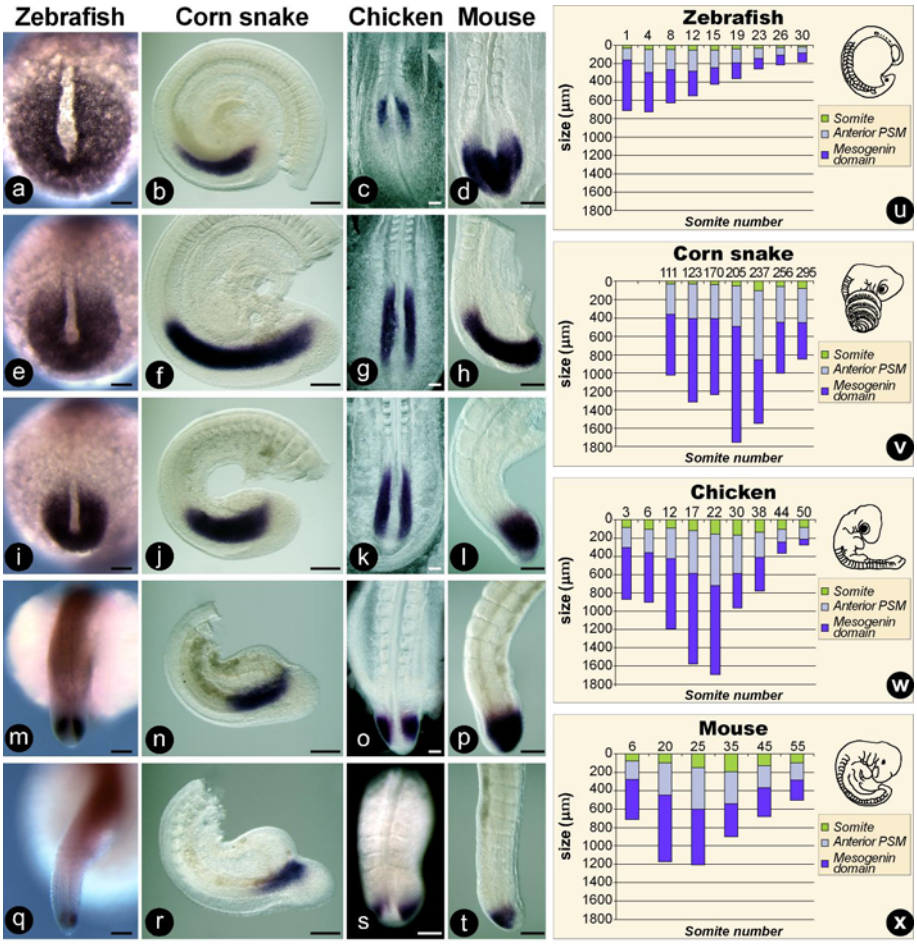
Zebrafish
Corn snake
Chicken
Mouse
a
b
c
d
e
f
g
h
i
j
k
l
m
n
o
p
q
r
s
t
Zebrafish
1 4 8 12 15 19 23 26 30
size (µm)
0 200 400 600 800 1000 1200 1400 1600 1800
Somite number
Somite
Anterior PSM
Mesogenin domain
u
Corn snake
111 123 170 205 237 256 295
v
Chicken
3 6 12 17 22 30 38 44 50
w
Mouse
6 20 25 35 45 55
x

Figure 3

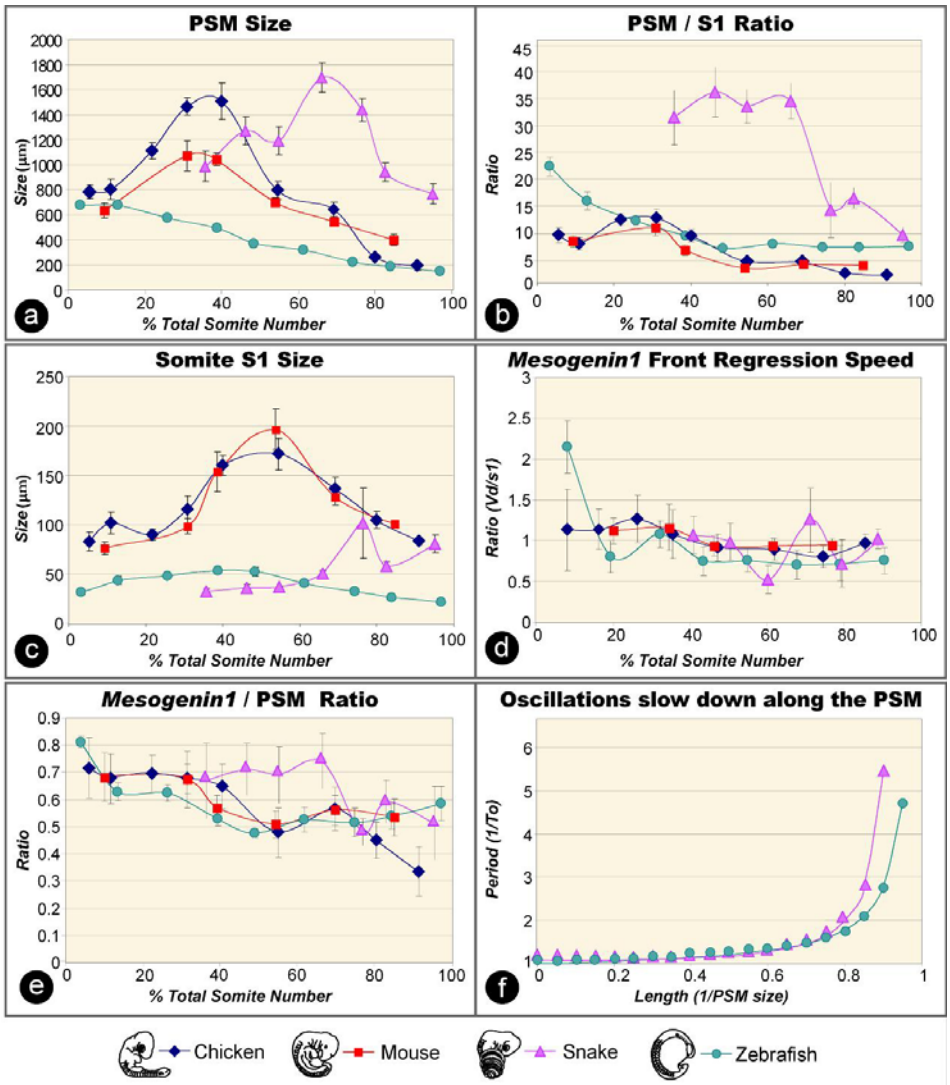
PSM Size
Size (µm)
% Total Somite Number
a
PSM / S1 Ratio
Ratio
% Total Somite Number
b
Somite S1 Size
Size (µm)
% Total Somite Number
c
Mesogenin1 Front Regression Speed
Ratio (Vd/s1)
% Total Somite Number
d
Mesogenin1 / PSM Ratio
Ratio
% Total Somite Number
e
Oscillations slow down along the PSM
Period (1/To)
Length (1/PSM size)
f
Chicken
Mouse
Snake
Zebrafish

Figure 4

Box 1: Why does the snake have so many more segments than other vertebrates?

We consider first the simplified case in which we assume that the cycle time of the segmentation clock, t_s, the length of the PSM, L, the length of a newly formed somite, s_1, and the growth rate in the PSM, α, are all constant over the period of somitogenesis.

Each somite is formed from the set of cells that emerge from the anterior end of the PSM in the course of one cycle of the segmentation clock. The total number of somites formed, n_s, is thus simply equal to the time t_{tot} for which the PSM remains in existence, divided by the duration of one cycle of the segmentation clock, t_s:

$$n_s = t_{tot} / t_s \ . \qquad (1)$$

In the snake, t_s has a value of about 1.5 hours, at least over the period that we are able to observe. This is similar to the value for the mouse or chick, and three times longer than that for the zebrafish, so that we can say immediately that the snake has more segments because somitogenesis continues for a much longer time.

A natural measure of time in a growing system such as the PSM is the tissue generation time. This can be defined as follows. In a time interval dt, the tissue that initially occupied the PSM will elongate, through growth, to a new length L (1 + α dt), where L is the length of the PSM and α is the *mean intrinsic growth rate* in the PSM. We define

$$t_2 = \ln 2 / \alpha \qquad (2)$$

as the *PSM generation time.* (If growth in the PSM is entirely by cell proliferation and is entirely directed along the cranio-caudal axis, it is easily shown that t_2 is simply equal to the cell population doubling time in the PSM.) Then we can write our formula for the number of somites thus:

$$n_s = n_g \, t_2 / t_s \qquad (3)$$

where

$$n_g = t_{tot} / t_2 \qquad (4)$$

is the number of tissue generations that occur in the PSM over the course of somitogenesis.

We can estimate t_2 as follows. If the PSM maintains a constant length, the amount of tissue emerging from it in one cycle t_s of the segmentation clock, and thus the size s_1 of the nascent somite will be equal to the amount of new tissue generated; thus, to a good approximation,

$$s_1 = \alpha \, L \, t_s = \ln 2 \, L \, t_s / t_2 \qquad (5)$$

or in other words,

$$t_2 = \ln 2 \, t_s \, L / s_1, \qquad (6)$$

which implies

$$n_g = (s_1 / L) \, . \, (n_s / \ln 2) \qquad (7)$$

From Figure 4b, we see that during the period of somitogenesis for which we have data in the snake, $[L / s_1]_{snake}$ averages about 25, while $[L / s_1]_{mouse} \sim 5$. Given that $[t_s]_{snake} \sim 90$ minutes, $[t_s]_{mouse} \sim 120$ minutes, and ln2 ~ 0.7, we get

$[t_2]_{snake} \sim 26$ hours

$[t_2]_{mouse} \sim 7$ hours

This important difference is consistent with the overall slower development of snakes.

If the L / s_1 values remained constant throughout somitogenesis, the corresponding estimates for the number of PSM tissue generations would be

$\left[n_g\right]_{snake} \sim 18$

$\left[n_g\right]_{mouse} \sim 19$

given that $[n_s]_{snake} = 315$ and $[n_s]_{mouse} = 65$.

From this rough calculation, we see that the difference of somite number between snake and mouse is accounted for almost entirely by the fact that the PSM generation time for the snake is very much longer than for the mouse (i.e. growth is very much slower). The number of PSM tissue generations required to generate the full set of somites is remarkably similar for the

two species. More exact calculations, allowing for the observed changes in PSM length and somite size over the period of somitogenesis, lead to similar conclusions (see Supplementary Information).

Box 2: Why does the snake have so many stripes in its PSM?

Once a steady state has been reached, in which somites are formed at a steady rate through a steady production process in the PSM - a condition that we can reasonably assume to hold good during the middle part of the period of somitogenesis - we can derive a simple relationship between the observed temporal and spatial oscillations of gene expression.

Let $\phi(x,t)$ denote the phase of the oscillation cycle for a cell at distance x from the tail end of the embryo at time t. If v is the velocity of the cell, its phase at time $t + \mathrm{d}t$ will be

$\phi(x + v\,\mathrm{d}t, t + \mathrm{d}t)$. Thus the rate of change of phase in this cell as it moves along its trajectory (the material derivative of ϕ) is

$$\frac{\mathrm{D}\phi}{\mathrm{D}t} = v\frac{\partial\phi}{\partial x} + \frac{\partial\phi}{\partial t}\,.$$

If we measure ϕ in cycles, $\frac{\mathrm{D}\phi}{\mathrm{D}t}$ is simply the intracellular oscillation frequency in cycles per unit time; in other words

$$\frac{\mathrm{D}\phi}{\mathrm{D}t} = \frac{1}{T}$$

where T is the current value of the period of oscillation in the given cell. We assume that the rate of cycling depends only on the position of the cell relative to the tailbud (as will be the case if, for example, it depends only on the concentration of FGF).

Cells reaching x at different times but having followed the same flowline since leaving the posterior PSM will differ in phase by an amount that simply reflects the difference in their time of exit from the posterior PSM. If cells in the posterior PSM all oscillate with period t_s, it follows that

$$\frac{\partial\phi}{\partial t} = \frac{1}{t_s}\,,$$

so that the spatial pattern in the PSM as a whole (posterior plus anterior) oscillates with period t_s (a snapshot of the PSM at time t looks the same as a snapshot at time $t + t_s$, after one additional somite has emerged from the anterior end of the PSM). t_s, the period of the fundamental oscillator in the posterior PSM, is thus equal to the time taken to form one extra somite, while the spatial stripes seen in the PSM reflect the slowing of the oscillation in each cell as it moves out along its flowline.

The number of stripes seen in the PSM is equal to the difference of phase $\Delta\phi$ (measured in cycles) between the posterior and anterior ends of the PSM:

$$\Delta\phi = -\int_0^L \frac{\partial\phi}{\partial x}\,dx\,.$$

From above,

$$\frac{\partial\phi}{\partial x} = \frac{1}{v}\left(\frac{1}{t_s} - \frac{1}{T}\right)$$

so that

$$\Delta\phi = \int_0^L \frac{1}{v}\left(\frac{1}{T} - \frac{1}{t_s}\right)dx.$$

Suppose, as a reasonable approximation, that the PSM tissue is growing uniformly with a growth rate α, so that each part of it increases in length by a factor $(1 + \alpha\,\mathrm{d}t)$ in a time interval $\mathrm{d}t$. Then the velocity at any point x, measured (as always) relative to the posterior end of the PSM, is simply

$v(x) = \alpha x$, so that

$$\Delta\phi = \int_0^L \frac{1}{\alpha x t_s}\left(\frac{t_s}{T} - 1\right)dx.$$

Let us define the fractional distance along the PSM as $y = \frac{x}{L}$. Then

$$\Delta\phi = \frac{1}{\alpha t_s}\int_0^1 \frac{1}{y}\left(\frac{t_s}{T} - 1\right)dy = \frac{t_2}{\ln 2\, t_s}\int_0^1 \frac{1}{y}\left(\frac{t_s}{T} - 1\right)dy$$

where t_2 is the PSM generation time as defined in Box 1.

The observations of the expression patterns of genes such as *Mesogenin1/Mespo* suggest that the segmentation clock of the snake slows down according to the *relative* position in the PSM in the same way as in other species. We can interpret this in terms of the way in which FGF regulates cell behavior and gene expression in the PSM: assuming that the FGF concentration gradient controls the pattern of expression of the genes that govern the slowing and stopping of the clock, the assertion is that the graph of FGF concentration as a function of y is the same in all species. This will be true, for example, if the difference between species is simply a difference in the FGF degradation rate, but with the same critical values of the FGF concentration marking the

points at which new genes come into play, including the point at which the PSM ends and somite differentiation begins. On this plausible assumption, t_s / T will be the same function of FGF concentration in all species, and in all species FGF concentration will be the same function of y. Consequently the integral $I = \int_0^1 \frac{1}{y} \left(\frac{t_s}{T} - 1 \right) dy$ will have the same value for all species. The number of stripes the snake shows in its PSM will then differ from other species simply in proportion to the value of $\frac{t_2}{t_s}$:

$$\Delta\phi = \frac{t_2}{\ln 2 \; t_s} I.$$

The large value of $\Delta\phi$ for the snake can thus be seen as the consequence of having a cell doubling time T_c that is very long compared with the somite cycle time T_0. During the middle part of somitogenesis, when the PSM length is not changing, we can use equation (6) of Box 1 to obtain

$$\Delta\phi = \frac{L}{s_1} I.$$

The numbers of PSM stripes during the middle period of somitogenesis in snake, mouse, chick, and zebrafish are thus predicted to be in the same ratios as their L / s_1 values, i.e., from Figure 4F, in roughly the ratios 35 : 5 : 5 : 8. In other words, the snake should have about seven times as many PSM stripes as mouse or chick, and about four times as many as zebrafish. This is in reasonably good agreement with the observations.

We thus conclude that the snake shows a large number of stripes in its PSM because the rate of growth in the PSM is slow compared with the segmentation clock rate - in other words, for just the same reason that this animal makes a large total number of somites.

Manuscript 2007-10-10531
Supplementary Information

The file contains Supplementary text and Figures S1-S2 with Legends

Summary:
The supplementary text describes the rigorous mathematical calculation of the relationship between the clock period and axis growth in the four different species.

Supplementary Fig. 1 shows expression of *Uncx4.1* and *MyoD* in two-day-old snake embryos. Supplementary Fig.2 shows the strategy used to measure the different somitogenesis parameters.

Supplementary Information

Why does the snake have so many more segments than other vertebrates?

Rigorous calculation - parameters varying with developmental stage

If we are to be precise, we cannot assume that t_s, L, s_1, α, or t_2 is a constant. To deal with the case where they may vary, let $N(t')$ be the number of somites formed up to time t':

$$N(t') = \int_{t_0}^{t'} \frac{1}{t_s}\, dt \qquad (8)$$

so that

$$n_s = N(t_0 + t_{\mathrm{tot}})$$

where somitogenesis begins at t_0 and ends at $t_0 + t_{\mathrm{tot}}$.

We define α and t_2 as before, with the proviso that they may vary with developmental stage. If we allow that L also may vary, we have to replace equation (5) above with the equation

$$s_1 = \alpha L t_s - \frac{dL}{dt} t_s = \frac{\ln 2}{t_2} L t_s - \frac{dL}{dt} t_s \qquad (5')$$

The formula for the number of PSM generations elapsing in the course of somitogenesis then becomes:

$$n_g = \int_{t_0}^{t_0+t_{\mathrm{tot}}} \frac{1}{t_2}\, dt \qquad (4')$$

$$= \int_{t_0}^{t_0+t_{\mathrm{tot}}} \frac{1}{t_s} \frac{s_1}{\ln 2\, L} + \frac{1}{\ln 2\, L} \frac{dL}{dt}\, dt$$

$$= \frac{1}{\ln 2} \left(\int_{t_0}^{t_0+t_{\mathrm{tot}}} \frac{s_1}{L} \frac{\mathrm{dN}}{\mathrm{dt}}\, dt + \ln \frac{L_{t_0+t_{\mathrm{tot}}}}{L_{t_0}} \right)$$

$$= \frac{1}{\ln 2} \left(\int_0^{n_s} \frac{s_1}{L}\, dN + \ln \frac{L_{t_0+t_{\mathrm{tot}}}}{L_{t_0}} \right)$$

If we treat the number of somites formed, $N(t)$, as an integer rather than a continuous variable, we can write the integral in the last line as a sum of values of s_1 / L over the cycles of the segmentation clock:

$$n_g = \frac{1}{\ln 2} \left(\sum_{N=0}^{n_s} \frac{s_1}{L} + \ln \frac{L_{t_0+t_{\mathrm{tot}}}}{L_{t_0}} \right) \qquad (7')$$

$$= \frac{n_s}{\ln 2} \left\langle \frac{s_1}{L} \right\rangle + \frac{1}{\ln 2} \ln \frac{L_{t_0+t_{\mathrm{tot}}}}{L_{t_0}}$$

where $\left\langle \frac{s_1}{L} \right\rangle$ is the mean somite size expressed as a fraction of the length of the PSM. From the graphs in Figure 4, it is easy to show that, for the three amniotes, the second term in the above equation is in fact fairly small ($\leq 15\%$) compared with the first, which essentially validates the previous equation (7) as a rough estimate.

Lastly, for comparison of growth rates, we define the average PSM generation time $\overline{t_2}$ by the equation

$$\overline{t_2} = t_{\mathrm{tot}} / n_g \qquad (9)$$

(Referring to equation (4'), we see that this means that $\overline{t_2}$ is the harmonic mean of t_2 over the period of somitogenesis.)

All the quantities in equation (7') are experimentally determined by the data graphed in Figure 4, allowing us to calculate n_g and $\overline{t_2}$ for each species. Note that the calculation of n_g does not depend on the value of t_s, or on whether t_s varies with developmental stage or is constant. The results are shown in Table X.

Table 1

	Snake	Mouse	Chick	Zebrafish
n_s	315	65	55	31
t_s	1.5h	2h	1.5h	0.5h

$<\frac{s_1}{L}>$	0.048	0.18	0.19	0.11
L_{t0}	994μm	639μm	789μm	680μm
$L_{t0+ttot}$	771μm	405μm	195μm	156μm
$\overline{t_2}$	22.0h	8.0h	6.3h	5.5h
n_g	21.3	16.6	13.1	2.7

Note: For the snake, we have data only for the latter two-thirds of the process of somitogenesis, and for the other species also our data do not quite extend to the very beginning and end of somitogenesis. Estimates in the Table are based on the extrapolations that L_{t0} and $L_{t0+ttot}$ are respectively equal to the values of L at the beginning and end of the period for which we have data, and that $<\frac{s_1}{L}>$ for the period of somitogenesis as a whole is the same as for the period for which we have data. If, for example, the value of $\frac{s_1}{L}$ in the snake was in fact as small during the first (unobservable) third of the period of somitogenesis as it is during the middle third, the estimate of $<\frac{s_1}{L}>$ would be 0.041, giving $\overline{t_2}$ = 25.8h and n_g = 18.4 for the snake.

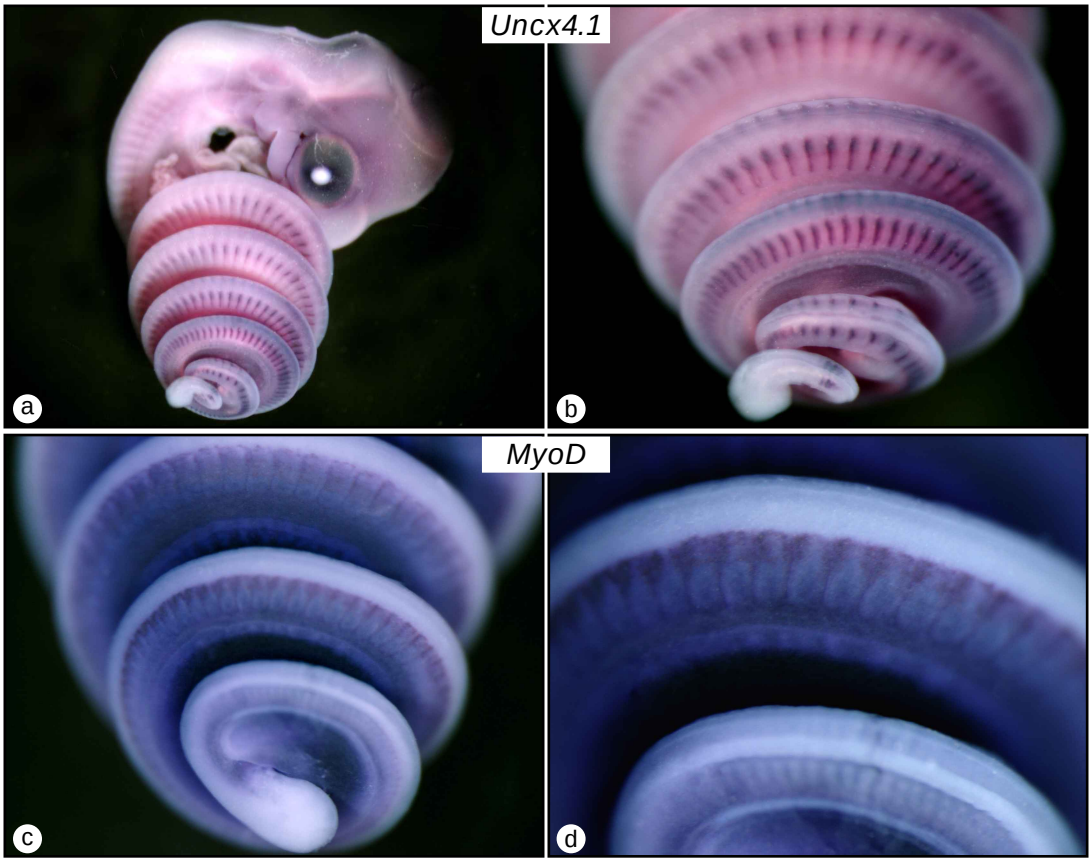

Supplementary figure 1 | In situ hybridization for *Uncx4.1* and *MyoD* in whole-mount corn snake embryos. (**a**) *Uncx4.1* staining on a whole-mount corn snake embryo at the 269-somite-stage. Anterior is to the top. (**b**) Enlargement of the posterior region of the embryo shown in (a). *Uncx4.1* marks somite posterior compartment. (**c**) Posterior region of a 230-somite-stage corn snake embryo stained with *MyoD*. (**d**) Enlargement of picture (**c**). *MyoD* marks somite medial part.

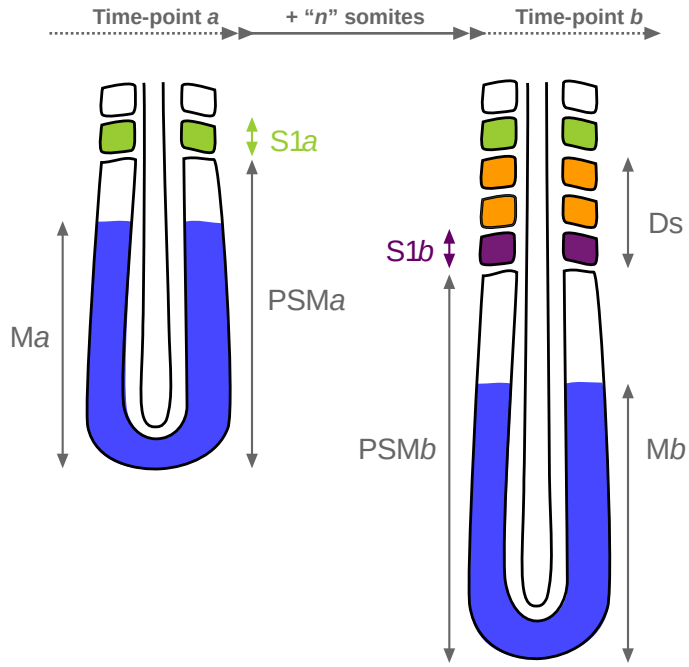

Supplementary figure 2 | Measurement of somitogenesis parameters. Schematic representation of the posterior part of an embryo before and after addition of three somites. Measurements in such consecutive time points are used to estimate the variation of size of the different domains and the speed described below. In the left panel, the newly formed somite s1 is shown in green. In the right panel, three somites have been added and the newly formed somite s1 is shown in purple. The orange somites have been formed during the two preceding somite cycles. The blue domain corresponds to the domain expressing *Mesogenin1/Mespo*.
Ma or Mb: *Mesogenin/Mespo* domain size for time-point a or b (in µm)
PSMa or PSMb: PSM size for time-point a or b (in µm)
S1a or S1b: Somite S1 size for time-point a or b (in µm)
n: Number of somites formed between time-point a and b
Ds: Length of the segmented mesoderm between time-points a and b (in µm).
Ds = ((S1a + S1b)/2) x n
Vt = Speed of tail bud elongation = (PSMb + Ds – PSMa)/n
Vd = Speed of *Mesogenin1/Mespo* front regression (determination front regression) = Vt - (Mb-Ma)/n

UNSUBMITTED DATA

I) Snake

1) Are there other genes dynamically expressed in corn snake PSM?

Genes from the Hairy/Hes family were shown to play a central role in the clock mechanisms, notably in generating their own periodic expression and in regulating other cyclic genes (Giudicelli et al., 2007; Lewis, 2003). Moreover, at least one member from this family was found cyclic in all the vertebrate species studied thus far (mouse, chicken, zebrafish, medaka, *Xenopus laevis*) suggesting that these genes are similarly regulated in the segmentation process over vertebrate evolution (Bessho et al., 2001; Damen et al., 2005; Dequeant et al., 2006; Gajewski et al., 2006; Henry et al., 2002; Holley et al., 2000; Jouve et al., 2000; Leimeister et al., 2000; Li et al., 2003; Palmeirim et al., 1997; Shankaran et al., 2007; Sieger et al., 2004).

I tried to clone a *Hairy/Hes* related gene in the corn snake. I designed degenerated primers against the bHLH region of *Drosophila melanogaster Hairy/Deadpan*, chicken *hairy1* and *Xenopus laevis hairy1*, and against the WRPW motif located in 3' of the genes (see Material and Methods and Figure 23). I first amplified a 115 bp fragment using the primers designed against the bHLH domain. The sequence of this fragment was closer to *Xenopus laevis hairy1* bHLH domain sequence (90 % identity at the nucleotide level). I then amplified an 816 bp fragment using specific primers against the cloned corn snake bHLH domain fragment and degenerated primers designed against the WRPW motif (Figure 23). The sequence of this fragment was closest to the mouse *Hes1* gene sequence (63.6% identity at the nucleotide level). Obtaining a good signal using this sequence as a probe for *in situ* hybridizations proved to be very difficult. I could obtain three different expression patterns (Figure 24). In the first one, corn snake *Hes1* was not expressed in the PSM. Only somites were stained. In the second one, some very faint stripes of corn snake *Hes1* were detected in the PSM. These stripes did not exactly look like *Lfng* stripes as they were closer to each other and allowed a larger gap between the last somite formed and the most anterior stripe. In the third one, only background was visible, leading to ubiquitously stained embryos. One embryo out of nine showed the first observed expression pattern; two embryos displayed the faint stripy expression pattern and the last six embryos were ubiquitously stained. Improving the *in situ* hybridization conditions would be needed to clarify these expression patterns. When the corn snake amino acid sequence of *Hes1* was aligned with the Hairy and enhancer

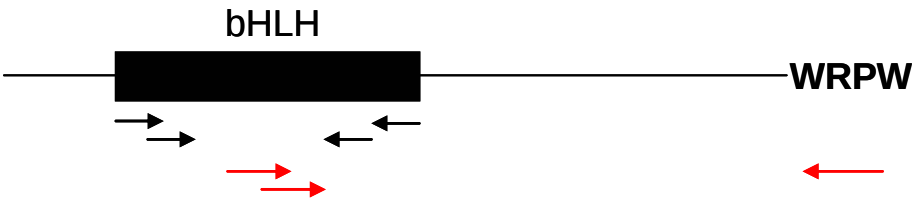

Figure 23. Cloning strategy for corn snake *Hes1* sequence.
In a first time, nested PCRs were performed on corn snake cDNA using primers designed against the bHLH domain of chicken *hairy1*, *Xenopus laevis hairy1* and Drosophila melanogaster *hairy* (black arrows). These primers correspond to pairs 1 and 2 in Table 2 in "Material and methods". In a second time, primers were designed against the corn snake *Hes1* bHLH sequence obtained during the first cloning step, and the WRPW domain at the C-terminus of the Hairy/Hes proteins (red primers, corresponding to pairs 3 and 4 in Table 2). Nested PCRs led to a 816 bp long corn snake fragment close to mouse *Hes1* sequence.

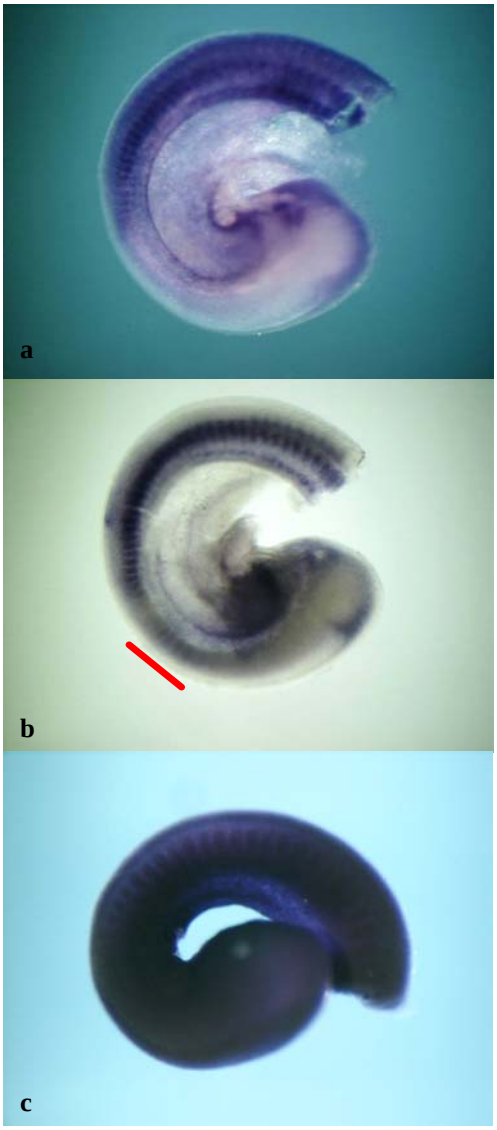

Figure 24. *Hes1* expression pattern in 230-somite corn snake tails.

a. in somites. b. in somites and as faint stripes in the PSM (red bar). c. Unspecific staining using *Hes1* probe. Anterior is to the top.

of split sequences of other amniotes (mouse and chicken), corn snake Hes1 grouped with “Hairy” sequences (mouse Hes1 and chicken hairy 1 and 2) (Figure 25). Finally, when the amino acid sequence of corn snake Hes1 was compared with its putative homologous mouse Hes1, chicken hairy2 and zebrafish her9, corn snake sequence was found closer to mouse Hes1, with 64.3 % identity (Table 4).

Nrarp, a gene belonging to Notch pathway and recently identified as cyclic in mouse PSM (Dequeant et al., 2006), showed a dynamic expression pattern in corn snake PSM, very reminiscent of mouse and chicken cyclic genes (Figure 26a,b). Corn snake *Nrarp* phases of expression were consistent with an onset in the posterior-most PSM/tail bud, followed by an anterior progression and narrowing of this expression domain in the PSM. Its amino acid sequence is closer to chicken and mouse with 98.5 % identity.

The Notch ligand *Delta* was identified as cyclic in mouse and zebrafish PSM (Jiang et al., 2000; Maruhashi et al., 2005). I cloned a *Delta* sequence in corn snake, closer to chicken *Delta1* at the amino acid level (89.2% identity). This gene was expressed in the entire corn snake PSM, but some embryos seemed to exhibit different intensities of staining at various posterior or more anterior areas of the PSM (Figure 26c,d), reminiscent of *Nrarp* expression pattern. The number of embryos showing such differences was low (4/12) and the definitive conclusion will wait further experiments.

2) Cultures

Corn snake *Lfng* stripy expression pattern first suggested that snakes could form several somites at the same time. One possibility to test this hypothesis was to directly visualize somite formation by time-lapse imaging on cultured snake tails (see material and methods). I tried these experiments on corn snake, and one year later, on “house snake” (*Lamprophis fuliginosus*), a new species of snake which arrived at the reptile facility. This colubridae species presented the advantage of laying eggs more often during the year, by clutches of 10 eggs on average. Eggs were incubated at 30ºC. Like corn snake embryos, house snake embryos exhibited more than 100 somites at oviposition. I used corn snake *Lfng* probe for performing *in situ* hybridization on house snake embryos and observed that *Lfng* expression pattern was conserved between corn and house snakes (Figure 27). Despite several trials using

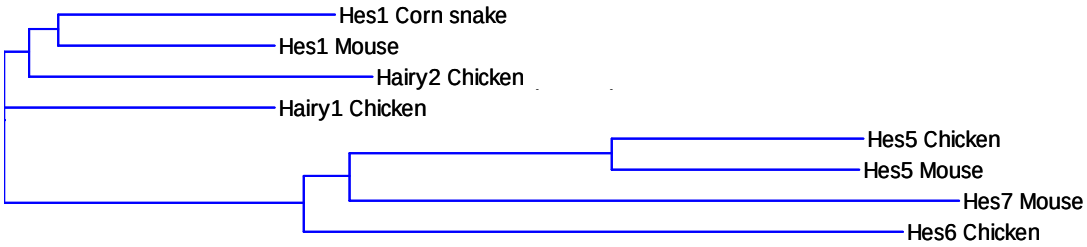

Figure 25. Comparison on a tree of the corn snake amino acid sequence for Hes1 with chicken and mouse hairy and enhancer of split sequences.
This tree was built using the Neighbor Joining method of Saitou and Nei (Vector NTI software).

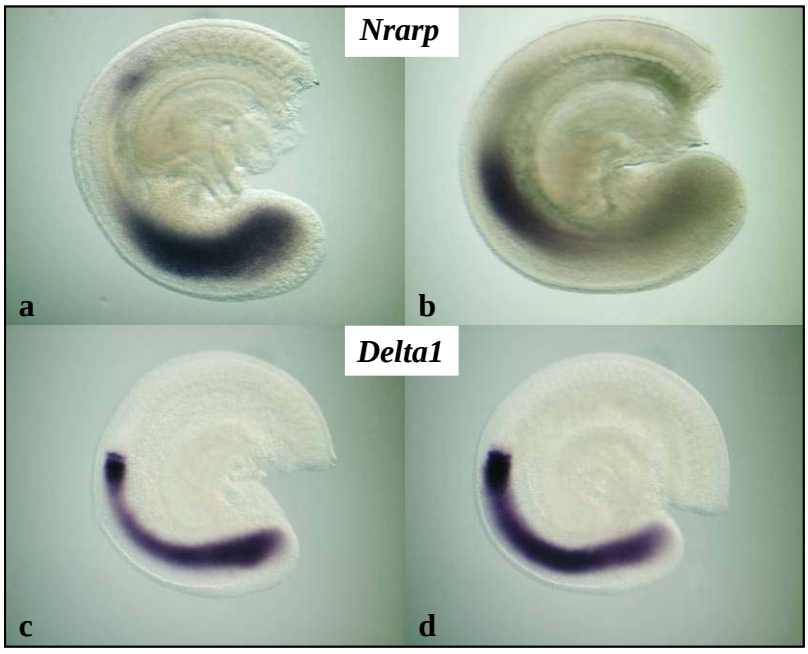

Figure 26. *Nrarp* and *Delta1* expression patterns in 230-somite corn snake tails.
a-b. *Nrarp*, c-d. *Delta1*; a,c. Phase I, b,d. Phase II. Anterior is to the top.

different culture media and oxygen concentration, I was unable to find the right conditions to culture snake tails (see Material and Methods). Finally, the only culture technique that worked was to graft the snake embryo tails on the aera opaca of a 2-day-old chicken embryo cultured *in vitro*. The chicken membrane was opened by a slit before grafting. This slit seemed to be important, as snake tails fused to the membrane were growing better than unfused tails, suggesting that nutrients were brougth more easily by chicken vascularization to the snake tail via its connection to the chicken membrane. In 8 hours at 34ºC and 5 % CO_2, four somites were added in the house snake tails (Figure 28). Unfortunately, it was not possible to generate time-lapse movies from this preparation, because of the lack of contrast.

II) Lizard

As corn snakes are seasonal, I spent my first six months in the laboratory learning to clone genes by nested PCR using degenerated primers and adapting the *in situ* hybridization protocol on a parthenogenetic species of lizard called *Aspidoscelis uniparens*. The advantage of this species is that individuals are all genetically identical. It also has a very long tail proportionally to its body (Figure 29), thus providing a good model for studying the mechanisms generating the caudal somites. This species exhibits between 65 and 70 vertebrae, based on counts done on X-rays. It lays eggs all year long, but remains seasonal, as eggs are more abundant in spring and summer. Clutches are composed of one to four eggs, not bigger than a finger nail (Figure 30). Eggs are soft-shelled, which makes the harvesting of the early stages (5-10 somite embryos) delicate. Fertile eggs are recognizable by a small light-brown spot at the surface of the shell. This spot locates the embryo in the egg. One possibility is to use a piece of tape to rigidify the shell at the spot area, and cut the shell around the tape, to allow the collection of the piece of shell containing the embryo, without the shell curling up and damaging the embryo. Then, the embryo and its membranes detach easily from the shell in PBS buffer. This technique allowed me to collect embryos at different stages throughout somitogenesis (Figure 31). The tissue of these embryos proved to be harder than chicken embryos and more difficult to dehydrate. These early steps of dehydration were then crucial for the success of the *in situ* hybridizations, as well as the finding of the right timing for proteinase K treatment.

The *A. uniparens* lizard forms at least 70 somites. I estimated the rate of

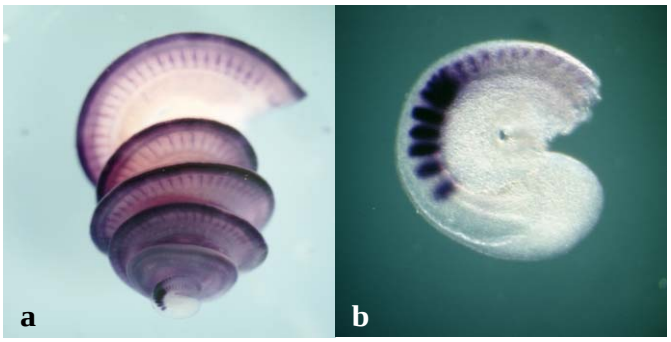

Figure 27. *Lfng* expression pattern in a 3 day-old house snake embryo.
a. Whole-mount embryo. Head was removed. b. Tail isolated from embryo in (a). Anterior is to the top.

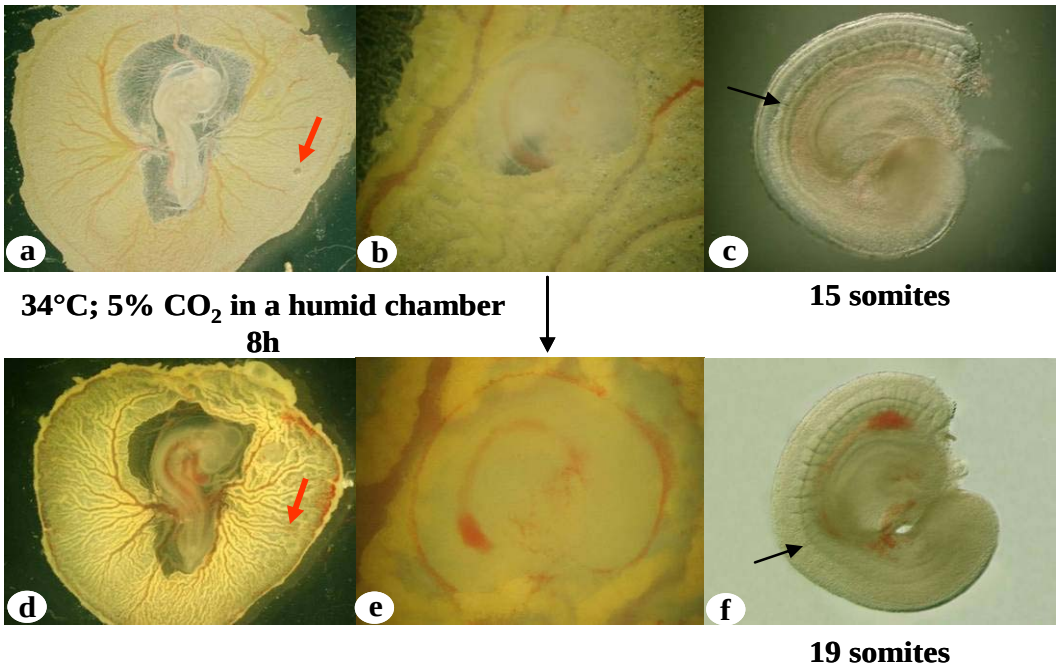

Figure 28. *In vitro* culture of 3-day-old house snake tails.
(a-c) Before culture, (d-f) After 8 hours culture at 34 °C and 5% CO_2 in a humid chanber.
a,d. 2-day-old chicken embryo. Red arrow indicates where the house snake tail was grafted on the chicken chorioallantoic membrane. b,e. Zoom on the graft in (a,d) respectively. c,f. Somite number of the house snake tail before (c) and after culture (f). Black arrow indicates the last somite boundary.

Figure 29. Picture of *Aspidoscelis uniparens* lizard. This lizard is also called the desert grassland whiptail, based on its living habitat and its long tail. It can measure up to 86 mm.

Figure 30. *A. uniparens* lizard's clutch of eggs. Clutch after one month incubation at 28ºC– 80% humidity. The red arrow indicates an unfertile egg.

somite formation to four hours by comparing the number of somites of different embryos, incubated for various amounts of time. I also cloned genes related to the clock, the determination front or the somites compartment in this lizard: *Axin2*, *Delta1*, *FGF8*, *Lfng*, *MyoD* and *Wnt3a*. *In situ* hybridizations only worked for *Wnt3a*, *Lfng* and *Delta1* (Figure 32). This may be due to the hybridization temperature that I kept at 68ºC for the lizards, whereas real improvements were obtained on snakes later, using 58ºC. *Wnt3a* displayed a conserved expression pattern with its transcripts expressed in the tail bud and neural tube. *Delta1* transcripts were found as one large stripe in the anterior PSM. Interestingly, *Lfng* was expressed as in zebrafish, as one narrow stripe in the anterior PSM and in the somites (Figure 32c). There was no evidence of stripes expressed more posterior in the PSM, as in snake, mouse and chicken. However, these data do not necessarily imply that this gene is not cycling in lizard PSM. The adaptation of the proteinase K treatment in corn snake proved to be crucial for detecting the more posterior *Lfng* stripes. More *in situ* hybridizations on lizard embryos, with optimizations of the proteinase K treatment, are therefore needed to draw definitive conclusions on lizard gene expression patterns.

Lizard gene sequences were compared to the corresponding orthologous sequences in corn snake, chicken, mouse, *Xenopus laevis* or *tropicalis* and zebrafish. Surprisingly, lizard and corn snake sequences were not always the closest in percentage of identity. Sometimes, either lizard or corn snake sequences were closer to chicken (see *MyoD*, *Delta1*, *Lfng* and *Wnt3a*, Table 4). However, these observations may not be significant, as these sequences do not represent the full length.

Another aspect of the lizard study was to try embryo culture and to generate a cell line to see if we could infect it with the RCAS virus (replication-competent avian sarcoma-leukosis virus). As reptiles are the closest relatives to birds, it was interesting to test if this avian virus could also infect lizard cells. If this worked, this could provide a tool for functional studies, by expressing molecules in the cell line, via the infection by the virus, and grafting a pellet of cell in a chosen area of the embryo. I generated a lizard fibroblastic cell line that grew well but slowly at 30ºC and 5% CO2 (see Material and Method). The infection by the RCAS virus did not work. Examples of reptile cell line generation exist in the literature (Clark et al., 1969), as well as an example of gecko cell lines infected by different kinds of viruses (Michalski et al., 1974). This information could be used to improve *Aspidoscelis uniparens* cell line

culture and provide candidate viruses capable of infecting reptile cells.

Figure 31. Normal developmental stages of the *A. uniparens* lizard up to mid-development post-oviposition.

a. 0-24 hours post-oviposition (hpo), 7 somites - b. 24-48 hpo, 15 somites - c. 48-72 hpo, 21 somites – d. 5 days post-oviposition (dpo), 30 somites – e. 5 dpo, 37 somites – f. 10-13 dpo, 63 somites – g. 14-20 dpo – h. 21-24 dpo – i. 25-28 dpo.

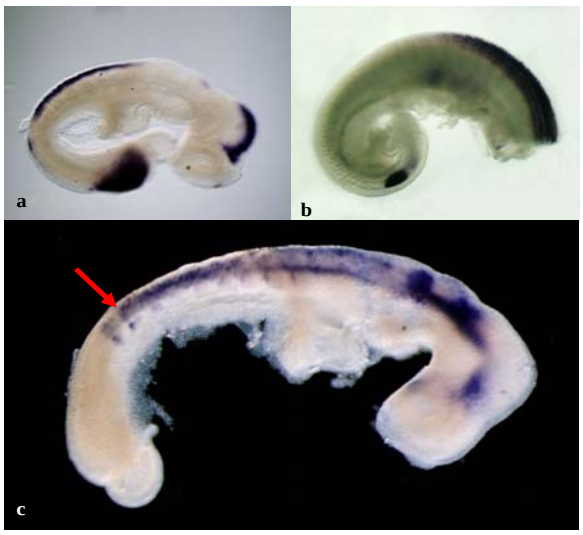

Figure 32. *In situ* hybridization in whole-mount *Aspidoscelis uniparens* embryos.

a. *Wnt3a*. b. *Delta*. c. *Lfng*. Red arrow indicates the last formed somite. (a,c), 15-somite, and (b) 30-somite embryos. Head was removed in (b). Anterior to the right.

DISCUSSION

This thesis presents a study on a new model species: the corn snake embryo (*Pantherophis guttatus*). Reptiles have always been the missing link in vertebrate research. Very few studies have been conducted on them because of the difficulties to maintain these species in the laboratory, their slow developmental rate and seasonal reproduction. Here, I report the detailed analysis of corn snake somitogenesis and its comparison with chicken, mouse and zebrafish. My major goal was to study the mechanisms of regulation of somite number in vertebrates.

1) Reptile somitogenesis in evolution

In order to have an idea of the conservation of the somitogenesis mechanisms in corn snake embryos compared with other vertebrates, I cloned genes involved in this process and revealed their expression profiles by *in situ* hybridization. Results strongly suggested that corn snake somitogenesis mechanisms were based on the "Clock and Wavefront" model like other vertebrates. The existence of a determination front was supported by the conserved formation of two opposite gradients of retinoic acid (see *Raldh2* expression Article Figure 2) and Wnt/Fgf signaling in the PSM. Moreover, a clock mechanism, albeit differently regulated, was evidenced by the dynamic expression of the Notch pathway genes *Nrarp* and *Lfng* in the PSM. I could not detect any cyclic genes from the Wnt and Fgf pathways, although some members of these pathways were identified as cyclic in mouse and chicken PSM (Aulehla et al., 2003; Dale et al., 2006; Dequeant et al., 2006; Ishikawa et al., 2004; Suriben et al., 2006). The Notch pathway is therefore the only one involved in the segmentation clock mechanism of all vertebrates studied thus far. Moreover, some members of this pathway are dynamically expressed in the growth zone of some chelicerate and myriapods, where they participate in segment formation (reviewed in (Damen, 2007)). More generally, *Notch* is expressed in somites and tail bud of the chordate amphioxus (Holland et al., 2001), and in the segmental founder cells of the annelid *Helobdella robusta* (Rivera et al., 2005), suggesting a role for *Notch* in the segmentation mechanism of these animals. All of this information are consistent with an ancestral role of the Notch pathway in segmentation and further raises the question of the segmentation of a common ancestor to the bilaterian.

Examination of the *Hes1* gene expression pattern in corn snake suggested that this gene may not be expressed in the PSM, whereas its homologous *chairy2* and

mHes1 are both cyclic in chicken and mouse. This absence of expression in the PSM could be similar to what is observed in zebrafish and medaka, where *her9*, the homolog of *chairy2/mHes1* is not expressed in the PSM (Gajewski et al., 2006; Leve et al., 2001). Alternatively, corn snake *Hes1* could have an expression pattern ressembling *Lfng*'s, with several dynamically expressed stripes in the PSM. This case would be a new example of the hairy and enhancer of split family involvement in segmentation clock mechanisms, as it is occuring in all other studied species. Further experiments would be needed to clarify this question.

When reviewing the literature, one can notice that the *Lfng* expression pattern is definitely lunatic. This pattern was described in chicken, mouse and zebrafish (Aulehla and Johnson, 1999; Forsberg et al., 1998; Leve et al., 2001; McGrew et al., 1998; Prince et al., 2001; Wu et al., 1996). A *Fringe* gene also exists in amphioxus and the grasshopper *Schistocerca gregaria* (short-germ arthropod) (Dearden and Akam, 2000; Mazet and Shimeld, 2003). In all these species, except amphioxus, the *Lfng* or *Fringe* gene is expressed at the level of the boundaries between the segments, suggesting that this gene participates in the segment maintenance and morphogenesis. Only in chicken and mouse, was this gene also recruited as a component of the segmentation clock. From these observations, a model was built to explain *Lfng* recruitment in vertebrate segmentation. It proposes that *Fringe* was initially unnecessary in chordate segmentation, as amphioxus does not express this gene in the mesoderm. In the vertebrate phylum, the *Lfng* gene would have subsequently been recruited for the segments boundaries maintenance and morphogenesis, in the same way as observed in arthropods (grasshopper). Later, the amniote group would have derived a new function for the *Lfng* gene in segment formation (Leve et al., 2001; Mazet and Shimeld, 2003), by involving it in segmentation clock mechanisms. The expression of *Lfng* in corn and house snake rather supports this model concerning the amniotes novelty. It would be interesting to check more closely the *Lfng* expression pattern in whiptail lizard embryos. If this pattern remained similar to zebrafish *Lfng*, whiptail lizard could become a candidate to challenge this model.

Finally, our experiments and mathematical modeling suggest that segment number in vertebrates is controlled on one hand by the number of PSM generations needed to reach the end of somitogenesis, and on the other hand, by the number of times the clock ticks during the completion of these PSM generations.

An additional example to illustrate this model is *Aspidoscelis uniparens* lizard

somitogenesis. Embryos from this species develop at a similar rate compared with corn snake embryos (it needs between two and three months between the start of development and hatching), but they make much less somites than corn snake (70 compared with 315). In agreement with this observation, the clock pace in lizard embryos was estimated at four hours (which is very slow compared with 90 minutes observed in corn snake). Hence, these observations further argue in favor of our model in which the regulation of the clock pace relative to axis growth rate would determine the total somite number in amniotes. This shows that the total duration of somitogenesis is not an important parameter explaining somite number variation, contrary to what could be assumed when comparing zebrafish, chicken, mouse and corn snake somitogenesis in our experiments. PSM generation numbers remain to be calculated in lizard to fully validate this proposition.

A mechanism partly explaining the transition between a lizard-like and a snake-like body can be hypothesized based on our observations. The pace of the clock in a lizard-like body could have gradually accelerated relative to axis growth rate, over evolution time, and led to elongated snake-like bodies exhibiting more segments. This hypothesis could be tested on the grass-lizard *Tetradactylus* embryos from southern Africa. This lizard has evolved three body forms which still co-exist: a lizard-like body (*Tetradactylus seps*), an “intermediate” body between lizard and snake in which the AP axis has elongated and limbs reduced in size (*Tetradactylus tetradactylus*), and a snake-like body with vestigial hindlimbs remaining on both sides of the cloaca, as observed in pythons (*Tetradactylus africanus*) (Figure 33) (Berger-Dell'Mour, 1985). Counting the total number of somites in these three specimens and measuring the pace of the clock relative to the PSM generation number and time could show if the clock pace indeed accelerated from *Tetradactylus seps* to *Tetradactylus africanus*, thus validating this mechanism.

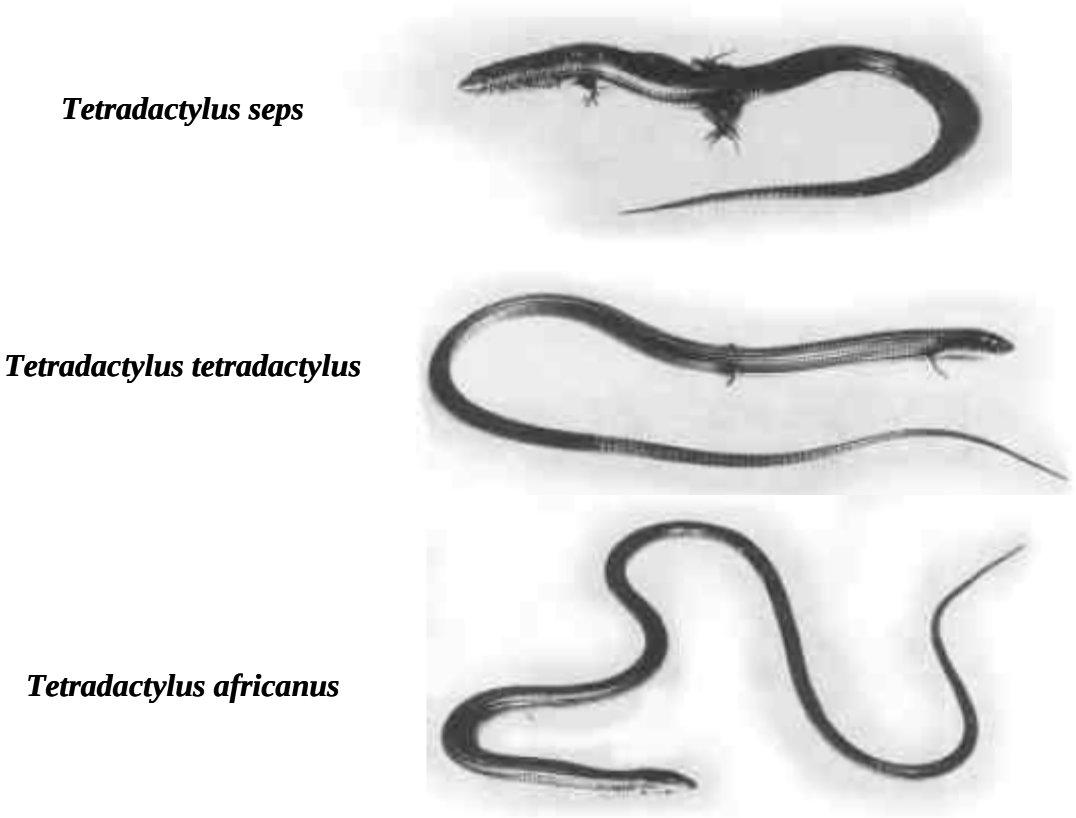

Figure 33. Different body forms in the lizard *Tetradactylus.*
After (Berger-Dell'Mour, 1985).

2) Control of PSM life time and somitogenesis arrest

We observed that amniote PSM first increases in size before decreasing until somitogenesis arrests. The transition between PSM enlargement and PSM shrinkage occurs at the lumbo-sacral level in amniotes (which corresponds to the cloacal region in corn snake). This transition occurs when *Hox10-11* paralogous groups are activated in the tail bud, suggesting that these genes could play a role in controling PSM life time. If this was the case, *Hox* genes from the paralogous group 13 would be expected to control somitogenesis arrest. However, no obvious experimental evidence supports this hypothesis as yet. For example, the simultaneous knock-out of all *Hox10* genes, which would be expected to lead to an increased somite number and axis length, only affect somite identity (the same results were obtained with the simultaneous knock-out of all *Hox11* genes) (Wellik and Capecchi, 2003). The lack of effects of these knock-outs on the total somite number could be explained by the fact that *Hox* genes from paralogous groups 12 and 13 are still active in the PSM and are able to compensate for the loss of *Hox* groups 10-11 in the regulation of PSM shrinking. Other studies show that the individual knock-outs of *Hox13* genes do not cause strong axial phenotype (Dolle et al., 1993; Economides et al., 2003; Fromental-Ramain et al., 1996; Godwin and Capecchi, 1998). *Hoxb13* knock-out is the more interesting because it causes an increase in the body length by increasing caudal vertebrae size (Economides et al., 2003). Some additional vertebrae are sometimes observed but not considered as a significative increase in the total vertebrae number. As functional redundancy has been described between the members of a same paralogous group among *Hox* genes, an interesting experiment would be to knock-out all the *Hox13* genes in mouse at once, and observe if the total number of somites, as well as axis length would be increased.

Zebrafish PSM maintenance seems to be differently regulated than in amniotes. The number of PSM generations in this species is much lower, leading to a “premature” PSM shrinking and somitogenesis arrest. In zebrafish, it has been shown that along the hoxd cluster, sequences of genes expressed anteriorly and involved in primordial structures patterning (like the hindbrain for example) have been highly conserved with other tetrapods, whereas sequences of genes involved in the patterning of more posterior structures have gradually diverged. For example, *Hoxd10* and *11* are the first genes along the zebrafish hoxd cluster where an increased divergence has

been detected at the amino acid level from other tetrapod sequences, and *hoxd12* and *13* completely diverged (van der Hoeven et al., 1996). This phenomenon was called "laxitas terminalis". It proposes that the function of posterior *hox* genes in zebrafish would have diverged to some extent from the function of posterior *hox* genes in other species. This mechanism could be responsible for the observed early shrinking of PSM size and reduced number of PSM generations in zebrafish embryo.

3) *Nrarp* and *Lfng* expression patterns

The present study proposes that the clock pace relative to axis growth rate could be illustrated by the number of cyclic gene waves, traveling at the same time in the PSM.

Conciliating *Nrarp* and *Lfng* expression patterns in this view is puzzling. Some cyclic genes are known to exhibit different expression patterns, due to mRNA stability difference. For example, *chairy2* is expressed for a longer time in the posterior PSM than *chairy1*, even if these genes cycle in synchrony in chicken PSM (Maroto et al., 2005). Another example in mouse shows that *Hes7* mRNA is more stable than *Lfng* mRNA and needs a longer time to refine as a narrow stripe in the anterior PSM than *Lfng* (Bessho et al., 2001). In zebrafish, different cyclic genes occupy different regions of the PSM. For example, *her11* is never expressed in the tailbud, like corn snake *Lfng* (Shankaran et al., 2007). Its oscillations start in posterior PSM and cycle in phase with *her1* and *her7*. In contrast, *her12* is continously expressed in the tail bud and its expression expands periodically anteriorly in the posterior PSM (Shankaran et al., 2007). Some stripes are expressed in a unique manner in the anterior PSM, out of synchrony with *her1*, *7* and *11*. Finally *her15* expression blinks in the tail bud/posterior PSM (Shankaran et al., 2007). One or two narrow stripes are expressed in the anterior PSM again differently from the other cyclic genes. These examples show that the segmentation clock is constituted of a serie of complex oscillators, the activity of which leads to the periodic formation of somites. The role of individual cyclic genes in somite formation is unclear. Some could be directly involved in somite boundary specification and AP patterning, whereas some others could be indirectly involved in the clock mechanism by interacting with the first class of cyclic genes and refining their activity. In corn snake, *Lfng* seems to be directly involved in somite boundary formation and

maintenance, as its expression is maintained in the somite anterior compartment after somite formation. It would be interesting to study the functional role of *Nrarp* in corn snake PSM and its interactions with *Lfng*. Some functional studies could be conducted in mouse and zebrafish. Some dissection and culture experiments in corn snake could allow the study of both gene dynamics relative to each other as well. One possibility would be to dissect out the left and right PSM of corn snake embryos and to hybridize them with *Lfng* probe on one side and *Nrarp* on the other side. This could first show if these genes oscillate in synchrony. Culturing left and right PSM as Palmeirim and colleagues (Palmeirim et al., 1997), but using the chicken chorioallantoic membrane system set up during my thesis for culture, would also allow to see the dynamics of these genes relative to somite formation.

4) Functional studies in the future?

Studies on corn snake embryos are limited by the absence of tools allowing functional studies. The long generation time of this species (two years) does not make genetic studies using transgenic animals very attractive. However, technics such as embryo culture or transient expression of molecules could be very useful for studying corn snake embryo development. Cultures could allow graft experiments as well as fate mapping, drug testing and real-time imaging. Microinjection or electroporation could allow overexpression of mRNAs, morpholinos, and diverse construct with dominant active or negative effects which could disturb the normal course of embryo development and help in its understanding.

I obtained positive culture results by grafting a house snake tail to the chorioallantoic membrane of a 2-days-old chicken embryo. The tail developed and new somites were added. Electroporation could be set up on this system. Snake tails exhibit a large neurenteric canal (Figure 34). This canal could be used for the injection of diverse molecules to be electroporated. The tails could be subsequently cultured on the chicken chorioallantoic membrane after electroporation. This system would target ectopic expression of molecules to the tail bud, notably the chordoneural hinge (posterior to the neurenteric canal), containing stem cells generating the medial PSM along the AP axis (Cambray and Wilson, 2002; Eloy-Trinquet and Nicolas, 2002; Iimura et al., 2007; Selleck and Stern, 1991). Hence, this system could allow diverse studies, particularly on axis growth, PSM formation and cyclic genes wave

generation.

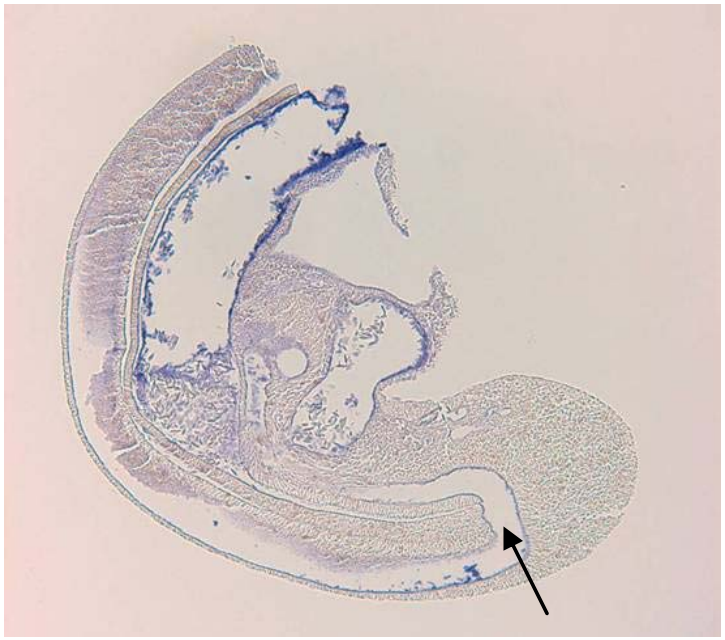

Figure 34. Sagittal section through a corn snake tail.
Arrow points at the neurenteric canal. Anterior to the top.

MATERIAL AND METHODS

1) Eggs and embryos

Corn and house snakes- Eggs were obtained from females mated in the institute. After oviposition, eggs were placed in humidified vermiculite and incubated for up to seven days in a humid atmosphere at 28°C. Embryos were harvested at different days after incubation in PBS-2 mM EGTA. They were then either fixed overnight at 4°C in 4%f ormaldehyde-2mM EGTA, rinsed in phosphate-buffered saline containing 0.1% Tween20 (PBT), dehydrated through a methanol series and stored in 100% methanol at -20°C, or directly frozen in liquid nitrogen and stored at -80°C for subsequent DNA or RNA extraction. Embryos were staged according to their number of somites.

Whiptail lizard- Eggs and embryos were harvested and treated identically to snake eggs.

Chicken- Fertilized chicken eggs were obtained from Ozark Hatcheries (Neosho, MO) and incubated at 38ºC in a humidified incubator. They were staged according to Hamburger and Hamilton (HH) (Hamburger and Hamilton, 1992) and by counting somites.

Mouse- Wild-type CD1 mice embryos were harvested from timed mated pregnant females between 8.0 and 13.5 days postcoitum (dpc) and staged by counting the number of somites.

Zebrafish- Studies on wild-type zebrafish (*Danio rerio*) were carried out in the Oregon AB background. Embryos obtained from natural crosses were maintained in 1/3 Ringer's solution (39 mM NaCl, 0.97 mM KCl, 1.8 mM $CaCl_2$, 1.7 mM Hepes at pH 7.2) at
28.5°C and staged according to age (hours postfertilization at 28.5°C) and somite number.

2) Cloning

Reptiles- One embryo was frozen after one day of incubation. Total RNA was isolated by Trizol extraction (Invitrogen). First-strand cDNA was synthetized using the "First-strand cDNA synthesis" kit from Invitrogen. Two nested PCRs ("Expand high fidelity PCR system" kit, Roche) were then performed on the cDNA using degenerated primers designed against conserved regions of the target genes. The primers sequences and Tm for each gene are available in the Table 2. PCR products presenting a good size on agarose gels were cloned in the pGEM-T easy vector (Promega) and sequenced using Sp6 and T7 promoters. Vectors containing right

sequences were further used to produce probes for *in situ* hybridization.

3) Whole mount *in situ* hybridization

Reptiles- Antisens DIG-labeled probes were produced from the constructs described above. The size of the probes and the enzymes used to linearize the vector and transcribe the probes are indicated in Table 3. Whole mount *in situ* hybridization was performed according to the procedure already described (Henrique et al., 1995) with a modified hybridization temperature at 58°C (except for *Delta1*, 68°C and *Mespo*, 55°C).

Chicken and Mouse- *cMespo* and m*Msgn1* probes were already described (Buchberger et al, 2000; Yoon et al, 2000). Whole mount *in situ* hybridizations were performed according to the procedure already described (Henrique et al., 1995).

Zebrafish- Zebrafish *Mespo* probe corresponds to the nucleotides 1 to 884 from the GenBank sequence NM_182882. Whole mount *in situ* hybridizations were performed according to the procedure already described (Ariza-McNaughton and Krumlauf, 2002).

4) "Mesogenin1/Mespo time-course" experiment and speeds calculation

In situ hybridizations using *Mesogenin1/Mespo* probe were performed on chicken, mouse, zebrafish and corn snake embryos at different time points along somitogenesis. Each time point regroups at least five embryos at the same stage (mouse, chicken, zebrafish) or at least three snake embryos at close stages. Close stage means: Time-point "111 somites": four embryos between 104 and 118 somites; Time-point "123 somites": 10 embryos between 131 and 154 somites. Time-point "170 somites": five embryos between 164 and 187 somites; Time-point "205 somites": four embryos between 200 and 215 somites; Time-point "237 somites": three embryos between 234 and 239 somites; Time-point "256 somites": 10 embryos between 243 and 269 somites and Time-point "295 somites": four embryos between 285 and 310 somites.

Embryos or tails were flat mounted and pictured. Size in micrometer of PSM, somite S1 and *Mesogenin1/Mespo* staining were measured using Zeiss LSM image Browser software. A correction taking into account PSM curvature was applied in early stage wholemount zebrafish embryos. PSMs were difficult to measure accurately because

of the difficulty to clearly distinguish the somite S0. Measurements corresponding to each somitogenesis time-point were averaged and a standard deviation calculated.
Local speeds between two time-points were calculated in µm/period. Speeds were calculated as follow:

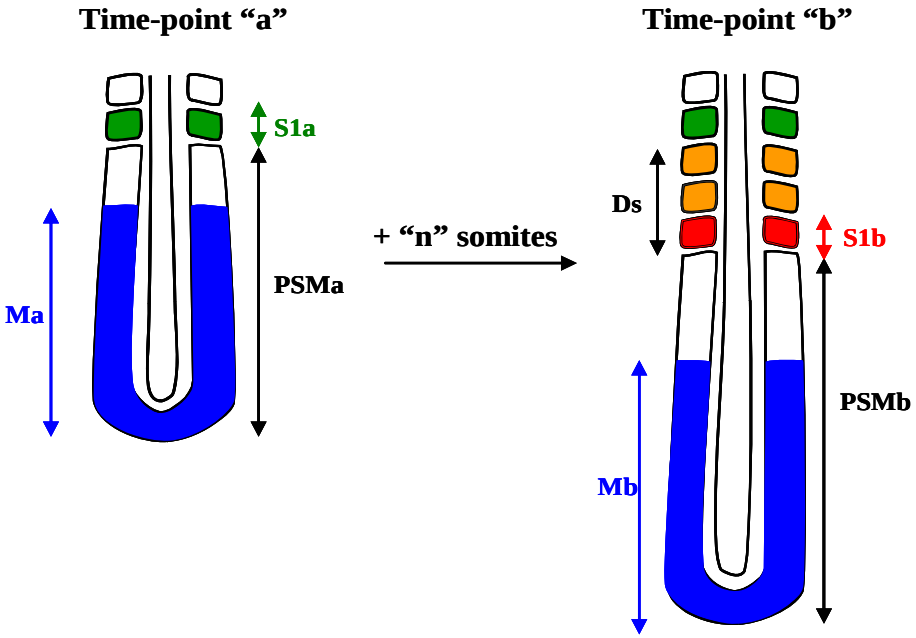

Ma or Mb: *Mesogenin1/Mespo* domain size for time-point a or b (in µm)
PSMa or PSMb: PSM size for time-point a or b (in µm)
S1a or S1b: Somite S1 size for time-point a or b (in µm)
n: Number of somites formed between time-point a and b
Ds: Length of the segmented mesodermmesoderm between time-points a and b (in µm)

$$Ds = ((S1a + S1b)/2) \times n$$

Vt = Speed of tail bud elongation = (PSMb + Ds – PSMa)/n
Vd = Speed of mesogenin front regression (determination front regression) = Vt - (Mb-Ma)/n

In Figure 22 of this thesis, determination front speed (Vd) was expressed in µm/minute by dividing each time-point value per the species specific clock period (90 minutes in chicken and corn snake, 120 minutes in mouse and 30 minutes in

zebrafish).

5) Corn snake skeletal prep

The corn snake skeletal prep and staining with Alizarin red (bone) and Alcian blue (cartilage) were performed as described (Kessel et al., 1990).

6) Lizard fibroblastic cell line

A lizard fibroblastic cell line was generated from a pool of four *A. uniparens* embryos at 34 days of incubation after oviposition (mid-development). Embryos were decapitated and emptied out. They were mashed through a syringe and trypsinized for 15 minutes. Supernatant was transferred to a fesh tube and digestion was stopped by adding fresh medium (F-12K basal medium (invitogen) supplemented with 15% Fetal Bovine Serum (FBS), 100µg/mL streptomycine and 100U/mL penicilline). After spinning 5 minutes at 1000 rpm, supernatant was discarded and cell resuspended in fresh medium. Cells were plated at 30ºC, in 5% CO_2. They were splitted every 4-6 days.

7) Lizard fibroblastic cell line infection with RCAS virus

RCAS strains A, B and E were used to try chicken and *Aspidoscelis uniparens* fibroblasts infection. Strain A can infect both chicken and quail, strain B infects chicken only and strain E infects quail only.

Cell transfection with the RCAS vector (Hughes et al., 1987) was done using the FUGENE reagent (Roche). Successful transfection was monitored by fluorescent immunodetection against the p27Gag viral protein. In short, cultures were fixed 20 minutes in PBS-Paraformaldehyde 4% and rinsed twice 10 minutes in PBS-Triton X-100 0.25%. They were then incubated 1 hour at room temperature in the primary antibody in PBS-Triton X-100 0.25% (anti-p27Gag 1/1000), rinsed 3 times and incubated in the same conditions in the secondary antibody (GAR-RITC, Southern Biotechnology associates 1/100) and rinsed 3 times. Slides were mounted in Mowiol or PBS-glycerol.

8) Cultures

Corn or House snake's tails were collected after cutting at the level of the somites S4 to S6. Several culture media were tried. Basal culture media consisted of DMEM

(high glucose, high glutamax), DMEM/F-12 or Leibovitz L15 (Invitrogen). Each of these media was supplemented with one or the other of the following combinations: 10% FBS or 10% FBS + 1% Chicken Serum (CS) or 10% FBS + 5% CS or 10% CS + 5% FBS or 10% Horse Serum + 5% Chicken extracts. After each mix, 100µg/mL streptomycine and 100U/mL penicilline were added. Cultures were performed in hanging drops, at 29°C, 5% CO_2.

The following culture medium was used on garter snake DMEM + 10% HS + 5% chicken extract + 2.4 mM Glutamine + 18 mM KCl + 20.5 mM Glucose + 100 µg/mL streptomycine and 100U/mL penicilline (Holtzman and Halpern, 1989). Alternatively, 10mM Hepes was added. Tails were cultured at 29°C without any addition of CO_2 or O_2.

Time-lapse movies were performed using "INC-2000 incubator system" culture chamber (Technology, Inc). Culture chamber was placed on an inverted microscope (Zeiss Axiovert 200M). AxioCam HRm camera was used for time-lapse movies in bright-field. The Software used was called "Axiovision 4.5". Tails were place in a special dish and covered with the following medium DMEM (high Glutamax and Glucose) + 10% FBS + 5% CS + 100 µg/mL streptomycine and 100 U/mL penicilline). Humidity was maintained in the culture chamber. 65% O_2 and 5% CO_2 were supplied. Culture's temperature was 30°C. Oxygen concentration was changed according to the try (80% O_2 or 25% O_2).

Table 2. Sequences and melting temperatures (Tm) of the primers used for cloning corn snake's and/or lizard's genes.

Gene	Primers	Sens	Antisens	Tm
Axin2	Pair 1	5' TGG ACC AAR TCY YTR CAY T 3'	5' TGR TGR TGG ATG TAG TGG TG 3'	52.4°C
	Pair 2	5' GAY CAR GAY GGT GCH YAH CT 3'	5' TAG TGG TGR TGR AYR TGC TT 3'	53.8°C
Delta1	Pair 1	5' GAR CTS AAG YTG CAG GAG TT 3'	5' TTR AAG CAM GGN CCR TCH GC 3'	55.2°C
	Pair 2	5' GGA GTT YKT MAA CAA GAA GG 3'	5' GTC ATK GCR CTM ARY TCA CA 3'	50.0°C
Dusp6	Pair 1	5' GTG GCT SAA SGA RCA GCT RG 3'	5' ATG TCR TAR GCA TCG TTC AT 3'	53.0°C
	Pair 2	5' ATG GAC TGC CGR SCD CAR GA 3'	5' TTG AGC TTC TGC ATR AGG TA 3'	53.0°C
EphA4	Pair 1	5' GAR GTG AGY ATH ATG GAT GA 3'	5' TGC GGA TGA GTT TGT CCA RC 3'	50.0°C
	Pair 2	5' TGC AAY GTR ATG GAR SCC AG 3'	5' GAC ATC ACT TCC CAC ATR AC 3'	52.0°C
FGF8	Pair 1	5' CTM RTS CGS ACC TAC CAR CT 3'	5' GGS ARS CKC TTC ATG AAG TG 3'	56.3°C
	Pair 2	5' ACC TAC CAR CTB TAC AGC CG 3'	5' ATG AAG TGS ACY TCV CGY TG 3'	57.1°C
Hes1	Pair 1	5' CAA RCC SAT YAT GGA GAA RMG 3'	5' CAG RTG YTT CAC YGT CAT CT 3'	53.5°C
	Pair 2	5' ATG GAG AAR MGW MGS MGR GC 3'	5' TRT CBG CCT TCT CCA GYT TG 3'	56.3°C
	Pair3	5' GGC AGC TCA AGA CGC TCA TC 3'	5' CCA NGG NCK CCA NAC 3'	55.0°C
	Pair4	5' CAC TCC AAG CTG GAG AAG GC 3'	5' CCA NGG NCK CCA NAC 3'	55.0°C
Lfng	Pair 1	5' TTC ATC GCH GTS AAR ACC AC 3'	5' AAC CTG GAW GGG TCV KCY TC 3'	55.2°C
	Pair 2	5' GTS AAR ACC ACY ARR AAG TT 3'	5' CKC TTG TTY TCA AAC ATD CC 3'	50.4°C
Mespo	Pair 1	5' AAR GCC AGY GAG MGR GAG AA 3'	5' GAT GTA STK GAT GGT GYA YT 3'	50.8°C
	Pair 2	5' GCC AGY GAG MGR GAG AAR CT 3'	5' GAT GGT GYA YTT SAR BGT YT 3'	52.1°C
MyoD	Pair 1	5' GAY GAC TTC TAY GAY GAY CC 3'	5' GGA RAT BCK CTC SAC DAT GC 3'	52.2ºC
	Pair 2	5' CTT YTT YGA RGA CYT GGA CC 3'	5' TCA TGC CRT CRG ARC AGT TG 3'	53.2ºC
Nrarp	Pair 1	5' AGG AGC TBC AST CDC TSC TG 3'	5' GTG ATS AGR TAD ARC ACG AT 3'	50.2ºC
	Pair 2	5' CTG CAR AAC ATG ACN AAC TG 3'	5' TAD ARC ACG ATG TCY TGR TG 3'	51.9ºC
Paraxis	Pair 1	5' ATG GCN TWY RCS MTG MTS CG 3'	5' YAK MAG VAG MAC RTT GGC CA 3'	56.6°C
	Pair 2	5' AYG AGG ARA AYC RSR GMG AG 3'	5' TTG GCC ARR TGB GMG ATG TA 3'	56.7°C
Pax-1	Pair 1	5' ACR TAY GGS GAR GTG AAY CA 3'	5' CGD ATK CCY ARK ATR TTG ST 3'	51.8°C
	Pair 2	5' GAR GTG AAY CAR CTB GGB GG 3'	5' ARK ATR TTG STR ACN GWR TG 3'	49.8°C
Raldh2	Pair 1	5' ATG GCN TCK CTS CAB CTS MT 3'	5' CCA TTK CCR GAC ATY TTG RA 3'	53.2°C
	Pair 2	5' TCK CTS CAB CTS MTG CCB TC 3'	5' CCR GAC ATY TTG RAB CCY CC 3'	57.3°C
Sprouty2	Pair 1	5' GAT GGA GRC SAG ARY WCA 3'	5' GTC RTA RCA SSC CTG GCA CA 3'	53.0°C
	Pair 2	5' TCY YTG GAH CAR ATM AGR RC 3'	5' ASG CAR CCC TTK GCY GGV AG 3'	53.0°C
T-box	Pair 1	5' DMY GGS AGR MGV ATG TTY CC 3'	5' AAD SCY TTN GCR AAN GGR TT 3'	54.9°C
	Pair 2	5' TAY ATY CAY CCN GAY WSN CC 3'	5' KSR TTC TGR TAR GCW GTV AC 3'	52.9°C
*Uncx4.1**	Pair 1	5' TGA TGG ASR GYC GSM TYC TG 3'	5' CTG MAC TCK GGA CTC SAC YA 3'	57.3°C
	Pair 2	5' CCB CAT GCC CAG TTY RRR GG 3'	5' ACT CKG GAC TCS ACY ARR TC 3'	55.8°C
Wnt3a	Pair 1	5' TVC GMT TCT GYM GSA AYT A 3'	5' RTA KAC NCK YRT RCA YTC YTG 3'	52.4°C
	Pair 2	5' TGG AGA TYA TGC CBA GYG T 3'	5' ACG TAG CAR CAC CAR TGG AA 3'	55.1°C

*: Unexpectedly, only the antisens primer of the second Uncx4.1pair (in red) amplified the sequence.

Table 3. Linearization and transcription enzymes used for the corn snake and whiptail lizard *in situ* probes.

Species	Gene name	Insert size in pGEM-T easy	Linearization enzyme	Transcription enzyme
Corn snake	***Axin2***	1283 bp	SalI	T7
	Delta-1	1059 bp	NcoI	Sp6
	Dusp6	860 bp	NcoI	Sp6
	EphA4	2485 bp	NcoI	Sp6
	FGF8	368 bp	NcoI	Sp6
	Hes1	816 bp	SalI	T7
	Lfng	668 bp	SalI	T7
	Mespo	132 bp	NcoI	Sp6
	MyoD	443 bp	SalI	T7
	Nrarp	206 bp	SacI	T7
	Paraxis	256 bp	NcoI	Sp6
	Raldh2	1406 bp	SacII	Sp6
	Sprouty2	701 bp	SalI	T7
	Uncx4.1	394 bp	NcoI	Sp6
	Wnt3a	832 bp	NcoI	Sp6
Whiptail lizard	***Axin2***	1342 bp	SalI	T7
	Delta-1	1077 bp	SalI	T7
	FGF8	368 bp	SalI	T7
	Lfng	668 bp	NcoI	Sp6
	MyoD	476 bp	SalI	T7
	Wnt3a	813 bp	NcoI	Sp6

APPENDIX

Table 4. Comparison of the gene sequences cloned in corn snake and whiptail lizard with other vertebrate species.

Comparisons are performed at the amino acid level. Numbers in tables correspond to percentages of identity between sequences. The name of the sequence is written at the top of the table. Numbers in brackets give the length in amino acids (aa) of the compared sequences.

Sequence names are given in alphabetic order. Genes which sequences were cloned both in corn snake and lizard are listed first.

Axin2 (427aa)

	Corn snake	Lizard *A. uniparens*	Chicken	Mouse	Zebrafish
Corn snake	100				
Lizard *A. uniparens*	89.7	100			
Chicken	87.1	86.2	100		
Mouse	80	78.6	80.5	100	
Zebrafish	69.6	68.8	72.5	67.9	100

Delta-1 (351 aa)

	Corn snake	Lizard *A. uniparens*	Chicken	Mouse	Zebrafish
Corn snake	100				
Lizard *A. uniparens*	88.9	100			
Chicken	89.2	88.8	100		
Mouse	84	84.1	88	100	
Zebrafish	77.2	77.9	81.3	78.8	100

FGF8 (122 aa)

	Corn snake	Lizard *A. uniparens*	Chicken	Mouse	*X. tropicalis*	Zebrafish
Corn snake	100					
Lizard *A. uniparens*	100	100				
Chicken	98.4	98.4	100			
Mouse	92.6	92.6	91.8	100		
X. tropicalis	92.6	92.6	91.8	88.5	100	
Zebrafish	91.8	91.8	91.8	89.3	89.3	100

Lfng (222 aa)

	Corn snake	Lizard *A. uniparens*	Chicken	Mouse	*X. tropicalis*	Zebrafish
Corn snake	100					
Lizard *A. uniparens*	91.4	100				
Chicken	93.7	92.8	100			
Mouse	82.9	81.1	82.9	100		
X. tropicalis	86	86.5	87.8	80.2	100	
Zebrafish	83.4	83	85.2	77.6	85.2	100

MyoD (147 aa)

	Corn snake	Lizard *A. uniparens*	Chicken	Mouse	*X. tropicalis*	Zebrafish
Corn snake	100					
Lizard *A. uniparens*	89.2	100				
Chicken	90.1	86.1	100			
Mouse	75.6	73.3	76.2	100		
X. tropicalis	87.1	81	84.1	76.2	100	
Zebrafish	87.1	82.9	86.1	75.6	90.8	100

Wnt3a (270 aa)

	Corn snake	Lizard *A. uniparens*	Chicken	Mouse	*X. laevis*	Zebrafish
Corn snake	100					
Lizard *A. uniparens*	96.3	100				
Chicken	97	97	100			
Mouse	88.9	89.6	89.3	100		
X. laevis	94.1	93.3	93.7	87.4	100	
Zebrafish	88.7	87.2	87.9	83.3	87.2	100

Dusp6 (286 aa)

	Corn snake	Chicken	Mouse	*X. tropicalis*	Zebrafish
Corn snake	100				
Chicken	93.7	100			
Mouse	91.6	94.1	100		
X. tropicalis	89.9	90.6	89.5	100	
Zebrafish	82.5	85	83.9	84.2	100

EphA4 (828 aa)

	Corn snake	Chicken	Mouse	Zebrafish
Corn snake	100			
Chicken	96.9	100		
Mouse	94.4	95.2	100	
Zebrafish	86.1	86.7	85.3	100

Hes1 (204 aa)

	Corn snake Hes1	Chicken hairy2	Mouse Hes1	Zebrafish her9
Corn snake Hes1	100			
Chicken hairy2	54.1	100		
Mouse Hes1	64.3	57.4	100	
Zebrafish her9	51.1	43.2	51.7	100

Mespo (44 aa)

	Corn snake	Chicken	Mouse	*X. laevis*	Zebrafish
Corn snake	100				
Chicken	93.2	100			
Mouse	90.9	95.5	100		
X. laevis	86.4	84.1	81.8	100	
Zebrafish	84.1	84.1	86.4	77.3	100

Nrarp (68 aa)

	Corn snake	Chicken	Mouse	Zebrafish
Corn snake	100			
Chicken	98.5	100		
Mouse	98.5	100	100	
Zebrafish	97.1	98.5	98.5	100

Paraxis full-length (183 aa)

	Corn snake	Chicken	Mouse	*X. laevis*	Zebrafish
Corn snake	100				
Chicken	67.4	100			
Mouse	65	72.6	100		
X. laevis	63.9	72.6	65	100	
Zebrafish	53.6	68.4	60.6	61.2	100

Pax1 (203 aa)

	Corn snake	Chicken	Mouse	*X. laevis*	Zebrafish
Corn snake	100				
Chicken	86.2	100			
Mouse	88.7	88.3	100		
X. laevis	78.8	83.2	85.7	100	
Zebrafish	75.4	78.6	79.5	79.1	100

Raldh2 (468 aa)

	Corn snake	Chicken	Mouse	*X. laevis*	Zebrafish
Corn snake	100				
Chicken	91.9	100			
Mouse	90.4	94.7	100		
X. laevis	86.3	90	89.5	100	
Zebrafish	79.5	79.5	79.3	79.1	100

Sprouty2 (233 aa)

	Corn snake	Chicken	Mouse	*X. tropicalis*	Zebrafish
Corn snake	100				
Chicken	84.1	100			
Mouse	79.2	82.6	100		
X. tropicalis	71.6	74.5	72.3	100	
Zebrafish	51.2	59.9	54.7	52.5	100

Uncx4.1 (130 aa)

	Corn snake	Mouse	*X. laevis*	Zebrafish
Corn snake	100			
Mouse	85.4	100		
X. laevis	76.2	79.2	100	
Zebrafish	73.8	76.8	84.6	100

Some corn snake sequences have been deposited to GenBank. Here are their accession numbers: *Axin2* (EU196456); *Fgf8* (EU196457); *Dusp6* (EU196465); *EphA4* (EU232010); *Lfng* (EU196458); *Mesogenin* (EU196459); *MyoD* (EU196460); *Paraxis* (EU196466); *Raldh2* (EU196461); *Sprouty2* (EU196464); *Uncx4.1* (EU196462); *Wnt3a* (EU196463).

Before coming in the Dr. Olivier Pourquié's laboratory, I spent my master's degree and my first year of PhD in the laboratory of the Dr De-Li Shi in Paris. This laboratory is interested in the molecular mechanisms of myogenesis in vertebrates. My question at that time was to understand if Tbx6, a T-box transcription factor involved in the maintenance of the paraxial mesoderm identity, was also involved in the early myogenesis of *Xenopus laevis*.

This work gave rise to the following article that I did not discuss in this thesis.

Available online at www.sciencedirect.com
SCIENCE DIRECT
Developmental Biology 290 (2006) 470 – 481
DEVELOPMENTAL BIOLOGY
www.elsevier.com/locate/ydbio

Genomes & Developmental Control

FGF8, *Wnt8* and *Myf5* are target genes of Tbx6 during anteroposterior specification in *Xenopus* embryo

Hong-Yan Li [1], Audrey Bourdelas [1], Clémence Carron, Céline Gomez, Jean-Claude Boucaut, De-Li Shi *

Groupe de Biologie Expérimentale, Laboratoire de Biologie du Développement, CNRS UMR 7622, Université Pierre et Marie-Curie, 9 quai Saint-Bernard, 75005 Paris, France

Received for publication 21 March 2005, revised 17 October 2005, accepted 14 November 2005
Available online 15 December 2005

Abstract

The T-box transcription factor Tbx6 is required for somite formation and loss-of-function or reduced activity of Tbx6 result in absence of posterior paraxial mesoderm or disorganized somites, but how it is involved in a regulatory hierarchy during *Xenopus* early development is not clear. We show here that *Tbx6* is expressed in the lateral and ventral mesoderm of early gastrula, and it is necessary and sufficient to directly and indirectly regulate the expression of a subset of early mesodermal and endodermal genes. Ectopic expression of Tbx6 inhibits early neuroectodermal gene expression by strongly inducing the expression of posterior mesodermal genes, and expands the mesoderm territory at the expense of neuroectoderm. Conversely, overexpression of a dominant negative Tbx6 mutant in the ventral mesoderm inhibits the expression of several mesodermal genes and results in neural induction in a dose-dependent manner. Using a hormone-inducible form of Tbx6, we have identified *FGF8*, *Xwnt8* and *XMyf5* as immediate early responsive genes of Tbx6, and the induction of these genes by Tbx6 is independent of Xbra and VegT. These target genes act downstream and mediate the function of Tbx6 in anteroposterior specification. Our results therefore identify a regulatory cascade governed by Tbx6 in the specification of posterior mesoderm during *Xenopus* early development.

Keywords: T-box; Tbx6; FGF8; Wnt8; Myf5; Myogenesis; Paraxial mesoderm; Anteroposterior patterning; Neural induction; *Xenopus*

Introduction

Members of the *T-box* gene family play central roles for the development of mesoderm. *T-box* genes are a family of developmental regulators with more than 20 members recently identified in invertebrates and vertebrates (reviewed by Papaioannou, 1997; Smith, 1999). Mutations in *T-box* genes have been found to cause several human diseases (Bamshad et al., 1997; Li et al., 1997; Basson et al., 1997). The founding family member, *Brachyury* (or *T*), was originally identified by mutation in the mouse (Dobrovolskaïa-Zavadskaïa, 1927) and then cloned (Herrmann et al., 1990). All of the *T-box* genes whose functions have been studied are essential for early development. *Brachyury* is required for mesoderm specification and morphogenetic movements of gastrulation (Conlon et al., 1996; Smith et al., 1991, 2000). *Eomesodermin* (*eomes*) is implicated in mesoderm development both in *Xenopus* and in mouse (Ryan et al., 1996; Russ et al., 2000). *Xenopus VegT* is a maternal mRNA and is zygotically expressed in the presumptive mesoderm and is restricted to the lateral and ventral mesoderm by the end of gastrulation (Zhang and King, 1996; Lustig et al., 1996; Stennard et al., 1996; Horb and Thomsen, 1997). Depletion experiments show that *VegT* function is required for endoderm and mesoderm development by regulating TGFβ family signaling molecules (Zhang et al., 1998; Clements et al., 1999; Kofron et al., 1999; Xanthos et al., 2001). In chick limb, Tbx5 and Tbx4 have been shown to regulate the expression of *Wnt* and *FGF* genes (Ng et al., 2002; Takeuchi et al., 2003), raising the possibility that *T-box* genes play a crucial role in gene regulatory hierarchy during vertebrate myogenesis.

Among different *T-box* genes, *Tbx6* is expressed in primitive streak, the paraxial mesoderm, and the tail-bud in different species (Chapman et al., 1996; Hug et al., 1997; Griffin et al., 1998; Uchiyama et al., 2001). It plays an important role in the

* Corresponding author. Fax: +33 1 44 27 34 51.
E-mail address: dshi@ccr.jussieu.fr (D.-L. Shi).
[1] These authors contributed equally to this work.

0012-1606/$ - see front matter © 2005 Elsevier Inc. All rights reserved.
doi:10.1016/j.ydbio.2005.11.020

formation of posterior paraxial mesoderm. In *Tbx6* null mutant mouse embryos, posterior paraxial mesoderm develops as neural tissues, suggesting that it is essential for the formation of posterior somitic mesoderm (Chapman and Papaioannou, 1998). In addition, it has been shown recently that the mouse rib-vertebrae mutation is a hypomorphic *Tbx6* allele (Watabe-Rudolph et al., 2002; White et al., 2003). This mutation affects somite formation, morphology and patterning, and leads to malformations of the axial skeleton such as split vertebrae and neural arches, and fusions of adjacent segments (Theiler and Varnum, 1985; Beckers et al., 2000; Nacke et al., 2000). Analyses of these mutations also reveal that Tbx6 interacts genetically with Notch pathway genes (White et al., 2003; Hofmann et al., 2004). Together, both loss-of-function and reduced activity of Tbx6 suggested that it occupies a key position in posterior paraxial mesoderm formation (Chapman et al., 1996; Chapman and Papaioannou, 1998; White et al., 2003).

Despite this important function, little is known about its regulation and its interaction with other factors involved in anteroposterior patterning and myogenesis. Since *Tbx6* is expressed in the posterior region in all vertebrates, another unanswered question is whether and how it is involved in the patterning of anteroposterior axis. In this report, we analyzed the activity of Tbx6 in mesoderm and neural induction, as well as in the patterning of anteroposterior axis. Our results show that Tbx6 regulates, both directly and indirectly, the expression of a subset of early mesodermal and endodermal genes. It protects posterior mesoderm from neural induction and directly interacts with *FGF8*, *Xwnt8* and *XMyf5* in anteroposterior patterning and in regulating *XMyoD* expression.

Materials and methods

Plasmid constructs and morpholino oligonucleotides

The *pCS2-Tbx6VP16* and *pCS2-Tbx6EnR* constructs were kindly provided by Dr. H. Uchiyama. A hormone-inducible construct of *Tbx6VP16* cloned in *pSP64T* vector (*pSP64T-Tbx6VP16-GR*) was obtained through fusion of *Tbx6VP16* with the ligand-binding domain of the human glucocorticoid receptor (amino acids 512–777, with an initiation methionine added to the amino-terminus). *pSP64T-Xbra*, *pSP64T-XbraEnR* and *pSP64T-VegT* were from Dr. J. Smith. *pSP35T-chordin* was from Dr E. De Robertis. *pSP6nucβgal* was from Dr. R. Harland and *pSP64T-XFD* was from Dr. M. Kirschner. *pCS2-FGF8* and *pCS2-Tbx6* were obtained by PCR amplification and cloned into the *pCS2* vector. *pCS2-VegTEnR* was also obtained by PCR amplification of *VegT* DNA binding domain (amino acids 1 to 284) and cloned inframe with the *Drosophilia Engrailed* repressor domain (amino acids 2 to 298). Synthetic capped mRNA was made by in vitro transcription as described (Djiane et al., 2000). The morpholino oligonucleotides for *XMyf5* (5′-ACCATCTCCATTCTGAATAGTGCTG-3′), *Xwnt8* (5′-AAAGTGGTGTTTTGCATGATGAAGG-3′) and control sequence were from Gene Tools, and suspended in sterile water at a concentration of 2 mg/ml.

Xenopus embryos and tissue explants

Xenopus eggs were obtained from females injected with 500 IU of human chorionic gonadotropin (Sigma), and artificially fertilized with minced testis. Eggs were dejellied with 2% cysteine hydrochloride (pH 7.8) and kept in 0.1× modified Barth solution (MBS) to appropriate stages (Nieuwkoop and Faber, 1967) for further manipulations. Microinjections of embryos at different stages were done in 0.1× MBS containing 3% Ficoll-400. After injections, embryos were kept in 3% Ficoll-400 solution for 3 h and then cultured in 0.1× MBS until they reached appropriate stages. After injection of *Tbx6VP16-GR* mRNA (20 to 100 pg), whole embryos or animal cap explants were cultured to different stages and then incubated in 10 μM of dexamethasone in the presence or absence of 10 μM of the protein synthesis inhibitor, cycloheximide.

In situ hybridization and cell lineage tracing

Whole-mount in situ hybridization was performed according to standard protocol (Harland, 1991). *Tbx6* probe was a 1.5 kb cDNA insert cloned in *pBluescript* vector and was obtained by systematic sequencing of a gastrula cDNA library. It was linearized with *Not*I and transcribed with T7 RNA polymerase to generate antisense RNA. Probes for *Xbra*, *Xwnt8*, *XMyf5*, *XMyoD* and *myosin light chain* were described previously (Shi et al., 2002). *Sox3* probe was provided by Dr. H. Grunz and *Sox17α* was from Dr. H. Woodland. They were linearized with *Eco*RI or *Sma*I, respectively, and transcribed with T7 RNA polymerase. *FGF8* probe was linearized from the *pCS2* expression plasmid with *Bam*HI and transcribed with T3 RNA polymerase. *LacZ* mRNA was injected as a cell lineage tracer and β-galactosidase staining was performed as described (Vize et al., 1991).

RT-PCR

Extraction of total RNA from whole embryo or animal cap explants was performed using guanidine isothiocyanate/phenol followed by LiCl precipitation to remove genomic DNA and polysaccharides. RNA samples were further treated with RNAse-free DNAse I (Roche) and were reverse-transcribed using 200 units SuperScript reverse transcriptase (Life Technologies). PCR primers for *Xbra*, *XMyoD*, *XMyf5*, *Xwnt8*, *chordin* and *ornithine decarboxylase* (*ODC*) were as described (Shi et al., 2002). Other primers are as follows: *Otx2* (F: 5′-GGATGGATTTGTTGCACCAGTC-3′, R: 5′-CACTCTCCGAGCTCACTTCTC-3′), *XAG1* (F: 5′-CTGACTGTCCGATCAGAC-3′, R: 5′-GAGTTGCTTCTCTGGCAT-3′), *N-CAM* (F: 5′-CACAGTTCCACCAAATGC-3′, R: 5′-GGAATCAAGCGGTACAGA-3′), *muscle actin* (F: 5′-GCTGACAGAATGCAGAAG-3′, R: 5′-TTGCTTGGAGGAGTGTGT-3′), *Hoxb9* (F: 5′-TACTTACGGGCTTGGCTGGA-3′, R: 5′-AGCGTGTAACCAGTTGGCTG-3′), *Xcad2* (F: 5′-ATAACAATCCGCAGGAAG-3′, R: 5′-TTGATGATGGAGATACCAAG-3′), *Mespo* (F: 5′-CTTACTACTGATGGAGACTC-3′, R: 5′-AATCGATAGCCAACCTCA-3′), *FGF8* (F: 5′-ATCCAACTGGCAACTGAGC-3′, R: 5′-AGAAATTACTGTCATAGTCC-3′), *FGF3* (F: 5′-TCGGCCATGCCACAATG-3′, R: 5′-AGTTTGCACCCCTCACTGTCC-3′), *Sizzled* (F: 5′-CAAACCTGATGGGACACACTAAC-3′, R: 5′-GCTTAGGCAATTCTTTTATAGGAG-3′), *goosecoid* (F: 5′-ACAACTGGAAGCACTGGA-3′, R: 5′-TCTTATTCCAGAGGAACC-3′), *En2* (F: 5′-CGGAATTCATCAGGTCCGACAATC-3′, R: 5′-GCGGATCCTTTGAAGTGGTCGCG-3′), *Sox17α* (F: 5′-GGACGAGTGCCAGATGATG-3′, R: 5′-CTGGCAAGTACATCTGTCC-3′), *Delta 1* (F: 5′-AATGAATAACCTGGCCAACTG-3′, 5′-GTGTCTTTTGACGTTGAGTAG-3′. One-twentieth of the reverse-transcribed cDNA was used for PCR amplification in a reaction mixture containing 1 μCi of [α-^{32}P]dCTP (ICN Pharmaceuticals). PCR products were resolved on a 5% non-denaturing polyacrylamide gel and visualized and quantified by a Phospho-Imager (BioRad).

Histology

Embryos or tissue explants were fixed in 3.7% formaldehyde buffered in MOPS. Histological sections were cut after embedding the embryos or explants in polyethylene glycol distearate.

Results

Tbx6 in dorsoventral and anteroposterior patterning

In *Xenopus* embryo, *Tbx6* is shown to be expressed in the posterior paraxial mesoderm as in other vertebrates (Uchiyama

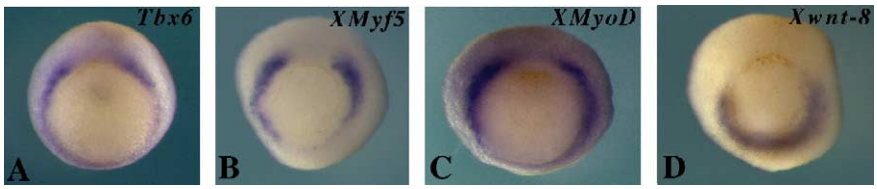

Fig. 1. Overlapping expression of *Tbx6*, *XMyf5*, *XMyoD* and *Xwnt8* at the early gastrula stage analyzed by in situ hybridization. (A) *Tbx6* is expressed in the lateral and ventral mesoderm of early gastrula. (B) *XMyf5* shows similar expression pattern but is expressed at a lower level in the most ventral region. (C) *XMyoD* is expressed in a very similar pattern as *Tbx6*. (D) The expression of *Xwnt8* is localized to the ventral region with a relatively lower level in the lateral mesoderm. The expression of all four genes is excluded in the dorsal region.

et al., 2001); however, the early expression was not reported. We have thus performed in situ hybridization to make the expression pattern of *Tbx6* in the early gastrula precise. The result shows that expression of *Tbx6* is localized to the lateral and ventral mesoderm of stage 10.5 early gastrula, and is excluded in the dorsal mesoderm. This expression pattern is nearly identical to that of *XMyf5* and *XMyoD*, and overlaps significantly that of *Xwnt8* (Fig. 1). Zygotic expression of these genes can be detected just before gastrulation by PCR, but we failed to detect their localization by in situ hybridization. From neurula stage onward, the expression of *XMyf5*, as well as *FGF8* (Christen and Slack, 1997), also overlaps that of *Tbx6*. This raises the question as for their interaction in dorsoventral and anteroposterior patterning.

We thus performed functional analyses using a constitutively active (Tbx6VP16) and a dominant negative (Tbx6EnR) mutant in order to examine how they affect dorsoventral and anteroposterior patterning. Embryos at 4-cell stage were

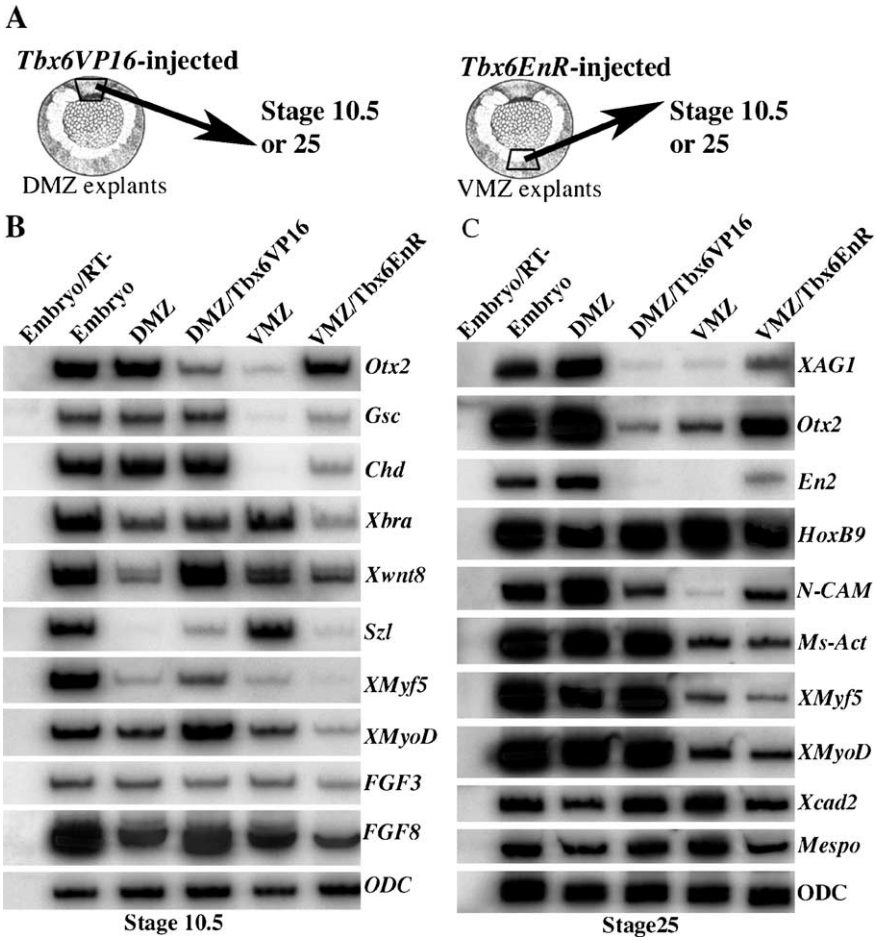

Fig. 2. Regulation of mesodermal and neural gene expression by Tbx6 in marginal zone explants. (A) Embryos at 4-cell stage were injected with *Tbx6VP16* mRNA in the DMZ region or with *Tbx6EnR* mRNA in the VMZ region. Injected embryos were cultured to early gastrula stage for dissection of DMZ and VMZ explants. (B) Gene expression in DMZ and VMZ explants at the early gastrula stage. Tbx6 inhibits the expression of dorsal genes like *Otx2* and induces the expression of ventral genes like *Xwnt8* and *szl* in the DMZ explants. In contrast, Tbx6EnR induces the expression of dorsal genes like *Otx2* in the VMZ explants, whereas it inhibits the expression of latero-ventral genes including *Xbra*, *szl*, *Xwnt8*, *XMyoD* and *FGF8*. (C) Gene expression in DMZ and VMZ explants expressing Tbx6VP16 or Tbx6EnR at early tail-bud stage. Tbx6 inhibits the expression of *Otx2* and *N-CAM*, but up-regulates posterior genes *Hoxb9*, *Xcad2* and *Mespo* in DMZ explants. Tbx6EnR induces the expression of neural markers *XAG1*, *Otx2*, *En2* and *N-CAM* in VMZ explants, while it inhibits the expression of posterior genes including *Hoxb9*, *Xcad2* and *Mespo*.

dorsally injected with *Tbx6VP16* mRNA (1 pg) or ventrally injected with *Tbx6EnR* mRNA (400 pg). Injected embryos were cultured to early gastrula stage (stage 10.5) for dissection of dorsal marginal zone (DMZ) or ventral marginal zone (VMZ) explants. Dissected tissues were either harvested immediately or cultured to stage 25 for RT-PCR analyses of dorsoventral and anteroposterior gene expression (Fig. 2A). At early gastrula stage, dorsal overexpression of Tbx6VP16 strongly inhibited the expression of the anterior mesendodermal gene *Otx2* while the expression of *goosecoid* and *chordin* was not significantly affected. Dorsal overexpression of Tbx6VP16 also induced the ectopic expression of *sizzled* (*szl*), a ventrally expressed gene (Salic et al., 1997). In addition, it up-regulated the expression of other latero-ventrally expressed genes like *Xwnt8*, *XMyf5*, *XMyoD* and *FGF8*. However, the expression level of *Xbra* and *FGF3* was not significantly affected. Conversely, ventral overexpression of Tbx6EnR strongly induced ectopic *Otx2* expression and moderately induced the ectopic expression of *goosecoid* and *chordin*. Tbx6EnR also decreased the expression level of *Xbra*, *Xwnt8*, *szl*, *XMyoD* and *FGF8* in VMZ explants (Fig. 2B). This analysis indicates that Tbx6 potently regulates the expression of a subset of latero-ventrally expressed mesodermal genes and may be a potent factor involved in early dorsoventral patterning.

At stage 25, Tbx6VP16 strongly inhibited the expression of anterior neuroectodermal markers *XAG1*, *Otx2* and *En2*, as well as the pan-neural marker *N-CAM* in DMZ explants, and up-regulated the expression of posterior mesodermal markers *Mespo* (Joseph and Cassetta, 1999), *Xcad2* (Pillemer et al., 1998) and *Hoxb9* (Fig. 2C). By contrast, VMZ explants expressing Tbx6EnR showed ectopic expression of *XAG1*, *Otx2*, *En2* and *N-CAM*, and had decreased expression level of *Hoxb9*, *Xcad2* and *Mespo* (Fig. 2C), indicating the occurrence of neural induction.

The effect of Tbx6EnR on gene expression was dose-dependent. At low dose (0.1 ng), it weakly inhibited the expression of *Xwnt8*, but significantly down-regulated the expression of *Xbra* and *XMyf5* at stages 10.5 and 25. At high dose (1.5 ng), more than 50% of inhibition of the expression of these genes was observed (Fig. 3). However, we did not obtain a complete block of the expression of these genes. This may be due to the mosaic distribution of injected mRNA. Other factors may be also involved in their regulation.

We next examined gene expression pattern in *Tbx6VP16*-injected whole gastrula by in situ hybridization. This provided further information compared with results from RT-PCR. We first found that Tbx6VP16 induced a condensation of pigmentation at the sites of injection (Figs. 4A, B), which might represent the formation of ectopic blastopore-like structure. However, in the absence of blastopore-specific marker gene, the exact nature of this structure remains to be determined. Interestingly, overexpression of Tbx6VP16 shifted *Xbra* expression to the presumptive neuroectoderm.

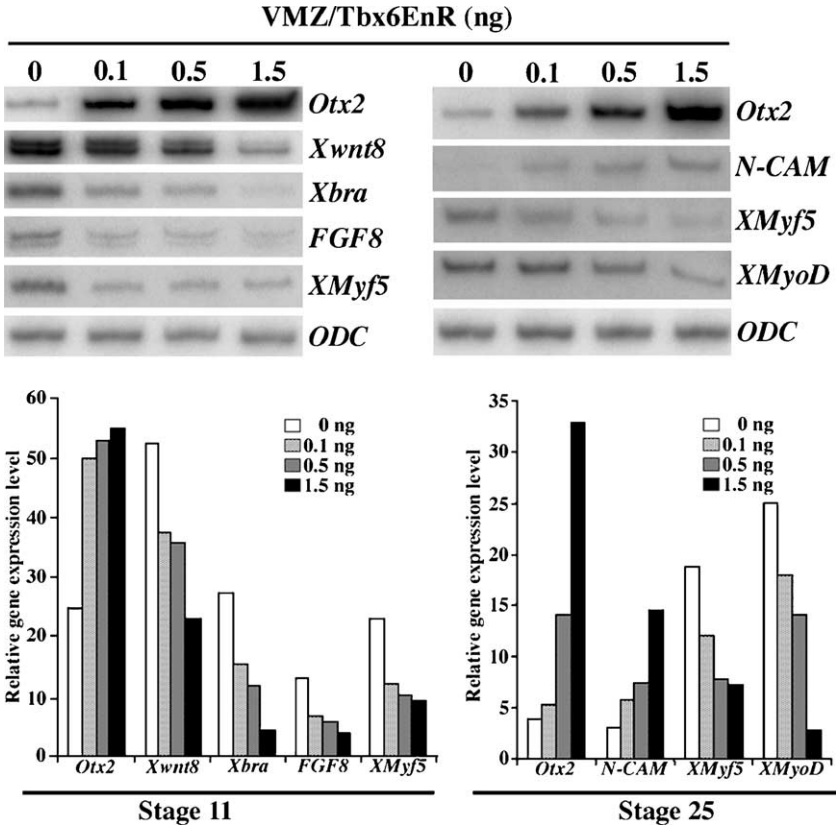

Fig. 3. Dose-dependent effect of Tbx6EnR on gene expression. Following injection of different amounts of Tbx6EnR mRNA in the ventral region at 4-cell stage, VMZ explants were dissected and RT-PCR was performed at stage 10.5 and 25. The intensity of each PCR product was normalized to *ODC*. This experiment was performed in triplicates with similar result.

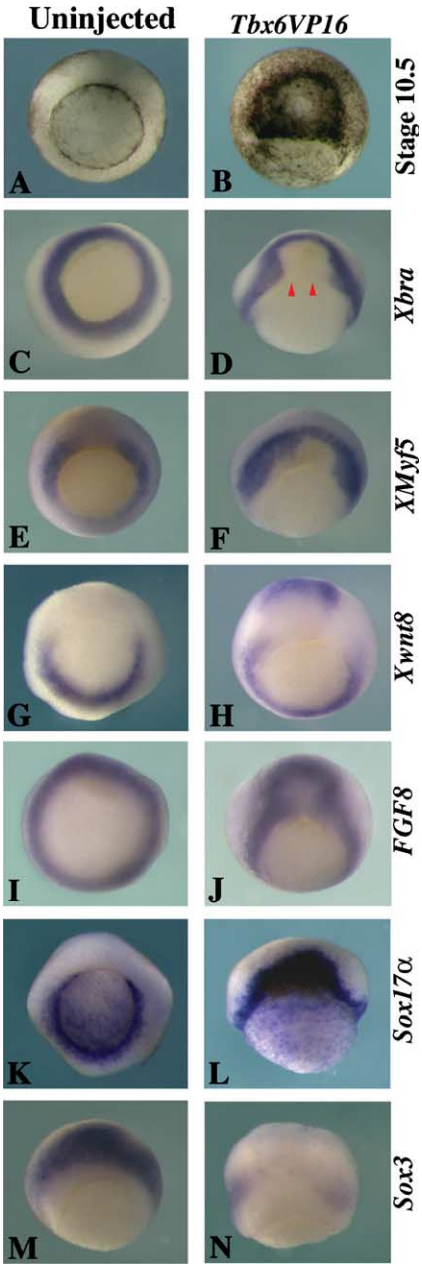

Fig. 4. Expression of mesoderm, endoderm and neural markers in *Tbx6VP16*-injected early gastrula. Embryos at 4-cell stage were dorsally injected with *Tbx6VP16* mRNA and cultured to early gastrula stage for in situ hybridization. (A) Vegetal view of an uninjected early gastrula. (B) Dorso-vegetal view of a *Tbx6VP16*-injected early gastrula with a condensation of pigmentation near injection sites. (C) Expression of *Xbra* in an uninjected early gastrula. (D) A *Tbx6VP16*-injected early gastrula showing a shift of *Xbra* expression domain to more anterior region. Arrowheads indicate the blastopore. (E) *XMyf5* expression in an uninjected early gastrula. (F) Ectopic expression of *XMyf5* in the dorsal region induced by Tbx6VP16. (G) *Xwnt8* expression in an uninjected early gastrula. (H) Ectopic expression of *Xwnt8* in a *Tbx6VP16*-injected early gastrula. (I) *FGF8* expression in an uninjected early gastrula is localized to the entire marginal zone. (J) Dorsal injection of *Tbx6VP16* shifted *FGF8* expression to a more anterior region. (K) *Sox17α* expression is located in the yolk plug and latero-ventral blastoporal lip with lower level in the dorsal region. (L) Tbx6VP16 strongly induces ectopic *Sox17α* expression in the dorsal region. (M) Expression of the neural marker *Sox3* in the dorsal ectoderm of an uninjected early gastrula. (N) Absence of *Sox3* expression in the dorsal ectoderm following injection of *Tbx6VP16*.

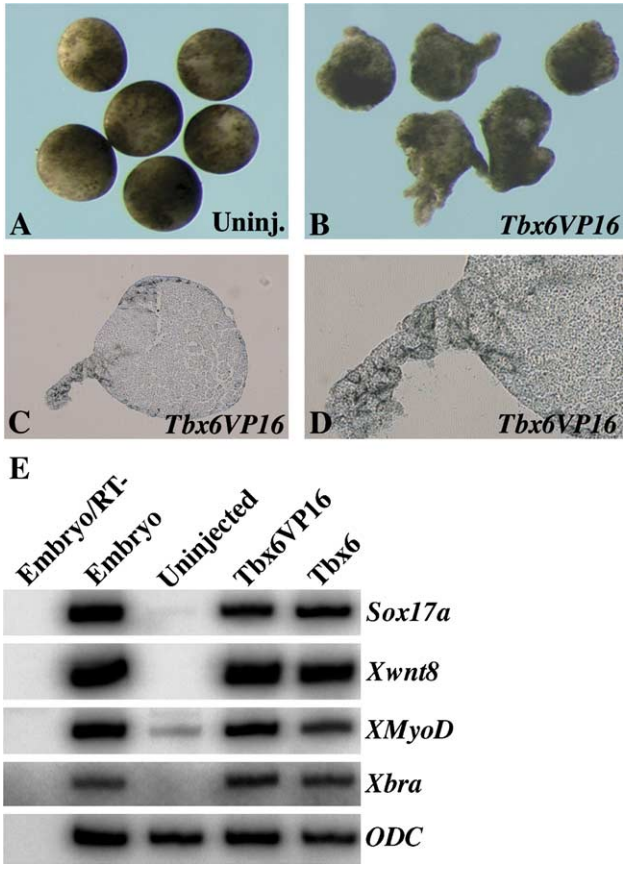

Fig. 5. Mesoderm and endoderm induction in ectoderm explants by Tbx6. Embryos at 4-cell stage were injected with *Tbx6VP16* or *Tbx6* mRNA in the animal pole region and ectodermal explants were cultured to stage 14. (A) Control uninjected explants. (B) *Tbx6VP16*-injected explants show elongation and protrusions. (C) Section from a *Tbx6VP16*-injected explant, low magnification. (D) Section from a *Tbx6VP16*-injected explant, high magnification. (E) RT-PCR analysis of mesoderm and endoderm markers. Both Tbx6VP16 and Tbx6 induce the expression of endodermal marker *Sox17α* in addition to latero-ventral mesoderm markers.

The newly induced expression domain of *Xbra* was located just above this ectopic blastopore-like structure (Figs. 4C, D). Although it is not clear if dorsal injection of *Tbx6VP16* induced ectopic *Xbra* expression or just shifted its expression pattern, it is clear that dorsal injection of *Tbx6VP16* induced ectopic expression of *XMyf5* (Figs. 4E, F) and *Xwnt8* (Figs. 4G, H). In addition, the ectopically induced expression domains of *XMyf5* and *Xwnt8* are distant to the endogenous blastopore. Furthermore, as in the case of *Xbra*, dorsal overexpression of Tbx6VP16 also shifted the expression domain of *FGF8* to more anterior region (Figs. 4I, J).

To see whether dorsal ectopic expression of Tbx6 indeed shifted the mesodermal domain to the presumptive neuroectoderm, we further analyzed the expression of the endodermal marker *Sox17α* (Hudson et al., 1997) and the early neuroectodermal marker *Sox3* (Penzel et al., 1997). In uninjected stage 10.5 gastrula, *Sox17α* is expressed around the blastopore and in the vegetal region fated to form endoderm (Fig. 4K; Hudson et al., 1997), with a lower level of expression in the dorsal blastoporal lip. However, in embryo dorsally injected with *Tbx6VP16* mRNA, strong expression of *Sox17α* was observed

in the dorsal region (Fig. 4L), indicating that Tbx6 is able to induce endoderm. Together with the expression pattern of *Xbra*, *XMyf5*, *FGF8* and *Xwnt8* in *Tbx6VP16*-injected early gastrula, this indicates that dorsal ectopic expression of Tbx6VP16 shifted the mesodermal domain further to the neuroectodermal region. Consistent with this conclusion, expression of *Sox3* was found to be strongly reduced or absent in early gastrula injected with *Tbx6VP16* mRNA (Figs. 4M, N).

To directly analyze the activity of Tbx6 in endoderm induction, we injected *Tbx6VP16* or wild-type *Tbx6* mRNA (200 pg) in the animal pole region and cultured animal cap explants to early neurula stage. Uninjected explants remained rounded (Fig. 5A), but *Tbx6VP16*-injected explants showed elongation and protrusions (Fig. 5B), which are formed by large cells in continuity with the epidermal layer (Figs. 5C, D). They likely result from cell shape change in the periphery of the explants. RT-PCR analysis indicated that both Tbx6VP16 and the wild-type Tbx6 potently induced the expression of the endodermal marker *Sox17α*, in addition to other latero-ventral mesodermal markers including *Xwnt8*, *XMyoD* and *Xbra* (Fig. 5E). This indicates that Tbx6 is able to induce both mesoderm and endoderm.

Tbx6 protects posterior mesoderm

The above observation suggests that Tbx6 induces mesoderm and endoderm at the expense of presumptive neuroectoderm. To further test this possibility, we directly assayed the effect of Tbx6VP16 to block neural induction promoted by overexpression of chordin (Piccolo et al., 1999). *Chordin* mRNA (500 pg) was injected either alone or coinjected with *Tbx6VP16* mRNA into animal pole region at 4-cell stage and ectodermal explants were dissected and cultured to stage 25 for analysis by RT-PCR of a panel of anteroposterior and mesodermal markers. When *chordin* mRNA was injected alone, ectodermal explants strongly express anterior neuroectodermal markers such as *Otx2* and *XAG1*, and the expression of *N-CAM* was also induced. Coinjection of *Tbx6VP16* mRNA with *chordin* mRNA strongly inhibited the expression of *Otx2*, *XAG1* and *N-CAM*. In these explants, somitic mesoderm markers like *muscle actin* and *XMyf5* genes were strongly expressed, as well as posterior mesodermal markers including *Hoxb9*, *Xcad2* and *Mespo* (Fig. 6A). This result indicates that Tbx6 exhibits a strong activity in posterior mesoderm

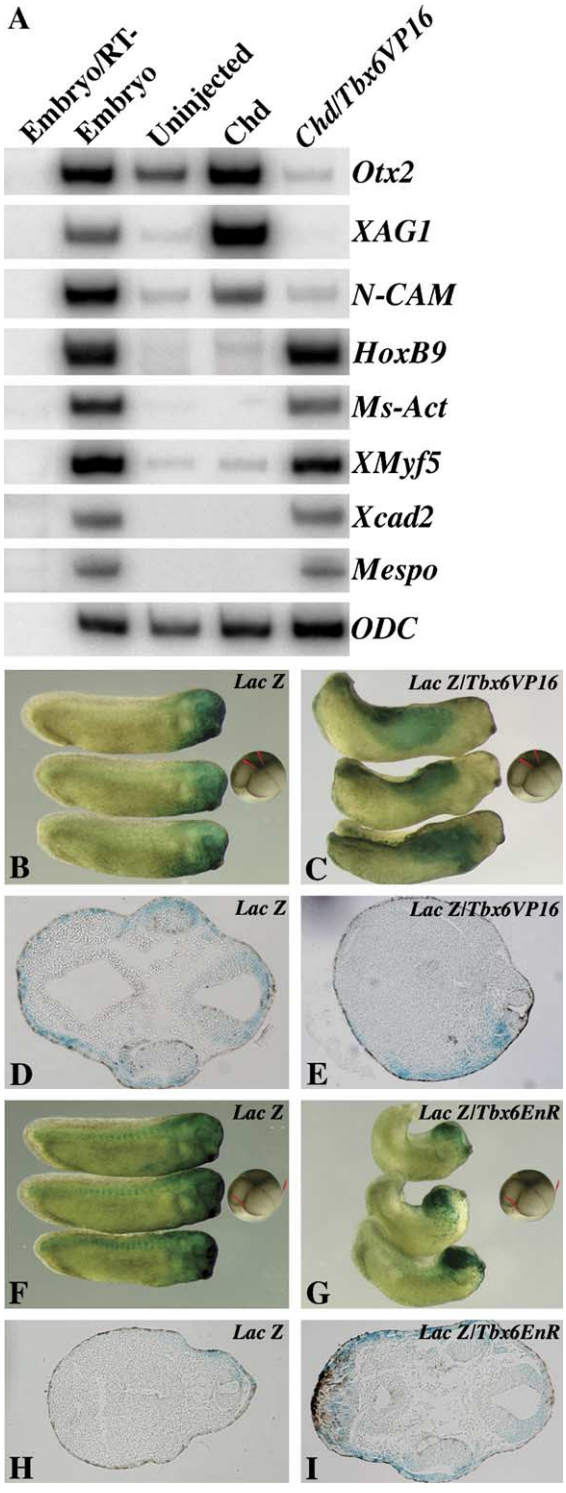

Fig. 6. Tbx6 inhibits neural induction in vitro and in vivo. (A) Tbx6 counterbalances the neuralizing activity of chordin. Embryos were injected with indicated mRNA and ectodermal explants were cultured to stage 25 for RT-PCR analysis. Overexpression of chordin induces the expression of anterior neuroectoderm markers *Otx2* and *XAG1*, as well as the pan-neural marker *N-CAM*. Coexpression of Tbx6VP16 with chordin strongly inhibits neural induction and induces the expression of different posterior mesoderm markers including *Hoxb9*, *Xcad2* and *Mespo*, in addition to somitic mesoderm markers *muscle actin* and *XMyf5*. (B–E) Cell lineage analysis in *Tbx6VP16*- and *Tbx6EnR*-injected embryos. *LacZ* mRNA was either injected alone or coinjected with *Tbx6VP16* or with *Tbx6EnR* mRNA in the indicated region at 8-cell stage. (B) Distribution of βgal-stained cells in the head and ventral regions in embryos injected with *LacZ* mRNA alone in the animal pole region of the two dorso-animal blastomeres. (C) Distribution of βgal-stained cells in the trunk region and somitic mesoderm following coinjection of *LacZ* mRNA with *Tbx6VP16* mRNA in the animal pole region of the two dorso-animal blastomeres. (D) Section at the head region of an embryo in panel B. (E) Section at the trunk region from an embryo in panel C. (F) βgal-stained cells are populated to the head region and somitic mesoderm when *LacZ* mRNA is injected alone in the marginal zone of the two dorso-animal blastomeres. (G) Coinjection of *Tbx6EnR* mRNA with *LacZ* mRNA in the marginal zone of the two dorso-animal blastomeres prevents somitic distribution of βgal-stained cells. (H) Section at the trunk region from an embryo in panel F. (I) Section at the head region from an embryo in panel G.

induction, and suggests that it induces posterior mesoderm at the expense of neural tissue.

Cell lineage tracing was then used to demonstrate the function of Tbx6 in protecting mesoderm. Synthetic mRNA corresponding to *LacZ* (500 pg) was either injected alone or coinjected with *Tbx6VP16* or *Tbx6EnR* mRNA at different regions of 8-cell stage embryos, and staining of β-galactosidase (βgal)-labeled cells was performed at the tail-bud stage. When *LacZ* mRNA was injected alone in the animal pole region of the two dorso-animal blastomeres, injected embryos developed normally and βgal-stained cells were mostly populated to the head region, with localization in both epidermis and neural tissue (Figs. 6B, D). Coinjection with *Tbx6VP16* mRNA in the same region resulted in embryos with anterior deficiency and reduced βgal-staining in the anterior region. In contrast, βgal-staining could be found in posterior and trunk somitic mesoderm and lateral plate mesoderm (Figs. 6C, E). This suggests that Tbx6VP16 changed the fate of neuroectodermal cells and induced them to become mesoderm. When *LacZ* mRNA was injected alone in the marginal zone of the two dorso-animal blastomeres, all injected embryos showed βgal-stained cells in the somitic mesoderm and in the head region (Figs. 6F, H). Strikingly, coinjection with *Tbx6EnR* mRNA prevented βgal-staining in the somites, and βgal-stained cells were essentially concentrated in the head region (Figs. 6G, I). This is consistent with the observation that Tbx6EnR induces anterior neural markers in VMZ explants (see Figs. 2C and 3). In this experiment, lower amounts of *Tbx6EnR* mRNA (100 pg) were used because injection of higher amounts of the mRNA blocked gastrulation movement (not shown).

Identification of Tbx6 target genes

Tbx6 regulates the expression of several latero-ventrally expressed mesodermal genes at the early gastrula stage (see Figs. 2B and 3), to identify the regulatory cascade between Tbx6 and these genes, we then set to identify direct target genes activated by Tbx6 at the early gastrula stage. We used a hormone-inducible form of Tbx6 (Fig. 7A) in which Tbx6VP16 was fused with the ligand-binding domain of the human glucocorticoid receptor (residues 512 to 777). The activity of this fusion protein (Tbx6VP16-GR) can be induced at appropriate stage by incubation of explants or whole embryos in dexamethasone (DEX). This approach was shown to be very efficient to identify direct T-box target genes (Tada et al., 1998). Synthetic mRNA corresponding to *Tbx6VP16-GR* (100 pg) was injected at 2-cell stage in the animal pole region and ectodermal explants were cut at stage 10.5. They were then treated with 10 μM DEX for 1.5 h in the absence or presence of 10 μM of the protein synthesis inhibitor, cycloheximide (CHX). The short-time induction by DEX and the presence of CHX will likely allow us to identify direct target genes of Tbx6. This is indeed the case. Following RT-PCR analysis of a panel of early mesodermal genes, we found that *FGF8*, *Xwnt8* and *XMyf5* were induced by Tbx6VP16-GR after 1.5 h of induction in DEX, either in the absence or presence of

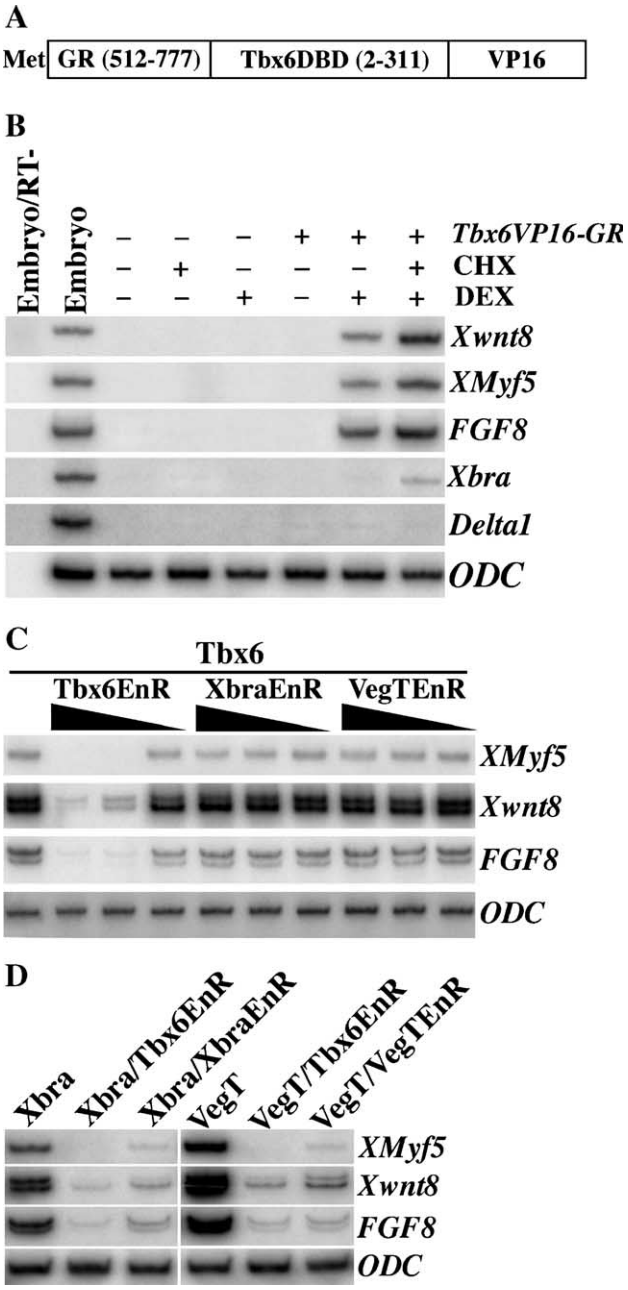

Fig. 7. Identification of Tbx6 direct targets genes. (A) Schematic representation of the inducible construct. (B) Embryos at 4-cell stage were injected with *Tbx6VP16-GR* mRNA and ectodermal explants were dissected and cultured to stage 10.5. Both uninjected and injected explants were treated with cycloheximide (CHX) or dexamethasone (DEX), or both, for 1.5 h. The expression of a panel of mesoderm and endoderm markers was analyzed by RT-PCR. Among these genes, the expression of *FGF8*, *Xwnt8* and *XMyf5* was rapidly and specifically induced and was not blocked in the presence of CHX. (C) Tbx6-induced expression of *XMyf5*, *Xwnt8* and *FGF8* was blocked by Tbx6EnR in a dose-dependent manner, but not by XbraEnR and VegTEnR. (D) Tbx6EnR strongly blocks the expression of *XMyf5*, *Xwnt8* and *FGF8* induced by Xbra and VegT. XbraEnR and VegTEnR also block the activity of Xbra and VegT, respectively.

CHX (Fig. 7B). No expression of any mesodermal marker was detected in *Tbx6VP16-GR*-injected ectodermal explants in the absence of DEX. This indicates that the induction of *FGF8*, *Xwnt8* and *XMyf5* by Tbx6VP16-GR in the presence of DEX is rapid and specific, and thus they represent direct

target genes of Tbx6 at the early gastrula stage. Tbx6VP16-GR did not induce *Xbra* expression following incubation in DEX, although a weak expression was observed in *Tbx6VP16-GR*-injected explants treated with both DEX and CHX (Fig. 7B). The same was true for *szl*, *XMyoD* and *Mespo* (not shown). Recently, *Delta 1* has been shown to be a target of Wnt signaling in synergy with Tbx6 in mouse embryo (Hofmann et al., 2004; White and Chapman, 2005), we also found that Tbx6VP16 was able to induce its expression in ectodermal explants at early gastrula stage. However, using the inducible *Tbx6VP16-GR* construct, and the condition described above, *Delta 1* expression was not detected (Fig. 7B). A similar result was obtained using mRNA ranging from 20 to 100 pg (not shown).

To see if *XMyf5*, *FGF8* and *Xwnt8* also represent targets of other T-box transcription factors such as Xbra and VegT, we injected 200 pg wild-type *Tbx6* mRNA alone or coinjected with different amounts (100 pg, 400 pg and 1000 pg) of *Tbx6EnR*, *XbraEnR* or *VegTEnR* mRNA in the animal pole region at 2-cell stage and cultured ectodermal explants to early gastrula stage. In this experiment, if Tbx6 is activating downstream targets of Xbra or VegT through low affinity interaction with the *T-box* binding sites, the induction of these genes should be inhibited by XbraEnR or by VegTEnR. The result shows that only Tbx6EnR potently inhibited the expression of all three genes induced by Tbx6 in a dose-dependent manner. However, XbraEnR and VegTEnR had no significant effect on the expression of *XMyf5*, *Xwnt8* and *FGF8* induced by Tbx6 (Fig. 7C). Similar result was obtained using Tbx6VP16 (not shown). Conversely, coinjection of 400 pg *Tbx6EnR* mRNA with 200 pg *Xbra* or *VegT* mRNA strongly blocked the expression of these genes induced by Xbra and VegT. A two-fold excess of *XbraEnR* and *VegTEnR* mRNA also inhibited the activity of Xbra and VegT,

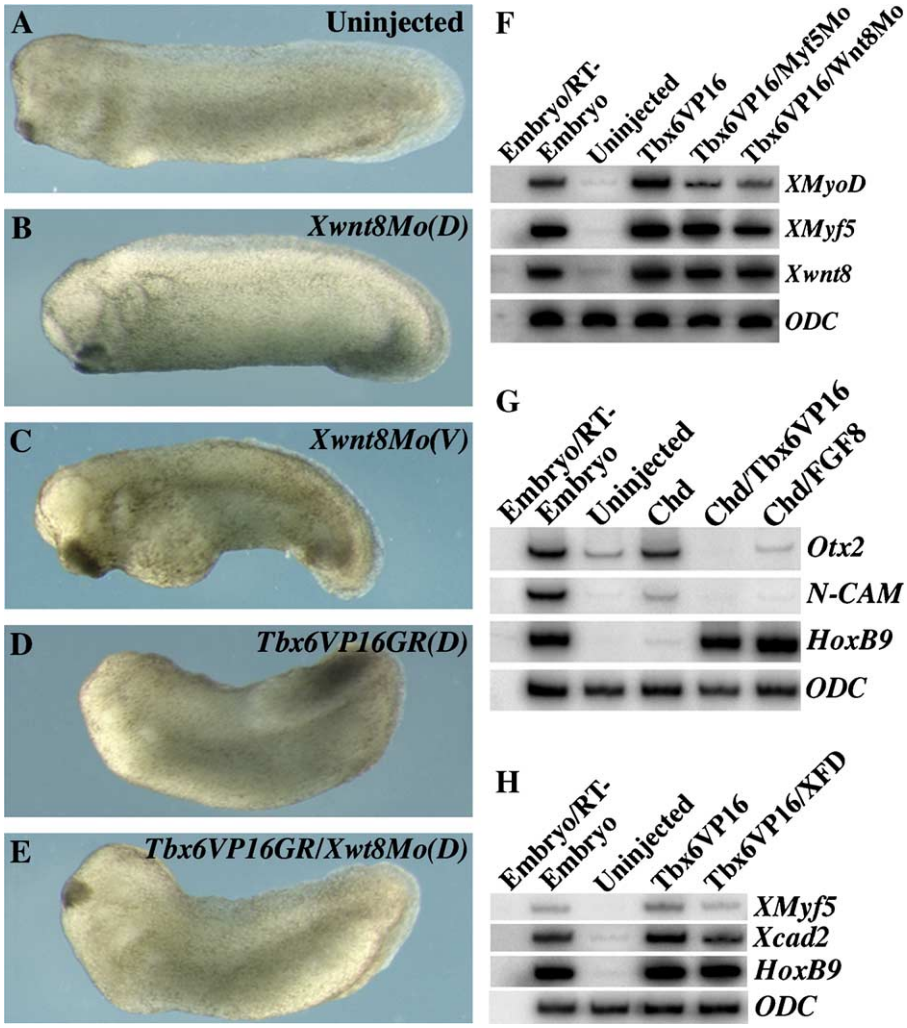

Fig. 8. Functional interaction between Tbx6, FGF8, Xwnt8 and XMyf5. (A–D) Interaction between Tbx6 and Xwnt8 in anteroposterior patterning. Embryos were injected at 4-cell stage and cultured to stage 35. (A) A control embryo. (B) A *Xwnt8Mo*-injected embryo in the dorsal region with slightly dorsalized phenotype. (C) A *Xwnt8Mo*-injected embryo in the ventral region with enlarged head and shortened anteroposterior axis. (D) A *Tbx6VP16-GR*-injected embryo incubated in DEX at stage 11 shows anterior deficiency at stage 35. (E) Coinjection of *Xwnt8Mo* with *Tbx6VP16-GR* mRNA rescues head development. (F) Interaction between Tbx6, Xwnt8 and XMyf5 in myogenesis. Embryos were injected at 2-cell stage and animal cap explants were cultured to stage 11 for RT-PCR analysis. Inhibition of Xwnt8 and XMyf5 activity strongly inhibits *XMyoD* expression induced by Tbx6VP16. (G) FGF8 exhibits similar activity as Tbx6VP16 in inhibiting neural induction in explants cultured to stage 25. A dominant negative FGF receptor (XFD) inhibits *XMyf5* and *Xcad2* expression induced by Tbx6VP16 in explants cultured to stage 25.

respectively (Fig. 7D). This result suggests that *XMyf5*, *Xwnt8* and *FGF8* likely represent specific targets of Tbx6.

Interaction between Tbx6 and its target genes in the specification of posterior mesoderm

This direct induction suggests that Tbx6 may interact with Xwnt8, XMyf5 and FGF8 in specifying posterior mesoderm. We first tested the interaction between Tbx6 and Xwnt8. We used *Xwnt8* antisense morpholino oligonucleotide (*Xwnt8Mo*) to specifically block the translation of *Xwnt8* mRNA and also took the advantage of the inducible Tbx6VP16-GR to induce its activity at the early gastrula stage. *Tbx6VP16-GR* mRNA was injected alone or coinjected with *Xwnt8Mo* (10 ng) at a 4-cell stage in the dorsal region and injected embryos at the early gastrula stage were incubated in the presence or absence of DEX until tail-bud stage. While dorsal injection of *Xwnt8Mo* produced only a moderately dorsalized phenotype (compare Figs. 8A and B), ventral injection resulted in embryos with enlarged head and shortened anteroposterior axis (Fig. 8C), a phenotype reminiscent of an inhibition of zygotic Wnt/β-catenin signaling (Glinka et al., 1998). However, embryos dorsally injected with *Tbx6VP16-GR* mRNA and treated with DEX exhibited anterior deficiency, characterized by an absence of eye and cement gland and microcephaly (Fig. 8D), a phenotype which is closely similar to that obtained by ectopic zygotic expression of Xwnt8 (Christian and Moon, 1993). Dorsal coinjection of *Xwnt8Mo* with *Tbx6VP16-GR* mRNA followed by DEX treatment at early gastrula stage significantly rescued head development, with embryos showing normal head and anteroposterior axis (Fig. 8E; Table 1). Therefore, *Xwnt8* may represent an immediate target, and relay the function of Tbx6 in dorsoventral and anteroposterior patterning.

To see if Xwnt8 and XMyf5 also relay the function of Tbx6 in myogenesis, we coinjected *Tbx6VP16* mRNA with *Xwnt8Mo* (10 ng) or *XMyf5Mo* (10 ng) in the animal pole region at 2-cell stage. Ectodermal explants were dissected and cultured to stage 10.5 for RT-PCR analysis. The result shows that coinjection of *Xwnt8Mo* or *XMyf5Mo* with *Tbx6VP16* strongly inhibited *XMyoD* expression induced by Tbx6VP16 (Fig. 8F), indicating that Tbx6 induces *XMyoD* expression through XMyf5 and Xwnt8. This is consistent with the observation that Myf5 acts upstream of MyoD (Tajbakhsh et al., 1997) and that Wnt/β-catenin signaling is required for the expression of *MyoD* (Hoppler et al., 1996). As for FGF8, the antisense morpholino approach showed no discernible effect on the phenotype (not shown; see also Lombardo and Slack, 1997), we first tested its activity in blocking neural induction in comparison with Tbx6. *Chordin* mRNA (500 pg) was injected alone or coinjected with *Tbx6VP16* mRNA (1 pg), or *FGF8* mRNA (10 pg) in the animal pole region at 4-cell stage. Ectodermal explants were dissected at blastula stage and cultured to stage 25. RT-PCR result shows that FGF8 exhibits a similar activity as Tbx6 in blocking neural induction and in inducing posterior genes, although to a lesser extent (Fig. 8G). We then used the dominant negative FGF receptor, which produces more strong and reproducible effect. *Tbx6VP16* mRNA was either injected alone or coinjected with *XFD* mRNA (500 pg) in the animal pole region at 2-cell stage and ectodermal explants were cultured to stage 25. The result showed that XFD decreased the expression of *XMyf5* and *Xcad2*, but had no effect on the expression of *HoxB9* (Fig. 8H). This indicates that FGF signaling relays the function of Tbx6 in the regulation of a subset of posterior genes.

Discussion

Tbx6 plays a key role in the specification of posterior paraxial mesoderm in all vertebrates. Here, we showed that *FGF8*, *Xwnt8* and *XMyf5* are target genes of Tbx6 and relay the function of Tbx6 in the specification of posterior mesoderm. These results identify a regulatory cascade governed by Tbx6 in this process.

Specification of lateral and ventral mesoderm by Tbx6

The involvement of several *Xenopus T-box* genes, including *Xbra* (Smith et al., 1991; Conlon et al., 1996), *eomes* (Ryan et al., 1996) and *VegT* (Zhang and King, 1996; Lustig et al., 1996; Stennard et al., 1996; Horb and Thomsen, 1997; Zhang et al., 1998; Clements et al., 1999; Kofron et al., 1999; Xanthos et al., 2002; White et al., 2002) in mesoderm induction and patterning has been more extensively investigated. However, relatively little is known about the function of *Tbx6*, another *T-box* gene, in these processes. In the present study, we showed that the expression pattern of *Tbx6* in the early gastrula overlaps those

Table 1
Functional interaction between Tbx6 and Xwnt8 in anteroposterior patterning

Injections phenotypes	Phenotypes				*n*
	Acephalic	Microcephalic	Enlarged head	Normal	
Uninjected		2		98	89
Tbx6VP16-GR/DEX (Dorso-animal)	84	16			95
Xwnt8Mo (Ventral)			73	27	98
Xwnt8Mo (Dorsal)			19	81	78
Tbx6VP16/Xwnt8Mo/DEX (Dorso-animal)		39	32	29	106

Embryos were injected at 4-cell stage and cultured to stage 35 for score of phenotypes. Acephalic embryos show absence of cement gland and eyes, microcephalic embryos exhibit reduced head structures with smaller cement gland and eyes, and embryos with enlarged head display strongly dorsalized phenotype with enlarged cement gland and reduced trunk and posterior regions. The results were expressed as percentage, except *n*, which refers to total embryos scored from three independent experiments.

of *XMyf5*, *XMyoD* and *Xwnt8*. Functional analyses show that, in vitro and in vivo, Tbx6 is both required and sufficient for the expression of several latero-ventrally expressed mesodermal genes. In particular, Tbx6 exhibited a strong activity to repress the expression of the dorsal mesodermal and anterior neural marker *Otx2*, while it potently induced, both directly and indirectly, the expression of ventral and posterior mesodermal genes including *FGF8*, *XMyf5*, *XMyoD*, *sizzled*, *Xwnt8*, *Xcad2*, *Mespo* and *Hoxb9*. Some of these genes may represent direct target genes of Tbx6 (see further discussion). Conversely, inhibition of Tbx6 activity in ventral mesoderm leads it to express dorsal and anterior mesodermal and neural marker *Otx2*. This suggests that Tbx6 is potently involved in early dorsoventral and anteroposterior patterning. In addition, both in whole embryo and in isolated ectodermal explants, Tbx6 is also able to induce endoderm, an activity that is shared by VegT (Clements et al., 1999; Casey et al., 1999; Xanthos et al., 2001; Stennard, 1998). It was shown that Tbx6 induces the expression of *VegT* (Uchiyama et al., 2001), raising the possibility of an interaction and a regulatory loop between these two genes in endoderm induction. It will be interesting in the future to examine this interaction.

Tbx6 protects posterior mesoderm

The shift of *Xbra* expression domain to neuroectoderm following ectopic expression of Tbx6 in the dorsal region suggests that Tbx6 possesses the ability to convert neuroectoderm into mesoderm. Indeed, our result showed that neural induction did not take place in ectoderm explants expressing chordin and Tbx6. By contrast, only the expression of posterior mesoderm markers could be detected. This indicates that Tbx6 may have a strong activity to induce posterior mesoderm and this may represent one of the mechanisms to explain its inhibitory effect on neural induction. Consistent with the result from gain-of-function analysis, inhibition of Tbx6 activity in ventral mesoderm strongly promoted neural induction (see Figs. 2C and 3), suggesting that the activity of endogenous Tbx6 is required to prevent neural induction. The cell lineage analysis of the distribution of Tbx6VP16- or Tbx6EnR-expressing cells further supports the conclusion that Tbx6 protects posterior mesoderm from neural induction. Therefore, these results are in accordance with previous observation showing that posterior mesoderm is transformed into neural tube in *Tbx6* knock-out mice (Chapman and Papaioannou, 1998). Since *Tbx6* is expressed in the tail-bud region, it likely functions to protect this region from neural induction.

Tbx6 target genes

The *T-box* gene family encodes related DNA-binding transcriptional regulators, at present little is known of the identities of their transcriptional targets (Showell et al., 2004). Recently, significant effort has been made to identify Xbra and VegT target genes using hormone-inducible constructs, which has allowed the identification of several homeobox genes involved in mesoderm and endoderm induction (Tada et al., 1998; Casey et al., 1999). We have used the same approach to identify Tbx6 target genes, and this has allowed us to show that *FGF8*, *Xwnt8* and *XMyf5* genes were directly regulated by Tbx6 in the early gastrula. Recently, it has been shown that Wnt8 activates the expression of *Tbx6* in zebrafish embryo (Szeto and Kimelman, 2004). Indeed, zygotic Wnt signaling is able to induce *Tbx6* expression in *Xenopus* ectodermal cells (data not shown; Uchiyama et al., 2001). This implies that there may be a positive regulatory loop between Xwnt8 and Tbx6. We found that the induction of *XMyf5*, *FGF8* and *Xwnt8* is independent on Xbra and VegT. However, although Xbra and VegT both induce *FGF8*, *Xwnt8* and *XMyf5*, the induction is strongly dependent on Tbx6. Thus, *XMyf5*, *FGF8* and *Xwnt8*, they may be indeed specific target genes of Tbx6, or at least Tbx6 binds to the T-box binding sites of these genes with higher affinity.

The direct regulation of *Xwnt8* by Tbx6 suggests that Tbx6 may act through Xwnt8, at least to some extent, in the specification of posterior mesoderm. Indeed, blocking specifically the translation of *Xwnt8* rescues the anterior deficiency produced by ectopic expression of Tbx6 at gastrula stage. From this observation, together with the similarity in phenotypes produced by overexpression of Tbx6 and Xwnt8 after midblastula transition (see further discussion), it is conceivable that Tbx6 and Xwnt8 function in the same cascade to regulate different aspects of embryonic patterning.

This genetic interaction also plays a role during myogenesis since Xwnt8 has been shown to regulate myogenic gene expression, and blockade of Wnt/β-catenin signaling inhibits the expression of *Myf5* and *MyoD* in *Xenopus* (Hoppler et al., 1996; Shi et al., 2002). In mice, Wnt/β-catenin signaling also functions synergistically with Tbx6 to control somite formation and patterning (Hofmann et al., 2004). In addition, Myf5 has been proposed to function upstream of MyoD (Tajbakhsh et al., 1997). In this study, we have shown that inhibition of XMyf5 and Xwnt8 function strongly inhibited *XMyoD* expression induced by Tbx6, indicating that XMyf5 and Xwnt8 act downstream of Tbx6 in myogenesis. Thus, Tbx6, by regulating the expression of *Xwnt8* and *XMyf5* genes, plays an important role in somitogenesis in *Xenopus* embryo (Fig. 9). *Tbx6* and *FGF8* also show overlapping expression at gastrula stage and they are coexpressed in the tail region at late stages. Conversely, inhibition of FGF signaling by a dominant negative FGF receptor down-regulated *XMyf5* and *Xcad2* expression at tail-bud stage. The regulation of *FGF8* by Tbx6 may also contribute to the protection of posterior mesoderm from neural induction and maintain myoblasts in an undifferentiated state. Indeed, consistent with its posteriorizing activity (Christen and Slack,

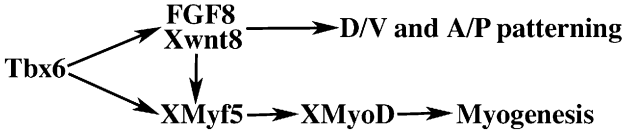

Fig. 9. Regulatory hierarchy in posterior mesoderm specification and myogenesis involving Tbx6, FGF8, Xwnt8 and XMyf5. Tbx6 functions upstream of these genes in both processes (see Discussion for detail).

1997), coexpression of FGF8 with chordin strongly reduced the expression level of anterior neural markers accompanied with an induction of posterior gene *Hoxb9*, raising the possibility that Tbx6 prevents neural induction through induction of *FGF8* expression. The regulation of FGF8 by Tbx6 may have an important implication in embryonic patterning in vertebrates because a gradient of *FGF8* mRNA has been shown to couple differentiation of embryonic tissues to axis elongation (Dubrulle and Pourquie, 2004).

Because of the strong phenotypes resulted from both gain-of-function and loss-of-function, it is clear that Tbx6 occupies a key position in the specification of posterior paraxial mesoderm and patterning of anteroposterior axis. It functions to induce the expression of posterior mesodermal genes and to inhibit neural induction. The present study strongly suggests that Tbx6 acts upstream of *FGF8*, *Xwnt8* and *XMyf5* in the specification of posterior mesoderm.

Acknowledgments

We would like to thank Drs. H. Uchiyama, J. Smith, R. Harland, E. De Robertis, H. Grunz and H. Woodland for sharing the plasmid constructs used in this study. This work was supported by grants from the Association Française de Myopathie (AFM), Ligue Nationale Contre le Cancer (LNCC) and Association pour la Recherche sur le Cancer (ARC). H.Y. Li was supported in part by a post-doctoral fellowship from the University Pierre et Marie-Curie.

References

Bamshad, M., Lin, R.C., Law, D.J., Watkins, W.C., Krakowiak, P.A., Moore, M.E., Franceschini, P., Lala, R., Holmes, L.B., Gebuhr, T.C., Bruneau, B.G., Schinzel, A., Seidman, J.G., Seidman, C.E., Jorde, L.B., 1997. Mutations in human TBX3 alter limb, apocrine and genital development in ulnar-mammary syndrome. Nat. Genet. 16, 311–315.

Basson, C.T., Bachinsky, D.R., Lin, R.C., Levi, T., Elkins, J.A., Soults, J., Grayzel, D., Kroumpouzou, E., Traill, T.A., Leblanc-Straceski, J., Renault, B., Kucherlapati, R., Seidman, J.G., Seidman, C.E., 1997. Mutations in human TBX5 cause limb and cardiac malformation in Holt-Oram syndrome. Nat. Genet. 15, 30–35.

Beckers, J., Schlautmann, N., Gossler, A., 2000. The mouse rib-vertebrae mutation disrupts anterior–posterior somite patterning and genetically interacts with a *Delta1* null allele. Mech. Dev. 95, 35–46.

Casey, E.S., Tada, M., Fairclough, L., Wylie, C.C., Heasman, J., Smith, J.C., 1999. Bix4 is activated directly by VegT and mediates endoderm formation in *Xenopus* development. Development 126, 4193–4200.

Chapman, D.L., Papaioannou, V.E., 1998. Three neural tubes in mouse embryos with mutations in the T-box gene *Tbx6*. Nature 391, 695–697.

Chapman, D.L., Agulnik, I., Hancock, S., Silver, L.M., Papaioannou, V.E., 1996. Tbx6, a mouse T-Box gene implicated in paraxial mesoderm formation at gastrulation. Dev. Biol. 180, 534–542.

Christen, B., Slack, J.M., 1997. FGF-8 is associated with anteroposterior patterning and limb regeneration in *Xenopus*. Dev. Biol. 192, 455–466.

Christian, J.L., Moon, R.T., 1993. Interactions between Xwnt-8 and Spemann organizer signaling pathways generate dorsoventral pattern in the embryonic mesoderm of *Xenopus*. Genes Dev. 7, 13–28.

Clements, D., Friday, R.V., Woodland, H.R., 1999. Mode of action of VegT in mesoderm and endoderm formation. Development 126, 4903–4911.

Conlon, F.L., Sedgwick, S.G., Weston, K.M., Smith, J.C., 1996. Inhibition of Xbra transcription activation causes defects in mesodermal patterning and reveals autoregulation of Xbra in dorsal mesoderm. Development 122, 2427–2435.

Djiane, A., Riou, J.F., Umbhauer, M., Boucaut, J.C., Shi, D.L., 2000. Role of *frizzled 7* in the regulation of convergent extension movements during gastrulation in *Xenopus laevis*. Development 127, 3091–3100.

Dobrovolskaïa-Zavadskaïa, N., 1927. Sur la mortification spontanée de la queue chez la souris nouveau-née et sur l'existence d'un caractère (facteur) héréditaire "non-viable". C. R. Seance Soc. Biol. 97, 114–116.

Dubrulle, J., Pourquie, O., 2004. fgf8 mRNA decay establishes a gradient that couples axial elongation to patterning in the vertebrate embryo. Nature 427, 419–422.

Glinka, A., Wu, W., Delius, H., Monaghan, A.P., Blumenstock, C., Niehrs, C., 1998. Dickkopf-1 is a member of a new family of secreted proteins and functions in head induction. Nature 391, 357–362.

Griffin, K.J., Amacher, S.L., Kimmel, C.B., Kimelman, D., 1998. Molecular identification of spadetail: regulation of zebrafish trunk and tail mesoderm formation by T-box genes. Development 125, 3379–3388.

Harland, R.M., 1991. In situ hybridization: an improved whole mount method for *Xenopus* embryos. In: Kay, B.K., Peng, H.B. (Eds.), Methods in Cell Biology, vol. 36. Academic Press, San Diego, pp. 685–695.

Herrmann, B.G., Labeit, S., Poustka, A., King, T.R., Lehrach, H., 1990. Cloning of the T gene required in mesoderm formation in the mouse. Nature 343, 617–622.

Hofmann, M., Schuster-Gossler, K., Watabe-Rudolph, M., Aulehla, A., Herrmann, B.G., Gossler, A., 2004. WNT signaling, in synergy with T/TBX6, controls Notch signaling by regulating Dll1 expression in the presomitic mesoderm of mouse embryos. Genes Dev. 18, 2712–2717.

Hoppler, S., Brown, J.D., Moon, R.T., 1996. Expression of a dominant-negative Wnt blocks induction of MyoD in *Xenopus* embryos. Genes Dev. 10, 2805–2817.

Horb, M.E., Thomsen, G.H., 1997. A vegetally localized T-box transcription factor in *Xenopus* eggs specifies mesoderm and endoderm and is essential for embryonic mesoderm formation. Development 124, 1689–1698.

Hudson, C., Clements, D., Friday, R.V., Stott, D., Woodland, H.R., 1997. Xsox17alpha and -beta mediate endoderm formation in *Xenopus*. Cell 91, 397–405.

Hug, B., Walter, V., Grunwald, D.J., 1997. *tbx6*, a Brachyury-related gene expressed by ventral mesendodermal precursors in the zebrafish embryo. Dev. Biol. 183, 61–73.

Joseph, E.M., Cassetta, L.A., 1999. Mespo: a novel basic helix–loop–helix gene expressed in the presomitic mesoderm and posterior tailbud of *Xenopus* embryos. Mech. Dev. 82, 191–194.

Kofron, M., Demel, T., Xanthos, J., Lohr, J., Sun, B., Sive, H., Osada, S., Wright, C., Wylie, C., Heasman, J., 1999. Mesoderm induction in *Xenopus* is a zygotic event regulated by maternal VegT via TGFbeta growth factors. Development 126, 5759–5770.

Lombardo, A., Slack, J.M.W., 1997. Inhibition of *eFGF* expression in *Xenopus* embryos by antisense mRNA. Dev. Dyn. 208, 162–169.

Li, Q.Y., Newbury-Ecob, R.A., Terrett, J.A., Wilson, D.I., Curtis, A.R., Yi, C.H., Gebuhr, T., Bullen, P.J., Robson, S.C., Strachan, T., Bonnet, D., Lyonnet, S., Young, I.D., Raeburn, J.A., Buckler, A.J., Law, D.J., Brook, J.D., 1997. Holt-Oram syndrome is caused by mutations in TBX5, a member of the Brachyury (T) gene family. Nat. Genet. 15, 21–29.

Lustig, K.D., Kroll, K.L., Sun, E.E., Kirschner, M.W., 1996. Expression cloning of a *Xenopus* T-related gene (*Xombi*) involved in mesodermal patterning and blastopore lip formation. Development 122, 4001–4012.

Nacke, S., Schafer, R., Habre de Angelis, M., Mundlos, S., 2000. Mouse mutant "rib-vertebrae" (rv): a defect in somite polarity. Dev. Dyn. 219, 192–200.

Ng, J.K., Kawakami, Y., Buscher, D., Raya, A., Itoh, T., Koth, C.M., Esteban, C.R., Rodriguez-Leon, J., Garrity, D.M., Fishman, M.C., Belmonte, J.C., 2002. The limb identity gene Tbx5 promotes limb initiation by interacting with Wnt2b and Fgf10. Development 129, 5161–5170.

Nieuwkoop, P.D., Faber, J., 1967. Normal Table of *Xenopus laevis* (Daudin). North Holland, Amsterdam.

Papaioannou, V.E., 1997. T-box family reunion. Trends Genet. 13, 212–213.

Penzel, R., Oschwald, R., Chen, Y., Tacke, L., Grunz, H., 1997. Characterization and early embryonic expression of a neural specific transcription factor *xSOX3* in *Xenopus laevis*. Int. J. Dev. Biol. 41, 667–677.

Piccolo, S., Sasai, Y., Lu, B., De Robertis, E.M., 1999. Dorsoventral patterning in *Xenopus*: inhibition of ventral signals by direct binding of chordin to BMP-4. Cell 86, 589–598.

Pillemer, G., Epstein, M., Blumberg, B., Yisraeli, J.K., De Robertis, E.M., Steinbeisser, H., Fainsod, A., 1998. Nested expression and sequential downregulation of the *Xenopus* caudal genes along the anterior–posterior axis. Mech. Dev. 71, 193–196.

Russ, A.P., Wattler, S., Colledge, W.H., Aparicio, S.A., Carlton, M.B., Pearce, J.J., Barton, S.C., Surani, M.A., Ryan, K., Nehls, M.C., Wilson, V., Evans, M.J., 2000. Eomesodermin is required for mouse trophoblast development and mesoderm formation. Nature 404, 95–99.

Ryan, K., Garrett, N., Mitchell, A., Gurdon, J.B., 1996. *Eomesodermin*, a key early gene in *Xenopus* mesoderm differentiation. Cell 87, 989–1000.

Salic, A.N., Kroll, K.L., Evans, L.M., Kirschner, M.W., 1997. Sizzled: a secreted Xwnt8 antagonist expressed in the ventral marginal zone of *Xenopus* embryos. Development 124, 4739–4748.

Shi, D.L., Bourdelas, A., Umbhauer, M., Boucaut, J.C., 2002. Zygotic Wnt/beta-catenin signaling preferentially regulates the expression of *Myf5* gene in the mesoderm of *Xenopus*. Dev. Biol. 245, 124–135.

Showell, C., Binder, O., Conlon, F.L., 2004. T-box genes in early embryogenesis. Dev. Dyn. 229, 201–218.

Smith, J.C., 1999. T-box genes: what they do and how they do it. Trends Genet. 15, 154–158.

Smith, J.C., Price, B.M.J., Green, J.B.A., Weigel, D., Herrmann, B.G., 1991. Expression of a *Xenopus* homolog of *Brachyury* (*T*) is an immediate-early response to mesoderm induction. Cell 67, 79–87.

Smith, J.C., Conlon, F.L., Saka, Y., Tada, M., 2000. *Xwnt11* and the regulation of gastrulation in *Xenopus*. Philos. Trans. R. Soc. Lond., B Biol. Sci. 355, 923–930.

Stennard, F., 1998. *Xenopus* differentiation: VegT gets specific. Curr. Biol. 8, R928–R930.

Stennard, F., Carnac, G., Gurdon, J.B., 1996. The *Xenopus T-box* gene, Antipodean, encodes a vegetally localised maternal mRNA and can trigger mesoderm formation. Development 122, 4179–4188.

Szeto, D.P., Kimelman, D., 2004. Combinatorial gene regulation by Bmp and Wnt in zebrafish posterior mesoderm formation. Development 131, 3751–3760.

Tada, M., Casey, E.S., Fairclough, L., Smith, J.C., 1998. Bix1, a direct target of *Xenopus* T-box genes, causes formation of ventral mesoderm and endoderm. Development 125, 3997–4006.

Tajbakhsh, S., Rocancourt, D., Cossu, G., Buckingham, M., 1997. Redefining the genetic hierarchies controlling skeletal myogenesis: Pax-3 and Myf-5 act upstream of MyoD. Cell 89, 127–138.

Takeuchi, J.K., Koshiba-Takeuchi, K., Suzuki, T., Kamimura, M., Ogura, K., Ogura, T., 2003. Tbx5 and Tbx4 trigger limb initiation through activation of the Wnt/Fgf signaling cascade. Development 130, 2729–2739.

Theiler, K., Varnum, D.S., 1985. Development of rib-vertebrae: a new mutation in the house mouse with accessory caudal duplications. Anat. Embryol. (Berl) 173, 111–116.

Uchiyama, H., Kobayashi, T., Yamashita, A., Ohno, S., Yabe, S., 2001. Cloning and characterization of the T-box gene *Tbx6* in *Xenopus laevis*. Dev. Growth Differ. 43, 657–669.

Vize, P.D., Hemmatie-Brivanlou, A., Harland, R.M., Melton, D.A., 1991. Assays for gene function in developing *Xenopus* embryos. In: Kay, B.K., Peng, H.B. (Eds.), Methods in Cell Biology, vol. 36. Academic Press, San Diego, pp. 367–387.

Watabe-Rudolph, M., Schlautmann, N., Papaioannou, V.E., Gossler, A., 2002. The mouse rib-vertebrae mutation is a hypomorphic *Tbx6* allele. Mech. Dev. 119, 251–256.

White, P.H., Chapman, D.L., 2005. Dll1 is a downstream target of Tbx6 in the paraxial mesoderm. Genesis 42, 193–202.

White, R.J., Sun, B.I., Sive, H.L., Smith, J.C., 2002. Direct and indirect regulation of derriere, a *Xenopus* mesoderm-inducing factor, by VegT. Development 129, 4867–4876.

White, P.H., Farkas, D.R., McFadden, E.E., Chapman, D.L., 2003. Defective somite patterning in mouse embryos with reduced levels of Tbx6. Development 130, 1681–1690.

Xanthos, J.B., Kofron, M., Wylie, C., Heasman, J., 2001. Maternal *VegT* is the initiator of a molecular network specifying endoderm in *Xenopus laevis*. Development 128, 167–180.

Xanthos, J.B., Kofron, M., Tao, Q., Schaible, K., Wylie, C., Heasman, J., 2002. The roles of three signaling pathways in the formation and function of the Spemann Organizer. Development 129, 4027–4043.

Zhang, J., King, M.L., 1996. *Xenopus VegT* RNA is localized to the vegetal cortex during oogenesis and encodes a novel T-box transcription factor involved in mesodermal patterning. Development 122, 4119–4129.

Zhang, J., Houston, D.W., King, M.L., Payne, C., Wylie, C., Heasman, J., 1998. The role of maternal VegT in establishing the primary germ layers in *Xenopus* embryos. Cell 94, 515–524.

BIBLIOGRAPHY

Agathon, A., Thisse, C. and Thisse, B. (2003). The molecular nature of the zebrafish tail organizer. *Nature* **424**, 448-452.
Amaya, E., Musci, T. J. and Kirschner, M. W. (1991). Expression of a dominant negative mutant of the FGF receptor disrupts mesoderm formation in Xenopus embryos. *Cell* **66**, 257-270.
Apesteguia, S. and Zaher, H. (2006). A Cretaceous terrestrial snake with robust hindlimbs and a sacrum. *Nature* **440**, 1037-1040.
Ariza-McNaughton, L. and Krumlauf, R. (2002). Non-radioactive in situ hybridization: simplified procedures for use in whole-mounts of mouse and chick embryos. *Int Rev Neurobiol* **47**, 239-250.
Artavanis-Tsakonas, S., Rand, M. D. and Lake, R. J. (1999). Notch signaling: cell fate control and signal integration in development. *Science* **284**, 770-776.
Aulehla, A. and Johnson, R. L. (1999). Dynamic expression of lunatic fringe suggests a link between notch signaling and an autonomous cellular oscillator driving somite segmentation. *Dev Biol* **207**, 49-61.
Aulehla, A., Wehrle, C., Brand-Saberi, B., Kemler, R., Gossler, A., Kanzler, B. and Herrmann, B. G. (2003). Wnt3a plays a major role in the segmentation clock controlling somitogenesis. *Dev Cell* **4**, 395-406.
Bagnall, K. M., Higgins, S. J. and Sanders, E. J. (1988). The contribution made by a single somite to the vertebral column: experimental evidence in support of resegmentation using the chick-quail chimaera model. *Development.* **103**, 69-85.
Balavoine, G. and Adoutte, A. (2003). The segmented Urbilateria: A testable hypothesis. *Int. Comp. Biol.* **43**, 137-147.
Beggs, K., Young, J., Georges, A. and West, P. (2000). Ageing the eggs and embryos of the pignosed turtle, Carettochelys insculpta (Chelonia: Carettochelydidae), from northern Australia. *Can J Zool* **78**, 373-392.
Bellairs, R. (1951). Development of early reptile embryos in vitro. *Nature* **167**, 687-688.
Bellairs, R. and Veini, M. (1980). An experimental analysis of somite segmentation in the chick embryo. *J.Embryol.Exp.Morphol.* **55**, 93-108.
Berger-Dell'Mour, H. A. E. (1985). The lizard genus Tetradactylus: a model case of an evolutionary process. In *Proceedings of the international symposium on African Vertebrates: Systematics, phylogeny and evolutionary ecology.*, (ed. K. L. Schuchmann), pp. 495-510. Bonn: Selbstverlag.
Bessho, Y., Hirata, H., Masamizu, Y. and Kageyama, R. (2003). Periodic repression by the bHLH factor Hes7 is an essential mechanism for the somite segmentation clock. *Genes Dev* **17**, 1451-1456.
Bessho, Y. and Kageyama, R. (2003). Oscillations, clocks and segmentation. *Curr Opin Genet Dev* **13**, 379-384.
Bessho, Y., Sakata, R., Komatsu, S., Shiota, K., Yamada, S. and Kageyama, R. (2001). Dynamic expression and essential functions of Hes7 in somite segmentation. *Genes Dev* **15**, 2642-2647.
Billett, F., Gans, C. and Maderson, P. F. A. (1985). Why study reptilian development? In *Biology of the Reptilia*, vol. 14. Development A. (ed. C. Gans F. Billett and P. F. A. Maderson), pp. 1-39. New York: John Wiley & Sons.
Bird, N. C. and Mabee, P. M. (2003). Developmental morphology of the axial skeleton of the zebrafish, Danio rerio (Ostariophysi: Cyprinidae). *Dev Dyn* **228**, 337-357.
Bleidorn, C., Vogt, L. and Bartolomaeus, T. (2003). New insights into polychaete

phylogeny (Annelida) inferred from 18S rDNA sequences. *Molecular phylogenetics and evolution* **29**, 279-288.
Blentic, A., Gale, E. and Maden, M. (2003). Retinoic acid signalling centres in the avian embryo identified by sites of expression of synthesising and catabolising enzymes. *Dev Dyn* **227**, 114-127.
Bottcher, R. T. and Niehrs, C. (2005). Fibroblast Growth Factor Signaling during Early Vertebrate Development. *Endocr Rev* **26**, 63-77.
Brent, A. E., Schweitzer, R. and Tabin, C. J. (2003). A somitic compartment of tendon progenitors. *Cell* **113**, 235-248.
Brent, A. E. and Tabin, C. J. (2002). Developmental regulation of somite derivatives: muscle, cartilage and tendon. *Curr Opin Genet Dev* **12**, 548-557.
Bronner-Fraser, M. (2000). Rostrocaudal differences within the somites confer segmental pattern to trunk neural crest migration. *Curr Top Dev Biol* **47**, 279-296.
Bronner-Fraser, M. and Stern, C. (1991). Effects of mesodermal tissues on avian neural crest cell migration. *Dev Biol.* **143**, 213-217.
Bruckner, K., Perez, L., Clausen, H. and Cohen, S. (2000). Glycosyltransferase activity of Fringe modulates Notch-Delta interactions. *Nature* **406**, 411-415.
Buchberger, A., Bonneick, S. and Arnold, H. (2000). Expression of the novel basic-helix-loop-helix transcription factor cMespo in presomitic mesoderm of chicken embryos. *Mech Dev* **97**, 223-226.
Bulman, M. P., Kusumi, K., Frayling, T. M., McKeown, C., Garrett, C., Lander, E. S., Krumlauf, R., Hattersley, A. T., Ellard, S. and Turnpenny, P. D. (2000). Mutations in the human delta homologue, DLL3, cause axial skeletal defects in spondylocostal dysostosis. *Nat Genet* **24**, 438-441.
Burgess, R., Rawls, A., Brown, D., Bradley, A. and Olson, E. N. (1996). Requirement of the paraxis gene for somite formation and musculoskeletal patterning. *Nature* **384**, 570-573.
Burke, A. C., Nelson, C. E., Morgan, B. A. and Tabin, C. (1995). Hox genes and the evolution of vertebrate axial morphology. *Development* **121**, 333-346.
Cambray, N. and Wilson, V. (2002). Axial progenitors with extensive potency are localised to the mouse chordoneural hinge. *Development* **129**, 4855-4866.
Cambray, N. and Wilson, V. (2007). Two distinct sources for a population of maturing axial progenitors. *Development* **134**, 2829-2840.
Caprette, C. L., Lee, M. S. Y., Shine, R., Mokany, A. and Downhower, J. F. (2004). The origin of snakes (Serpentes) as seen through eye anatomy. *Biological Journal of the Linnean Society* **81**, 469-482.
Catala, M., Teillet, M. A., De Robertis, E. M. and Le Douarin, M. L. (1996). A spinal cord fate map in the avian embryo: while regressing, Hensen's node lays down the notochord and floor plate thus joining the spinal cord lateral walls. *Development.* **122**, 2599-2610.
Catala, M., Teillet, M. A. and Le Douarin, N. M. (1995). Organization and development of the tail bud analyzed with the quail- chick chimaera system. *Mech.Dev* **51**, 51-65.
Cebra-Thomas, J., Tan, F., Sistla, S., Estes, E., Bender, G., Kim, C., Riccio, P. and Gilbert, S. F. (2005). How the turtle forms its shell: a paracrine hypothesis of carapace formation. *Journal of experimental zoology. Part B* **304**, 558-569.
Cebra-Thomas, J. A., Betters, E., Yin, M., Plafkin, C., McDow, K. and Gilbert, S. F. (2007). Evidence that a late-emerging population of trunk neural crest cells forms the plastron bones in the turtle Trachemys scripta. *Evol Dev* **9**, 267-277.
Chapman, D. L. and Papaioannou, V. E. (1998). Three neural tubes in mouse

embryos with mutations in the T-box gene Tbx6. *Nature* **391**, 695-697.
Cheyette, B. N., Waxman, J. S., Miller, J. R., Takemaru, K., Sheldahl, L. C., Khlebtsova, N., Fox, E. P., Earnest, T. and Moon, R. T. (2002). Dapper, a Dishevelled-associated antagonist of beta-catenin and JNK signaling, is required for notochord formation. *Dev Cell* **2**, 449-461.
Choe, C. P., Miller, S. C. and Brown, S. J. (2006). A pair-rule gene circuit defines segments sequentially in the short-germ insect Tribolium castaneum. *Proc Natl Acad Sci U S A* **103**, 6560-6564.
Christ, B., Huang, R. and Scaal, M. (2007). Amniote somite derivatives. *Dev Dyn*.
Christ, B., Huang, R. and Wilting, J. (2000). The development of the avian vertebral column. *Anat Embryol (Berl)* **202**, 179-194.
Christ, B., Jacob, H. J. and Jacob, M. (1974). Somitogenesis in the chick embryo. Determination of the segmentation direction. *Verh.Anat.Ges.* **68**, 573-579.
Ciruna, B. and Rossant, J. (2001). FGF signaling regulates mesoderm cell fate specification and morphogenetic movement at the primitive streak. *Dev Cell* **1**, 37-49.
Clark, H. F., Cohen, M. M. and Karzon, D. T. (1969). Characterization of Reptilian Cell Lines Established at Incubation Temperatures of 23 to 36. *PSEBM* **133**, 1039-1047.
Clark, K., Bender, G., Murray, B. P., Panfilio, K., Cook, S., Davis, R., Murnen, K., Tuan, R. S. and Gilbert, S. F. (2001). Evidence for the neural crest origin of turtle plastron bones. *Genesis* **31**, 111-117.
Cohn, M. J. and Tickle, C. (1999). Developmental basis of limblessness and axial patterning in snakes. *Nature* **399**, 474-479.
Cole, S. E., Levorse, J. M., Tilghman, S. M. and Vogt, T. F. (2002). Clock Regulatory Elements Control Cyclic Expression of Lunatic fringe during Somitogenesis. *Dev Cell* **3**, 75-84.
Conlon, R. A., Reaume, A. G. and Rossant, J. (1995). Notch1 is required for the coordinate segmentation of somites. *Development.* **121**, 1533-1545.
Cooke, J. (1975). Control of somite number during morphogenesis of a vertebrate, Xenopus laevis. *Nature* **254**, 196-199.
Cooke, J. and Zeeman, E. C. (1976). A clock and wavefront model for control of the number of repeated structures during animal morphogenesis. *J Theor Biol* **58**, 455-476.
Cordes, R., Schuster-Gossler, K., Serth, K. and Gossler, A. (2004). Specification of vertebral identity is coupled to Notch signalling and the segmentation clock. *Development* **131**, 1221-1233.
Correia, K. M. and Conlon, R. A. (2000). Surface ectoderm is necessary for the morphogenesis of somites. *Mech Dev* **91**, 19-30.
Crastz, F. (1982). Embryological stages of the marine turtle Lepidochelys olivacea (Eschscholtz). *Rev Biol Trop* **30**, 113-120.
Dale, J. K., Malapert, P., Chal, J., Vilhais-Neto, G., Maroto, M., Johnson, T., Jayasinghe, S., Trainor, P., Herrmann, B. and Pourquie, O. (2006). Oscillations of the snail genes in the presomitic mesoderm coordinate segmental patterning and morphogenesis in vertebrate somitogenesis. *Dev Cell* **10**, 355-366.
Dale, J. K., Maroto, M., Dequeant, M. L., Malapert, P., McGrew, M. and Pourquie, O. (2003). Periodic Notch inhibition by Lunatic Fringe underlies the chick segmentation clock. *Nature* **421**, 275-278.
Dale, L. and Jones, C. M. (1999). BMP signalling in early Xenopus development. *Bioessays* **21**, 751-760.
Damen, W. G. (2007). Evolutionary conservation and divergence of the segmentation

process in arthropods. *Dev Dyn* **236**, spc1.
Damen, W. G., Janssen, R. and Prpic, N. M. (2005). Pair rule gene orthologs in spider segmentation. *Evol Dev* **7**, 618-628.
Davis, G. K. and Patel, N. H. (1999). The origin and evolution of segmentation. *Trends Cell Biol* **9**, M68-72.
Davis, R. L. and Kirschner, M. W. (2000). The fate of cells in the tailbud of Xenopus laevis. *Development* **127**, 255-267.
De Robertis, E. M. (1997). Evolutionary biology. The ancestry of segmentation *Nature* **387**, 25-26.
de Rosa, R., Prud'homme, B. and Balavoine, G. (2005). Caudal and even-skipped in the annelid Platynereis dumerilii and the ancestry of posterior growth. *Evol Dev* **7**, 574-587.
Dearden, P. and Akam, M. (2000). A role for Fringe in segment morphogenesis but not segment formation in the grasshopper, Schistocerca gregaria. *Dev Genes Evol* **210**, 329-336.
del Barco Barrantes, I., Elia, A., Wunnsch, K., Hrabde De Angelis, M., Mak, T., Rossant, J., Conlon, R., Gossler, A. and Luis de la Pompa, J. (1999). Interaction between Notch signalling and Lunatic Fringe during somite boundary formation in the mouse. *Current Biology* **9**, 470-480.
Delfini, M. C., Dubrulle, J., Malapert, P., Chal, J. and Pourquie, O. (2005). Control of the segmentation process by graded MAPK/ERK activation in the chick embryo. *Proc Natl Acad Sci U S A* **102**, 11343-11348.
Delsuc, F., Brinkmann, H., Chourrout, D. and Philippe, H. (2006). Tunicates and not cephalochordates are the closest living relatives of vertebrates. *Nature* **439**, 965-968.
Dendy, A. (1899). Outlines of the development of the tuatara, Sphenodon (Hatteria) punctatus. *Q J Microsc Sci* **42**, 1-87.
Dequeant, M. L., Glynn, E., Gaudenz, K., Wahl, M., Chen, J., Mushegian, A. and Pourquie, O. (2006). A complex oscillating network of signaling genes underlies the mouse segmentation clock. *Science* **314**, 1595-1598.
Dietrich, S., Schubert, F. R. and Lumsden, A. (1997). Control of dorsoventral pattern in the chick paraxial mesoderm. *Development.* **124**, 3895-3908.
Diez del Corral, R., Olivera-Martinez, I., Goriely, A., Gale, E., Maden, M. and Storey, K. (2003). Opposing FGF and retinoid pathways control ventral neural pattern, neuronal differentiation, and segmentation during body axis extension. *Neuron* **40**, 65-79.
Dockter, J. L. and Ordahl, C. P. (1998). Determination of sclerotome to the cartilage fate. *Development.* **125**, 2113-2124.
Dolle, P., Dierich, A., LeMeur, M., Schimmang, T., Schuhbaur, B., Chambon, P. and Duboule, D. (1993). Disruption of the Hoxd-13 gene induces localized heterochrony leading to mice with neotenic limbs. *Cell* **75**, 431-441.
Dottori, M., Hartley, L., Galea, M., Paxinos, G., Polizzotto, M., Kilpatrick, T., Bartlett, P. F., Murphy, M., Kontgen, F. and Boyd, A. W. (1998). EphA4 (Sek1) receptor tyrosine kinase is required for the development of the corticospinal tract. *Proc Natl Acad Sci U S A* **95**, 13248-13253.
Dougan, S. T., Warga, R. M., Kane, D. A., Schier, A. F. and Talbot, W. S. (2003). The role of the zebrafish nodal-related genes squint and cyclops in patterning of mesendoderm. *Development* **130**, 1837-1851.
Duband, J. L., Dufour, S., Hatta, K., Takeichi, M., Edelman, G. M. and Thiery, J. P. (1987). Adhesion molecules during somitogenesis in the avian embryo. *J.Cell*

Biol. **104**, 1361-1374.
Duboule, D. and Morata, G. (1994). Colinearity and functional hierarchy among genes of the homeotic complexes. *Trends Genet* **10**, 358-364.
Dubrulle, J., McGrew, M. J. and Pourquie, O. (2001). FGF signaling controls somite boundary position and regulates segmentation clock control of spatiotemporal Hox gene activation. *Cell* **106**, 219-232.
Dubrulle, J. and Pourquie, O. (2004a). Coupling segmentation to axis formation. *Development* **131**, 5783-5793.
Dubrulle, J. and Pourquie, O. (2004b). fgf8 mRNA decay establishes a gradient that couples axial elongation to patterning in the vertebrate embryo. *Nature* **427**, 419-422.
Dufaure, J. P. and Hubert, J. (1961). Table de developpement de Lezard vivipare Lacerta (Zootoca) vivipara Jacquin. *Arch Anat Microsc Morphol Exp* **50**, 309-327.
Durbin, L., Brennan, C., Shiomi, K., Cooke, J., Barrios, A., Shanmugalingam, S., Guthrie, B., Lindberg, R. and Holder, N. (1998). Eph signaling is required for segmentation and differentiation of the somites. *Genes Dev* **12**, 3096-3109.
Durbin, L., Sordino, P., Barrios, A., Gering, M., Thisse, C., Thisse, B., Brennan, C., Green, A., Wilson, S. and Holder, N. (2000). Anteroposterior patterning is required within segments for somite boundary formation in developing zebrafish. *Development* **127**, 1703-1713.
Economides, K. D., Zeltser, L. and Capecchi, M. R. (2003). Hoxb13 mutations cause overgrowth of caudal spinal cord and tail vertebrae. *Dev Biol* **256**, 317-330.
Eloy-Trinquet, S. and Nicolas, J. F. (2002). Cell coherence during production of the presomitic mesoderm and somitogenesis in the mouse embryo. *Development* **129**, 3609-3619.
Evrard, Y. A., Lun, Y., Aulehla, A., Gan, L. and Johnson, R. L. (1998). lunatic fringe is an essential mediator of somite segmentation and patterning *Nature* **394**, 377-381.
Fan, C. M., Lee, C. S. and Tessier-Lavigne, M. (1997). A role for WNT proteins in induction of dermomyotome. *Dev Biol.* **191**, 160-165.
Fan, C. M. and Tessier-Lavigne, M. (1994). Patterning of mammalian somites by surface ectoderm and notochord: evidence for sclerotome induction by a hedgehog homolog. *Cell* **79**, 1175-1186.
Faure, S., Lee, M. A., Keller, T., ten Dijke, P. and Whitman, M. (2000). Endogenous patterns of TGFbeta superfamily signaling during early Xenopus development. *Development* **127**, 2917-2931.
Forsberg, H., Crozet, F. and Brown, N. A. (1998). Waves of mouse Lunatic fringe expression, in four-hour cycles at two-hour intervals, precede somite boundary formation. *Curr.Biol.* **8**, 1027-1030.
Fromental-Ramain, C., Warot, X., Messadecq, N., LeMeur, M., Dolle, P. and Chambon, P. (1996). Hoxa-13 and Hoxd-13 play a crucial role in the patterning of the limb autopod. *Development* **122**, 2997-3011.
Gajewski, M., Elmasri, H., Girschick, M., Sieger, D. and Winkler, C. (2006). Comparative analysis of her genes during fish somitogenesis suggests a mouse/chick-like mode of oscillation in medaka. *Dev Genes Evol* **216**, 315-332.
Gajewski, M., Sieger, D., Alt, B., Leve, C., Hans, S., Wolff, C., Rohr, K. B. and Tautz, D. (2003). Anterior and posterior waves of cyclic her1 gene expression are differentially regulated in the presomitic mesoderm of zebrafish. *Development* **130**, 4269-4278.
Galceran, J., Farinas, I., Depew, M. J., Clevers, H. and Grosschedl, R. (1999). Wnt3a-/--like phenotype and limb deficiency in Lef1(-/-)Tcf1(-/-) mice. *Genes Dev*

13, 709-717.
Gaunt, S. J., Sharpe, P. T. and Duboule, D. (1988). Spatially restricted domains of homeo-gene transcripts in mouse embryos: relation to a segmented body plan. *Development* **104**, 169-179.
Gee, H. (2006). Evolution: careful with that amphioxus. *Nature* **439**, 923-924.
Geling, A., Steiner, H., Willem, M., Bally-Cuif, L. and Haass, C. (2002). A gamma-secretase inhibitor blocks Notch signaling in vivo and causes a severe neurogenic phenotype in zebrafish. *EMBO Rep* **3**, 688-694.
Gilbert, S. F., Loredo, G. A., Brukman, A. and Burke, A. C. (2001). Morphogenesis of the turtle shell: the development of a novel structure in tetrapod evolution. *Evol Dev* **3**, 47-58.
Gilland, E. H. and Burke, A. C. (2004). Gastrulation in reptiles. In *Gastrulation : from cells to embryo,* (ed. C. D. Stern), pp. 205-218. Cold Spring Harbor, N.Y.: Cold Spring Harbor Laboratory Press.
Giudicelli, F., Ozbudak, E. M., Wright, G. J. and Lewis, J. (2007). Setting the Tempo in Development: An Investigation of the Zebrafish Somite Clock Mechanism. *PLoS Biol* **5**, e150.
Godwin, A. R. and Capecchi, M. R. (1998). Hoxc13 mutant mice lack external hair. *Genes Dev* **12**, 11-20.
Goldman, D. C., Martin, G. R. and Tam, P. P. (2000). Fate and function of the ventral ectodermal ridge during mouse tail development. *Development* **127**, 2113-2123.
Goldstein, R. S. and Kalcheim, C. (1992). Determination of epithelial half-somites in skeletal morphogenesis. *Development.* **116**, 441-445.
Gont, L. K., Steinbeisser, H., Blumberg, B. and de Robertis, E. M. (1993). Tail formation as a continuation of gastrulation: the multiple cell populations of the Xenopus tailbud derive from the late blastopore lip. *Development* **119**, 991-1004.
Graham, A., Papalopulu, N. and Krumlauf, R. (1989). The murine and Drosophila homeobox gene complexes have common features of organization and expression. *Cell* **57**, 367-378.
Greco, T. L., Takada, S., Newhouse, M. M., McMahon, J. A., McMahon, A. P. and Camper, S. A. (1996). Analysis of the vestigial tail mutation demonstrates that Wnt-3a gene dosage regulates mouse axial development. *Genes Dev* **10**, 313-324.
Green, J. B., New, H. V. and Smith, J. C. (1992). Responses of embryonic Xenopus cells to activin and FGF are separated by multiple dose thresholds and correspond to distinct axes of the mesoderm. *Cell* **71**, 731-739.
Greenbaum, E. (2002). A standardized series of embryonic stages for the emydid turtle Trachemys scripta. *Can J Zool* **80**, 1350-1370.
Greenbaum, E. and Carr, J. L. (2002). Staging criteria for embryos of the spiny softshell turtle, Apalone spinifera (Testudines: Trionychidae). *Journal of morphology* **254**, 272-291.
Greene, H. W. and Cundall, D. (2000). Perspectives: evolutionary biology. Limbless tetrapods and snakes with legs. *Science* **287**, 1939-1941.
Grenard, S. (1994). Medical herpetology. Pottsville, PA: Reptile & Amphibian Magazine.
Griffin, K., Patient, R. and Holder, N. (1995). Analysis of FGF function in normal and no tail zebrafish embryos reveals separate mechanisms for formation of the trunk and the tail. *Development* **121**, 2983-2994.
Griffith, C. M., Wiley, M. J. and Sanders, E. J. (1992). The vertebrate tail bud: three germ layers from one tissue. *Anat Embryol (Berl)* **185**, 101-113.

Grimaldi, A., Tettamanti, G., Martin, B. L., Gaffield, W., Pownall, M. E. and Hughes, S. M. (2004). Hedgehog regulation of superficial slow muscle fibres in Xenopus and the evolution of tetrapod trunk myogenesis. *Development* **131**, 3249-3262.
Gritsman, K., Talbot, W. S. and Schier, A. F. (2000). Nodal signaling patterns the organizer. *Development* **127**, 921-932.
Guyot, G., Pieau, C. and Renous, S. (1994). Developpement embryonnaire d'une tortue terrestre, la tortue d'Hermann, Testudo hermanni Gmelin, 1789. *Ann Sci Nat Zool Paris* **15**, 115-137.
Hamburger, V. and Hamilton, H. L. (1992). A series of normal stages in the development of the chick embryo (1951). *Dev.Dyn.* **195**, 231-272.
Hara, K. (1978). Spemann's organizer in birds. In *Organizer: a Milestone of a Half-Century from Spemann*, (ed. O. Nakamura and S. Toivonen), pp. 221-226.
Head, J. J. and David Polly, P. (2007). Dissociation of somatic growth from segmentation drives gigantism in snakes. *Biology letters* **3**, 296-298.
Heisenberg, C. P., Tada, M., Rauch, G. J., Saude, L., Concha, M. L., Geisler, R., Stemple, D. L., Smith, J. C. and Wilson, S. W. (2000). Silberblick/Wnt11 mediates convergent extension movements during zebrafish gastrulation. *Nature* **405**, 76-81.
Henrique, D., Adam, J., Myat, A., Chitnis, A., Lewis, J. and Ish-Horowicz, D. (1995). Expression of a Delta homologue in prospective neurons in the chick. *Nature* **375**, 787-790.
Henry, C. A., Urban, M. K., Dill, K. K., Merlie, J. P., Page, M. F., Kimmel, C. B. and Amacher, S. L. (2002). Two linked hairy/Enhancer of split-related zebrafish genes, her1 and her7, function together to refine alternating somite boundaries. *Development* **129**, 3693-3704.
Herrmann, B. G., Labeit, S., Poustka, A., King, T. R. and Lehrach, H. (1990). Cloning of the T gene required in mesoderm formation in the mouse. *Nature* **343**, 617-622.
Hessling, R. and Westheide, W. (2002). Are Echiura derived from a segmented ancestor? Immunohistochemical analysis of the nervous system in developmental stages of Bonellia viridis. *Journal of morphology* **252**, 100-113.
Hirata, H., Bessho, Y., Kokubu, H., Masamizu, Y., Yamada, S., Lewis, J. and Kageyama, R. (2004). Instability of Hes7 protein is crucial for the somite segmentation clock. *Nat Genet* **36**, 750-754.
Hirata, H., Yoshiura, S., Ohtsuka, T., Bessho, Y., Harada, T., Yoshikawa, K. and Kageyama, R. (2002). Oscillatory expression of the bHLH factor Hes1 regulated by a negative feedback loop. *Science* **298**, 840-843.
Hofmann, M., Schuster-Gossler, K., Watabe-Rudolph, M., Aulehla, A., Herrmann, B. G. and Gossler, A. (2004). WNT signaling, in synergy with T/TBX6, controls Notch signaling by regulating Dll1 expression in the presomitic mesoderm of mouse embryos. *Genes Dev* **18**, 2712-2717.
Holder, L. A. and Bellairs, A. d. A. (1962). The use of reptiles in experimental embryology. . *Br J Herpetol* **3**, 54-61.
Holland, L. Z., Kene, M., Williams, N. A. and Holland, N. D. (1997). Sequence and embryonic expression of the amphioxus engrailed gene (AmphiEn): the metameric pattern of transcription resembles that of its segment-polarity homolog in Drosophila. *Development.* **124**, 1723-1732.
Holland, L. Z., Rached, L. A., Tamme, R., Holland, N. D., Kortschak, D., Inoko, H., Shiina, T., Burgtorf, C. and Lardelli, M. (2001). Characterization and developmental expression of the amphioxus homolog of Notch (AmphiNotch):

evolutionary conservation of multiple expression domains in amphioxus and vertebrates. *Dev Biol* **232**, 493-507.
Holley, S. A., Geisler, R. and Nusslein-Volhard, C. (2000). Control of her1 expression during zebrafish somitogenesis by a delta-dependent oscillator and an independent wave-front activity. *Genes Dev* **14**, 1678-1690.
Holley, S. A., Julich, D., Rauch, G. J., Geisler, R. and Nusslein-Volhard, C. (2002). her1 and the notch pathway function within the oscillator mechanism that regulates zebrafish somitogenesis. *Development* **129**, 1175-1183.
Holmdahl, D. E. (1925). Experimentelle Untersuchungen über die lage der Grenze zwischen Primärer und sekundärer Körperentwicklung beim Huhn. *Anatomischer Anzeiger* **59**, 393-396.
Holtzman, D. A. and Halpern, M. (1989). In vitro technique for studying garter snake (Thamnophis sp.) development. *J Exp Zool* **250**, 283-288.
Hoppler, S. and Moon, R. T. (1998). BMP-2/-4 and Wnt-8 cooperatively pattern the Xenopus mesoderm. *Mech Dev* **71**, 119-129.
Horikawa, K., Radice, G., Takeichi, M. and Chisaka, O. (1999). Adhesive subdivisions intrinsic to the epithelial somites. *Dev Biol* **215**, 182-189.
Hrabe de Angelis, M., McIntyre, J. and Gossler, A. (1997). Maintenance of somite borders in mice requires the Delta homologue DII1. *Nature* **386**, 717-721.
Hubert, J. and Dufaure, J. P. (1968). Table de developpement de la vipere aspic, Vipera aspis. L. *Bull Soc Zool France* **93**, 135-148.
Hubert, J., Dufaure, J. P. and Collin, J. P. (1966). Materiaux pour une table de developpement de Vipera aspis aspis L. La periode d'organogenese. *Bull Soc Zool France* **91**, 779-788.
Hughes, S. H., Greenhouse, J. J., Petropoulos, C. J. and Sutrave, P. (1987). Adaptor plasmids simplify the insertion of foreign DNA into helper-independent retroviral vectors. *Journal of virology* **61**, 3004-3012.
Iimura, T. and Pourquie, O. (2006). Collinear activation of Hoxb genes during gastrulation is linked to mesoderm cell ingression. *Nature* **442**, 568-571.
Iimura, T. and Pourquie, O. (2007). Hox genes in time and space during vertebrate body formation. *Development, growth & differentiation* **49**, 265-275.
Iimura, T., Yang, X., Weijer, C. J. and Pourquie, O. (2007). Dual mode of paraxial mesoderm formation during chick gastrulation. *Proc Natl Acad Sci U S A* **104**, 2744-2749.
Ingham, P. W. and Martinez Arias, A. (1992). Boundaries and fields in early embryos. *Cell* **68**, 221-235.
Irvine, K. D. and Rauskolb, C. (2001). Boundaries in development: formation and function. *Annu Rev Cell Dev Biol* **17**, 189-214.
Ishikawa, A., Kitajima, S., Takahashi, Y., Kokubo, H., Kanno, J., Inoue, T. and Saga, Y. (2004). Mouse Nkd1, a Wnt antagonist, exhibits oscillatory gene expression in the PSM under the control of Notch signaling. *Mech Dev* **121**, 1443-1453.
Jaeger, J. and Goodwin, B. C. (2002). Cellular oscillators in animal segmentation. *In silico biology* **2**, 111-123.
Jenner, R. A. (2000). Evolution of animal body plans: the role of metazoan phylogeny at the interface between pattern and process. *Evol Dev* **2**, 208-221.
Jiang, Y. J., Aerne, B. L., Smithers, L., Haddon, C., Ish-Horowicz, D. and Lewis, J. (2000). Notch signalling and the synchronization of the somite segmentation clock. *Nature* **408**, 475-479.
Jiang, Y. J., Brand, M., Heisenberg, C. P., Beuchle, D., Furutani-Seiki, M., Kelsh, R. N., Warga, R. M., Granato, M., Haffter, P., Hammerschmidt, M. et al.

(1996). Mutations affecting neurogenesis and brain morphology in the zebrafish, Danio rerio. *Development.* **123**, 205-216.
Jouve, C., Iimura, T. and Pourquie, O. (2002). Onset of the segmentation clock in the chick embryo: evidence for oscillations in the somite precursors in the primitive streak. *Development* **129**, 1107-1117.
Jouve, C., Palmeirim, I., Henrique, D., Beckers, J., Gossler, A., Ish-Horowicz, D. and Pourquie, O. (2000). Notch signalling is required for cyclic expression of the hairy-like gene HES1 in the presomitic mesoderm. *Development* **127**, 1421-1429.
Kalcheim, C., Cinnamon, Y. and Kahane, N. (1999). Myotome formation: a multistage process. *Cell Tissue Res* **296**, 161-173.
Kanatsu, M. and Nishikawa, S. I. (1996). In vitro analysis of epiblast tissue potency for hematopoietic cell differentiation. *Development* **122**, 823-830.
Kanki, J. P. and Ho, R. K. (1997). The development of the posterior body in zebrafish. *Development* **124**, 881-893.
Kawamura, A., Koshida, S., Hijikata, H., Ohbayashi, A., Kondoh, H. and Takada, S. (2005). Groucho-associated transcriptional repressor ripply1 is required for proper transition from the presomitic mesoderm to somites. *Dev Cell* **9**, 735-744.
Kerszberg, M. and Wolpert, L. (2000). A clock and trail model for somite formation, specialization and polarization. *J Theor Biol* **205**, 505-510.
Kessel, M., Balling, R. and Gruss, P. (1990). Variations of cervical vertebrae after expression of a Hox-1.1 transgene in mice. *Cell* **61**, 301-308.
Kessel, M. and Gruss, P. (1991). Homeotic transformations of murine vertebrae and concomitant alteration of Hox codes induced by retinoic acid. *Cell* **67**, 89-104.
Kikuchi, A. (1999). Roles of Axin in the Wnt signalling pathway. *Cellular signalling* **11**, 777-788.
Kim, S. H., Jen, W. C., De Robertis, E. M. and Kintner, C. (2000). The protocadherin PAPC establishes segmental boundaries during somitogenesis in xenopus embryos. *Curr Biol* **10**, 821-830.
Kimelman, D. (2006). Mesoderm induction: from caps to chips. *Nat Rev Genet* **7**, 360-372.
Kimelman, D. and Griffin, K. J. (2000). Vertebrate mesendoderm induction and patterning. *Curr Opin Genet Dev* **10**, 350-356.
Knezevic, V., De Santo, R. and Mackem, S. (1998). Continuing organizer function during chick tail development. *Development* **125**, 1791-1801.
Kohler, G. (2005a). 1. Introduction. In *Incubation of Reptile Eggs: Basics, Guidelines, Experiences*, pp. 8-9. Malabar, Florida: Krieger Publishing Company.
Kohler, G. (2005b). 2. Morphology of Reptile Eggs. In *Incubation of Reptile Eggs: Basics, Guidelines, Experiences*, pp. 9-14. Malabar, Florida: Krieger Publishing Company.
Kohler, G. (2005c). 6. Physiological Foundations of Reptilian Incubation. In *Incubation of Reptile Eggs: Basics, Guidelines, Experiences*, pp. 30-49. Malabar, Florida: Krieger Publishing Company.
Koizumi, K., Nakajima, M., Yuasa, S., Saga, Y., Sakai, T., Kuriyama, T., Shirasawa, T. and Koseki, H. (2001). The role of presenilin 1 during somite segmentation. *Development* **128**, 1391-1402.
Krumlauf, R. (1994). Hox genes in vertebrate development. *Cell* **78**, 191-201.
Kulesa, P. M. and Fraser, S. E. (2002). Cell dynamics during somite boundary formation revealed by time-lapse analysis. *Science* **298**, 991-995.
Kusumi, K., Sun, E. S., Kerrebrock, A. W., Bronson, R. T., Chi, D. C., Bulotsky, M. S., Spencer, J. B., Birren, B. W., Frankel, W. N. and Lander, E. S. (1998). The

mouse pudgy mutation disrupts Delta homologue Dll3 and initiation of early somite boundaries. *Nat Genet* **19**, 274-278.
Lawrence, P. A. (1992). The Making of a Fly. Oxford: Blackwell Science.
Leimeister, C., Dale, K., Fischer, A., Klamt, B., Hrabe de Angelis, M., Radtke, F., McGrew, M. J., Pourquie, O. and Gessler, M. (2000). Oscillating expression of c-hey2 in the presomitic mesoderm suggests that the segmentation clock may use combinatorial signaling through multiple interacting bHLH factors. *Dev Biol* **227**, 91-103.
Lekven, A. C., Thorpe, C. J., Waxman, J. S. and Moon, R. T. (2001). Zebrafish wnt8 encodes two wnt8 proteins on a bicistronic transcript and is required for mesoderm and neurectoderm patterning. *Dev Cell* **1**, 103-114.
Lemus, D., Illanes, J., Fuenzalida, M., Paz De La Vega, Y. and Garcia, M. (1981). Comparative analysis of the development of the lizard, Liolaemus tenuis tenuis. II. A series of normal postlaying stages in embryonic development. *Journal of morphology* **169**, 337-349.
Leve, C., Gajewski, M., Rohr, K. B. and Tautz, D. (2001). Homologues of c-hairy1 (her9) and lunatic fringe in zebrafish are expressed in the developing central nervous system, but not in the presomitic mesoderm. *Dev Genes Evol* **211**, 493-500.
Lewis, J. (2003). Autoinhibition with transcriptional delay: a simple mechanism for the zebrafish somitogenesis oscillator. *Curr Biol*.
Li, Q., Ishikawa, T. O., Miyoshi, H., Oshima, M. and Taketo, M. M. (2005). A targeted mutation of Nkd1 impairs mouse spermatogenesis. *J Biol Chem* **280**, 2831-2839.
Li, Y., Fenger, U., Niehrs, C. and Pollet, N. (2003). Cyclic expression of esr9 gene in Xenopus presomitic mesoderm. *Differentiation* **71**, 83-89.
Lindell, L. E. (1994). The evolution of vertebral number and body size in snakes. *Functional Ecology* **8**, 708-719.
Liu, C., Knezevic, V. and Mackem, S. (2004). Ventral tail bud mesenchyme is a signaling center for tail paraxial mesoderm induction. *Dev Dyn* **229**, 600-606.
Loredo, G. A., Brukman, A., Harris, M. P., Kagle, D., Leclair, E. E., Gutman, R., Denney, E., Henkelman, E., Murray, B. P., Fallon, J. F. et al. (2001). Development of an evolutionarily novel structure: fibroblast growth factor expression in the carapacial ridge of turtle embryos. *J Exp Zool* **291**, 274-281.
Lou, X., Fang, P., Li, S., Hu, R. Y., Kuerner, K. M., Steinbeisser, H. and Ding, X. (2006). Xenopus Tbx6 mediates posterior patterning via activation of Wnt and FGF signalling. *Cell research* **16**, 771-779.
Lustig, B., Jerchow, B., Sachs, M., Weiler, S., Pietsch, T., Karsten, U., van de Wetering, M., Clevers, H., Schlag, P. M., Birchmeier, W. et al. (2002). Negative feedback loop of Wnt signaling through upregulation of conductin/axin2 in colorectal and liver tumors. *Mol Cell Biol* **22**, 1184-1193.
Lutz, H. and Dufaure, J. P. (1960). [Culture of embryos and organs of the viviparous lizard (Lacerta vivipara).]. *Comptes rendus hebdomadaires des seances de l'Academie des sciences* **250**, 2456-2458.
Maden, M., Graham, A., Zile, M. and Gale, E. (2000). Abnormalities of somite development in the absence of retinoic acid. *Int J Dev Biol* **44**, 151-159.
Magnusson, W. E. and Taylor, J. A. (1980). A description of developmental stages in Crocodylus porosus, for use in aging eggs in the field. *Aust Wildl Res* **7**, 479-485.
Mahmoud, I. Y., Hess, G. L. and Klicka, J. (1973). Normal embryonic stages of the western painted turtle, Chrysemys picta belli. *Journal of morphology* **141**, 269-280.
Marcelle, C., Stark, M. R. and Bronner-Fraser, M. (1997). Coordinate actions of

BMPs, Wnts, Shh and Noggin mediate patterning of the dorsal somite. *Development.* **124**, 3955-3963.
Maroto, M., Dale, J. K., Dequeant, M. L., Petit, A. C. and Pourquie, O. (2005). Synchronised cycling gene oscillations in presomitic mesoderm cells require cell-cell contact. *Int J Dev Biol* **49**, 309-315.
Maruhashi, M., Van De Putte, T., Huylebroeck, D., Kondoh, H. and Higashi, Y. (2005). Involvement of SIP1 in positioning of somite boundaries in the mouse embryo. *Dev Dyn* **234**, 332-338.
Masamizu, Y., Ohtsuka, T., Takashima, Y., Nagahara, H., Takenaka, Y., Yoshikawa, K., Okamura, H. and Kageyama, R. (2006). Real-time imaging of the somite segmentation clock: revelation of unstable oscillators in the individual presomitic mesoderm cells. *Proc Natl Acad Sci U S A* **103**, 1313-1318.
Mathukkaruppan, V. R., Kanakambika, R., Manichavel, V. and Veeraraghvan, K. (1970). Analysis of the development of the lizard, Calotes versicolor. I. A series of normal stages in the embryonic development. *Journal of morphology* **130**, 479-489.
Mazet, F. and Shimeld, S. M. (2003). Characterisation of an amphioxus Fringe gene and the evolution of the vertebrate segmentation clock. *Dev Genes Evol* **213**, 505-509.
McDowell, N. and Gurdon, J. B. (1999). Activin as a morphogen in Xenopus mesoderm induction. *Semin Cell Dev Biol* **10**, 311-317.
McGinnis, W., Hart, C. P., Gehring, W. J. and Ruddle, F. H. (1984). Molecular cloning and chromosome mapping of a mouse DNA sequence homologous to homeotic genes of Drosophila. *Cell* **38**, 675-680.
McGrew, M. J., Dale, J. K., Fraboulet, S. and Pourquie, O. (1998). The lunatic fringe gene is a target of the molecular clock linked to somite segmentation in avian embryos. *Curr Biol* **8**, 979-982.
Meinhardt, H. (1986). Models of segmentation. In *Somites in Developing Embryos*, (ed. B. R E. DA and L. JW), pp. 179-191. New York and London: Plenum press.
Menkes, B. and Sandor, S. (1977). Somitogenesis, regulation potencies, sequence determination and primordial interactions. In *Vertebrate limb and somite morphogenesis. British Society Developmental Biology Symposium 3*, (ed. D. A. Ede D. A. Hinchcliffe and M. Balls), pp. 405-419. Cambridge: Cambridge University Press.
Michalski, F., Cohen, M. M. and Clark, H. F. (1974). Adult and embryonic gecko cells in vitro: growth characteristics, infection by rabies, sindbis and polyoma viruses, and transformation by SV40. *Proc Soc Exp Biol Med* **146**, 337-348.
Miller, J. D. (1985). Embryology of marine turtles. In *Biology of the Reptilia*, vol. 14. Development A. (ed. C. Gans F. Billett and P. F. A. Maderson), pp. 269-328. New York: John Wiley & Sons.
Mittapalli, V. R., Huang, R., Patel, K., Christ, B. and Scaal, M. (2005). Arthrotome: a specific joint forming compartment in the avian somite. *Dev Dyn* **234**, 48-53.
Miura, S., Davis, S., Klingensmith, J. and Mishina, Y. (2006). BMP signaling in the epiblast is required for proper recruitment of the prospective paraxial mesoderm and development of the somites. *Development* **133**, 3767-3775.
Moffat, L. A. (1985). Embryonic development and aspects of reproductive biology in the tuatara, Sphenodon punctatus. In *Biology of the Reptilia*, vol. 14. Development A. (ed. C. Gans F. Billett and P. F. A. Maderson), pp. 493-522. New York: John Wiley & Sons.
Moloney, D. J., Panin, V. M., Johnston, S. H., Chen, J., Shao, L., Wilson, R., Wang, Y., Stanley, P., Irvine, K. D., Haltiwanger, R. S. et al. (2000). Fringe is a

glycosyltransferase that modifies Notch. *Nature* **406**, 369-375.
Monk, N. A. M. (2003). Oscillatory expression of Hes1, p53 and NF-kB driven by transcriptional time delays. *Curr Biol*.
Morales, A. V., Yasuda, Y. and Ish-Horowicz, D. (2002). Periodic Lunatic fringe Expression Is Controlled during Segmentation by a Cyclic Transcriptional Enhancer Responsive to Notch Signaling. *Dev Cell* **3**, 63-74.
Moreno, T. A. and Kintner, C. (2004). Regulation of segmental patterning by retinoic acid signaling during Xenopus somitogenesis. *Dev Cell* **6**, 205-218.
Morimoto, M., Sasaki, N., Oginuma, M., Kiso, M., Igarashi, K., Aizaki, K., Kanno, J. and Saga, Y. (2007). The negative regulation of Mesp2 by mouse Ripply2 is required to establish the rostro-caudal patterning within a somite. *Development* **134**, 1561-1569.
Morimoto, M., Takahashi, Y., Endo, M. and Saga, Y. (2005). The Mesp2 transcription factor establishes segmental borders by suppressing Notch activity. *Nature* **435**, 354-359.
Morin-Kensicki, E. M., Melancon, E. and Eisen, J. S. (2002). Segmental relationship between somites and vertebral column in zebrafish. *Development* **129**, 3851-3860.
Nagashima, H., Uchida, K., Yamamoto, K., Kuraku, S., Usuda, R. and Kuratani, S. (2005). Turtle-chicken chimera: an experimental approach to understanding evolutionary innovation in the turtle. *Dev Dyn* **232**, 149-161.
Nakajima, Y., Morimoto, M., Takahashi, Y., Koseki, H. and Saga, Y. (2006). Identification of Epha4 enhancer required for segmental expression and the regulation by Mesp2. *Development* **133**, 2517-2525.
New, D. A. T. (1966). Reptiles. In *The culture of vertebrate embryos*, pp. 99-119. London,
New York, London,: Logos P.;
Academic P.
Niederreither, K., Vermot, J., Le Roux, I., Schuhbaur, B., Chambon, P. and Dolle, P. (2003). The regional pattern of retinoic acid synthesis by RALDH2 is essential for the development of posterior pharyngeal arches and the enteric nervous system. *Development* **130**, 2525-2534.
Oates, A. C. and Ho, R. K. (2002). Hairy/E(spl)-related (Her) genes are central components of the segmentation oscillator and display redundancy with the Delta/Notch signaling pathway in the formation of anterior segmental boundaries in the zebrafish. *Development* **129**, 2929-2946.
Ohya, Y. K., Kuraku, S. and Kuratani, S. (2005). Hox code in embryos of Chinese soft-shelled turtle Pelodiscus sinensis correlates with the evolutionary innovation in the turtle. *Journal of experimental zoology. Part B* **304**, 107-118.
Oka, C., Nakano, T., Wakeham, A., de la Pompa, J. L., Mori, C., Sakai, T., Okazaki, S., Kawaichi, M., Shiota, K., Mak, T. W. et al. (1995). Disruption of the mouse RBP-J kappa gene results in early embryonic death. *Development.* **121**, 3291-3301.
Ordahl, C. P. and Le Douarin, N. M. (1992). Two myogenic lineages within the developing somite. *Development* **114**, 339-353.
Ordahl, C. P., Williams, B. A. and Denetclaw, W. (2000). Determination and morphogenesis in myogenic progenitor cells: an experimental embryological approach. *Curr Top Dev Biol* **48**, 319-367.
Packard, D. S. J. (1978). Chick somite determination: the role of factors in young somites and the segmental plate. *J.Exp.Zool.* **203**, 295-306.

Packard, D. S. J. (1980). Somite formation in cultured embryos of the snapping turtle. Chelydra serpentina. *J.Embryol.Exp.Morphol.* **59**, 113-130.
Packard, D. S. J. and Jacobson, A. (1976). The influence of axial structures on chick somite formation. *Dev Biol.* **53**, 36-48.
Packard, D. S. J. and Meier, S. (1984). Morphological and experimental studies of the somitomeric organization of the segmental plate in snapping turtle embryos. *J.Embryol.Exp.Morphol.* **84**, 35-48.
Palmeirim, I., Dubrulle, J., Henrique, D., Ish-Horowicz, D. and Pourquié, O. (1998). Uncoupling segmentation and somitogenesis in the chick presomitic mesoderm. *Dev Genet.* **23**, 77-85.
Palmeirim, I., Henrique, D., Ish-Horowicz, D. and Pourquié, O. (1997). Avian hairy gene expression identifies a molecular clock linked to vertebrate segmentation and somitogenesiss. *Cell* **91**, 639-648.
Pasteels, J. (1937a). Etudes sur la gastrulation des Vertébrés méroblastiques. . *Arch.Biol.* **48**, 105-184.
Pasteels, J. (1937b). Etudes sur la gastrulation des Vertébrés méroblastiques. III. Oiseaux. IV. Conclusions générales. *Arch.Biol.* **48**, 381-488.
Peel, A. (2004). The evolution of arthropod segmentation mechanisms. *Bioessays* **26**, 1108-1116.
Peel, A. and Akam, M. (2003). Evolution of segmentation: rolling back the clock. *Curr Biol* **13**, R708-710.
Polly, P. D., Head, J. J. and Cohn, M. J. (2001). Testing modularity and dissociation: the evolution of regional proportions in snakes. In *Beyond heterochrony : the evolution of development*, (ed. M. Zelditch), pp. 305-335. New York: Wiley-Liss.
Pough, F. H. (2004a). Herpetology as a field of study. In *Herpetology*, pp. 3-20. Upper Saddle River, NJ: Prentice Hall.
Pough, F. H. (2004b). Reproduction and life histories of reptiles. In *Herpetology*, pp. 331-351. Upper Saddle River, NJ: Prentice Hall.
Pourquie, O. (2004). The chick embryo: a leading model in somitogenesis studies. *Mech Dev* **121**, 1069-1079.
Pourquie, O., Coltey, M., Breant, C. and Le Douarin, N. M. (1995). Control of somite patterning by signals from the lateral plate. *Proc Natl Acad Sci U S A* **92**, 3219-3223.
Pourquie, O., Coltey, M., Teillet, M. A., Ordahl, C. and Le Douarin, N. M. (1993). Control of dorsoventral patterning of somitic derivatives by notochord and floor plate. *Proc Natl Acad Sci U S A* **90**, 5242-5246.
Pourquie, O., Fan, C. M., Coltey, M., Hirsinger, E., Watanabe, Y., Breant, C., Francis-West, P., Brickell, P., Tessier-Lavigne, M. and Le Douarin, N. M. (1996). Lateral and axial signals involved in avian somite patterning: a role for BMP4. *Cell* **84**, 461-471.
Pourquie, O. and Tam, P. P. (2001). A nomenclature for prospective somites and phases of cyclic gene expression in the presomitic mesoderm. *Dev Cell* **1**, 619-620.
Primmett, D. R., Norris, W. E., Carlson, G. J., Keynes, R. J. and Stern, C. D. (1989). Periodic segmental anomalies induced by heat shock in the chick embryo are associated with the cell cycle. *Development.* **105**, 119-130.
Primmett, D. R., Stern, C. D. and Keynes, R. J. (1988). Heat shock causes repeated segmental anomalies in the chick embryo. *Development.* **104**, 331-339.
Prince, V. E., Holley, S. A., Bally-Cuif, L., Prabhakaran, B., Oates, A. C., Ho, R. K. and Vogt, T. F. (2001). Zebrafish lunatic fringe demarcates segmental boundaries.

Mech Dev **105**, 175-180.
Prud'homme, B., de Rosa, R., Arendt, D., Julien, J. F., Pajaziti, R., Dorresteijn, A. W., Adoutte, A., Wittbrodt, J. and Balavoine, G. (2003). Arthropod-like expression patterns of engrailed and wingless in the annelid Platynereis dumerilii suggest a role in segment formation. *Curr Biol* **13**, 1876-1881.
Psychoyos, D. and Stern, C. D. (1996). Fates and migratory routes of primitive streak cells in the chick embryo. *Development.* **122**, 1523-1534.
Rauskolb, C. and Irvine, K. D. (1999). Notch-mediated segmentation and growth control of the Drosophila leg. *Dev Biol* **210**, 339-350.
Raynaud, A. (1959a). [Development and growth of embryos of the blindworm (Anguis fragilis L.) in the egg incubated in vitro.]. *Comptes rendus hebdomadaires des seances de l'Academie des sciences* **249**, 1813-1815.
Raynaud, A. (1959b). [A technic for the development of eggs of the blindworm (Anguis fragilis L.) outside of the maternal organism.]. *Comptes rendus hebdomadaires des seances de l'Academie des sciences* **249**, 1715-1717.
Reese, A. M. (1915). The Alligator and Its Allies. New York: GP Putnam's Sons.
Renous, S., Rimblot-Baly, F., Fretey, J. and Pieau, C. (1989). Caracteristiques du developpement embryonnaire de la tortue Luth, Dermochelys coriacea (Vandelli, 1961). *Ann Sci Nat Zool Paris* **10**, 197-229.
Richardson, M. K., Allen, S. P., Wright, G. M., Raynaud, A. and Hanken, J. (1998). Somite number and vertebrate evolution. *Development.* **125**, 151-160.
Rivera, A. S., Gonsalves, F. C., Song, M. H., Norris, B. J. and Weisblat, D. A. (2005). Characterization of Notch-class gene expression in segmentation stem cells and segment founder cells in Helobdella robusta (Lophotrochozoa; Annelida; Clitellata; Hirudinida; Glossiphoniidae). *Evol Dev* **7**, 588-599.
Robb, L. and Tam, P. P. (2004). Gastrula organiser and embryonic patterning in the mouse. *Semin Cell Dev Biol* **15**, 543-554.
Saga, Y., Hata, N., Koseki, H. and Taketo, M. M. (1997). Mesp2: a novel mouse gene expressed in the presegmented mesoderm and essential for segmentation initiation. *Genes Dev* **11**, 1827-1839.
Sakai, Y., Meno, C., Fujii, H., Nishino, J., Shiratori, H., Saijoh, Y., Rossant, J. and Hamada, H. (2001). The retinoic acid-inactivating enzyme CYP26 is essential for establishing an uneven distribution of retinoic acid along the anterio-posterior axis within the mouse embryo. *Genes Dev* **15**, 213-225.
Sanders, E. J., Khare, M. K., Ooi, V. C. and Bellairs, R. (1986). An experimental and morphological analysis of the tail bud mesenchyme of the chick embryo. *Anat.Embryol.(Berl).* **174**, 179-185.
Sanger, T. J. and Gibson-Brown, J. J. (2004). The developmental bases of limb reduction and body elongation in squamates. *Evolution; international journal of organic evolution* **58**, 2103-2106; discussion 2107-2108.
Saude, L., Woolley, K., Martin, P., Driever, W. and Stemple, D. L. (2000). Axis-inducing activities and cell fates of the zebrafish organizer. *Development* **127**, 3407-3417.
Sawada, A., Shinya, M., Jiang, Y. J., Kawakami, A., Kuroiwa, A. and Takeda, H. (2001). Fgf/MAPK signalling is a crucial positional cue in somite boundary formation. *Development* **128**, 4873-4880.
Scaal, M. and Wiegreffe, C. (2006). Somite compartments in anamniotes. *Anat Embryol (Berl)* **211 Suppl 1**, 9-19.
Schier, A. F. and Talbot, W. S. (2005). Molecular genetics of axis formation in zebrafish. *Annu Rev Genet* **39**, 561-613.

Schoenwolf, G. C. (1977). Tail (end) bud contributions to the posterior region of the chick embryo. *J Exp Zool* **201**, 227-246.
Schoenwolf, G. C., Chandler, N. B. and Smith, J. L. (1985). Analysis of the origins and early fates of neural crest cells in caudal regions of avian embryos. *Dev Biol* **110**, 467-479.
Schohl, A. and Fagotto, F. (2002). Beta-catenin, MAPK and Smad signaling during early Xenopus development. *Development* **129**, 37-52.
Scholtz, G. (2002). The articulata hypothesis - or what is a segment? *Org. Divers. Evol.* **2**, 197-215.
Schoppmeier, M. and Damen, W. G. (2005). Suppressor of Hairless and Presenilin phenotypes imply involvement of canonical Notch-signalling in segmentation of the spider Cupiennius salei. *Dev Biol* **280**, 211-224.
Schubert, M., Holland, L. Z. and Holland, N. D. (2000). Characterization of an amphioxus wnt gene, AmphiWnt11, with possible roles in myogenesis and tail outgrowth. *Genesis* **27**, 1-5.
Schubert, M., Holland, L. Z., Stokes, M. D. and Holland, N. D. (2001). Three amphioxus Wnt genes (AmphiWnt3, AmphiWnt5, and AmphiWnt6) associated with the tail bud: the evolution of somitogenesis in chordates. *Dev Biol* **240**, 262-273.
Schulte-Merker, S., van Eeden, F. J., Halpern, M. E., Kimmel, C. B. and Nusslein-Volhard, C. (1994). no tail (ntl) is the zebrafish homologue of the mouse T (Brachyury) gene. *Development.* **120**, 1009-1015.
Selleck, M. A. and Stern, C. D. (1991). Fate mapping and cell lineage analysis of Hensen's node in the chick embryo. *Development.* **112**, 615-626.
Shankaran, S. S., Sieger, D., Schroter, C., Czepe, C., Pauly, M. C., Laplante, M. A., Becker, T. S., Oates, A. C. and Gajewski, M. (2007). Completing the set of h/E(spl) cyclic genes in zebrafish: her12 and her15 reveal novel modes of expression and contribute to the segmentation clock. *Dev Biol* **304**, 615-632.
Shen, J., Bronson, R. T., Chen, D. F., Xia, W., Selkoe, D. J. and Tonegawa, S. (1997). Skeletal and CNS defects in Presenilin-1-deficient mice. *Cell* **89**, 629-639.
Shinde, S. L. and Goel, S. C. (1980). A simple technique for maintaining the lizard (Calotes versicolor) embryos in culture till hatching. *Indian journal of experimental biology* **18**, 1101-1103.
Shine, R. (2000). Vertebral numbers in male and female snakes: the roles of natural, sexual and fecundity selection. *J Evol Biol* **13**, 455-465.
Shine, R. (2003). Reproductive strategies in snakes. *Proceedings* **270**, 995-1004.
Sieger, D., Tautz, D. and Gajewski, M. (2003). The role of Suppressor of Hairless in Notch mediated signalling during zebrafish somitogenesis. *Mech Dev* **120**, 1083-1094.
Sieger, D., Tautz, D. and Gajewski, M. (2004). her11 is involved in the somitogenesis clock in zebrafish. *Dev Genes Evol* **214**, 393-406.
Soderberg, D. (2006). Corn snakes in captivity. Lansing, Michigan: ECO Herpetological Publishing & Distribution.
Sosic, D., Brand-Saberi, B., Schmidt, C., Christ, B. and Olson, E. N. (1997). Regulation of paraxis expression and somite formation by ectoderm- and neural tube-derived signals. *Dev Biol.* **185**, 229-243.
Sparrow, D. B., Chapman, G., Wouters, M. A., Whittock, N. V., Ellard, S., Fatkin, D., Turnpenny, P. D., Kusumi, K., Sillence, D. and Dunwoodie, S. L. (2006). Mutation of the LUNATIC FRINGE gene in humans causes spondylocostal dysostosis with a severe vertebral phenotype. *Am J Hum Genet* **78**, 28-37.
Spemann, H. (1931). Uber den anteil von implantat und wirtskem an der orientierung

und beschaffenheit der induzierten embryalanlage. *Wilhelm Roux Arch Entwicklungsmech Org* **123**, 389-517.
Spemann, H. and H., M. (1924). Uber induktion von embryoalanlangen durch implatation artfremder organisatoren *Roux Arch EntwMmech Org* **100**, 599-638.
St Johnston, D. and Nusslein-Volhard, C. (1992). The origin of pattern and polarity in the Drosophila embryo. *Cell* **68**, 201-219.
Stern, C. D., Artinger, K. B. and Bronner-Fraser, M. (1991). Tissue interactions affecting the migration and differentiation of neural crest cells in the chick embryo. *Development.* **113**, 207-216.
Stickney, H. L., Barresi, M. J. and Devoto, S. H. (2000). Somite development in zebrafish. *Dev Dyn* **219**, 287-303.
Stollewerk, A., Schoppmeier, M. and Damen, W. G. (2003). Involvement of Notch and Delta genes in spider segmentation. *Nature* **423**, 863-865.
Sun, X., Meyers, E. N., Lewandoski, M. and Martin, G. R. (1999). Targeted disruption of Fgf8 causes failure of cell migration in the gastrulating mouse embryo. *Genes Dev* **13**, 1834-1846.
Suriben, R., Fisher, D. A. and Cheyette, B. N. (2006). Dact1 presomitic mesoderm expression oscillates in phase with Axin2 in the somitogenesis clock of mice. *Dev Dyn* **235**, 3177-3183.
Szeto, D. P. and Kimelman, D. (2006). The regulation of mesodermal progenitor cell commitment to somitogenesis subdivides the zebrafish body musculature into distinct domains. *Genes Dev* **20**, 1923-1932.
Tada, M. and Smith, J. C. (2000). Xwnt11 is a target of Xenopus Brachyury: regulation of gastrulation movements via Dishevelled, but not through the canonical Wnt pathway. *Development* **127**, 2227-2238.
Takada, S., Stark, K. L., Shea, M. J., Vassileva, G., McMahon, J. A. and McMahon, A. P. (1994). Wnt-3a regulates somite and tailbud formation in the mouse embryo. *Genes Dev* **8**, 174-189.
Takahashi, Y., Koizumi, K., Takagi, A., Kitajima, S., Inoue, T., Koseki, H. and Saga, Y. (2000). Mesp2 initiates somite segmentation through the Notch signalling pathway. *Nat Genet* **25**, 390-396.
Tam, P. P. (1981). The control of somitogenesis in mouse embryos. *J.Embryol.Exp.Morphol.* **65 Suppl**, 103-128.
Tam, P. P. and Tan, S. S. (1992). The somitogenetic potential of cells in the primitive streak and the tail bud of the organogenesis-stage mouse embryo. *Development* **115**, 703-715.
Tautz, D. (2004). Segmentation. *Dev Cell* **7**, 301-312.
Tokita, M. and Kuratani, S. (2001). Normal embryonic stages of the Chinese softshelled turtle Pelodiscus sinensis (Trionychidae). *Zoological Science (Tokyo)* **18**, 705-715.
Tonegawa, A., Funayama, N., Ueno, N. and Takahashi, Y. (1997). Mesodermal subdivision along the mediolateral axis in chicken controlled by different concentrations of BMP-4. *Development* **124**, 1975-1984.
Tonegawa, A. and Takahashi, Y. (1998). Somitogenesis controlled by Noggin. *Dev Biol.* **202**, 172-182.
Treadwell, R. W. (1962). Time and sequence of appearance of certain gross structures in Pituophis melanoleucus sayi embryos. *Herpetologica* **18**, 120-124.
Turing, A. M. (1952). The chemical basis of morphogenesis. *Philosophical Transactions of the Royal Society of London* **B 237**, 37-72.
van der Hoeven, F., Sordino, P., Fraudeau, N., Izpisua-Belmonte, J. C. and

Duboule, D. (1996). Teleost HoxD and HoxA genes: comparison with tetrapods and functional evolution of the HOXD complex. *Mech Dev* **54**, 9-21.
van Eeden, F. J., Granato, M., Schach, U., Brand, M., Furutani-Seiki, M., Haffter, P., Hammerschmidt, M., Heisenberg, C. P., Jiang, Y. J., Kane, D. A. et al. (1996). Mutations affecting somite formation and patterning in the zebrafish, Danio rerio. *Development.* **123**, 153-164.
Veini, M. and Bellairs, R. (1983). Experimental analysis of control mechanisms in somite segmentation in avian embryos. I. Reduction of material at the blastula stage in Coturnix coturnix japonica. *J.Embryol.Exp.Morphol.* **74**, 1-14.
Vidal, N. and Hedges, S. B. (2004). Molecular evidence for a terrestrial origin of snakes. *Proceedings* **271 Suppl 4**, S226-229.
Vincent, C., Bontoux, M., Le Douarin, N. M., Pieau, C. and Monsoro-Burq, A. H. (2003). Msx genes are expressed in the carapacial ridge of turtle shell: a study of the European pond turtle, Emys orbicularis. *Dev Genes Evol* **213**, 464-469.
Von Ebner, V. (1888). Urwirbel und Neugliederung der WirbelSäule. *Sitzungsber.Akad.Wiss.Wien* **III/97**, 194-206.
Wang, J., Li, S., Chen, Y. and Ding, X. (2007). Wnt/beta-catenin signaling controls Mespo expression to regulate segmentation during Xenopus somitogenesis. *Dev Biol* **304**, 836-847.
Ward, A. B. and Brainerd, E. L. (2007). Evolution of axial patterning in elongate fishes. *Biological Journal of the Linnean Society* **90**, 97-116.
Wellik, D. M. and Capecchi, M. R. (2003). Hox10 and Hox11 genes are required to globally pattern the mammalian skeleton. *Science* **301**, 363-367.
Wharton, K. A., Jr., Zimmermann, G., Rousset, R. and Scott, M. P. (2001). Vertebrate proteins related to Drosophila Naked Cuticle bind Dishevelled and antagonize Wnt signaling. *Dev Biol* **234**, 93-106.
Whittock, N. V., Sparrow, D. B., Wouters, M. A., Sillence, D., Ellard, S., Dunwoodie, S. L. and Turnpenny, P. D. (2004). Mutated MESP2 causes spondylocostal dysostosis in humans. *Am J Hum Genet* **74**, 1249-1254.
Wiens, J. J. (2004). Development and evolution of body form and limb reduction in squamates: a response to Sanger and Gibson-Brown. *Evolution* **58**, 2107-2108.
Wiens, J. J. and Slingluff, J. L. (2001). How lizards turn into snakes: a phylogenetic analysis of body-form evolution in anguid lizards. *Evolution; international journal of organic evolution* **55**, 2303-2318.
Wilson, V., Manson, L., Skarnes, W. C. and Beddington, R. S. (1995). The T gene is necessary for normal mesodermal morphogenetic cell movements during gastrulation. *Development* **121**, 877-886.
Winnier, G., Blessing, M., Labosky, P. A. and Hogan, B. L. (1995). Bone morphogenetic protein-4 is required for mesoderm formation and patterning in the mouse. *Genes Dev* **9**, 2105-2116.
Wong, P. C., Zheng, H., Chen, H., Becher, M. W., Sirinathsinghji, D. J., Trumbauer, M. E., Chen, H. Y., Price, D. L., Van der Ploeg, L. H. and Sisodia, S. S. (1997). Presenilin 1 is required for Notch1 and DII1 expression in the paraxial mesoderm. *Nature* **387**, 288-292.
Wu, J. Y., Wen, L., Zhang, W. J. and Rao, Y. (1996). The secreted product of Xenopus gene lunatic Fringe, a vertebrate signaling molecule [published erratum appears in Science 1996 Oct 25;274(5287):485]. *Science* **273**, 355-358.
Yamaguchi, T. P., Bradley, A., McMahon, A. P. and Jones, S. (1999a). A Wnt5a pathway underlies outgrowth of multiple structures in the vertebrate embryo. *Development* **126**, 1211-1223.

Yamaguchi, T. P., Harpal, K., Henkemeyer, M. and Rossant, J. (1994). fgfr-1 is required for embryonic growth and mesodermal patterning during mouse gastrulation. *Genes Dev* **8**, 3032-3044.
Yamaguchi, T. P., Takada, S., Yoshikawa, Y., Wu, N. and McMahon, A. P. (1999b). T (Brachyury) is a direct target of Wnt3a during paraxial mesoderm specification. *Genes Dev* **13**, 3185-3190.
Yamamoto, A., Kemp, C., Bachiller, D., Geissert, D. and De Robertis, E. M. (2000). Mouse paraxial protocadherin is expressed in trunk mesoderm and is not essential for mouse development. *Genesis* **27**, 49-57.
Yang, X., Dormann, D., Munsterberg, A. E. and Weijer, C. J. (2002). Cell movement patterns during gastrulation in the chick are controlled by positive and negative chemotaxis mediated by FGF4 and FGF8. *Dev Cell* **3**, 425-437.
Yasuhiko, Y., Haraguchi, S., Kitajima, S., Takahashi, Y., Kanno, J. and Saga, Y. (2006). Tbx6-mediated Notch signaling controls somite-specific Mesp2 expression. *Proc Natl Acad Sci U S A* **103**, 3651-3656.
Yntema, C. L. (1964). Procurement and Use of Turtle Embryos for Experimental Procedures. *Anat Rec* **149**, 577-583.
Yntema, C. L. (1968). A series of stages in the embryonic development of Chelydra serpentina. *Journal of morphology* **125**, 219-251.
Yoon, J. K., Moon, R. T. and Wold, B. (2000). The bHLH class protein pMesogenin1 can specify paraxial mesoderm phenotypes [In Process Citation]. *Dev Biol* **222**, 376-391.
Yoon, J. K. and Wold, B. (2000). The bHLH regulator pMesogenin1 is required for maturation and segmentation of paraxial mesoderm. *Genes Dev* **14**, 3204-3214.
Yu, H. M., Jerchow, B., Sheu, T. J., Liu, B., Costantini, F., Puzas, J. E., Birchmeier, W. and Hsu, W. (2005). The role of Axin2 in calvarial morphogenesis and craniosynostosis. *Development* **132**, 1995-2005.
Zakany, J., Kmita, M., Alarcon, P., de la Pompa, J. L. and Duboule, D. (2001). Localized and transient transcription of Hox genes suggests a link between patterning and the segmentation clock. *Cell* **106**, 207-217.
Zehr, D. R. (1962). Stages in the normal development of the common garter snake, Thamnophis sirtalis sirtalis. *Copeia* **1962**, 322-329.
Zhang, N. and Gridley, T. (1998). Defects in somite formation in lunatic fringe-deficient mice *Nature* **394**, 374-377.
Zhang, S., Cagatay, T., Amanai, M., Zhang, M., Kline, J., Castrillon, D. H., Ashfaq, R., Oz, O. K. and Wharton, K. A., Jr. (2007). Viable mice with compound mutations in the Wnt/Dvl pathway antagonists nkd1 and nkd2. *Mol Cell Biol* **27**, 4454-4464.
Zug, G. R., Vitt, L. J. and Caldwell, J. P. (2001). Snakes. In *Herpetology : an introductory biology of amphibians and reptiles*, pp. 503-532. San Diego, Calif.: Academic Press.